RF CIRCUIT NONLINEARITY CHARACTERIZATION AND MODELING FOR EMBEDDED TEST

By

CHOONGEOL CHO

A DISSERTATION PRESENTED TO THE GRADUATE SCHOOL
OF THE UNIVERSITY OF FLORIDA IN PARTIAL FULFILLMENT
OF THE REQUIREMENTS FOR THE DEGREE OF
DOCTOR OF PHILOSOPHY

UNIVERSITY OF FLORIDA

2005

This document is dedicated to the graduate students of the University of Florida.

ACKNOWLEDGMENTS

I would like to express my sincere appreciation to my advisor, Professor William R. Eisenstadt, whose encouragement, guidance, and support throughout my work have been invaluable, I also would like to thank Professors Robert M. Fox, John G. Harris, and Oscar D. Crisalle for their interest in this work and their guidance as the thesis committee members.

I thank Motorola Company for financial support. I also thank Bob Stengel and Enrique Ferrer for their dedication to my research. In addition, I thank all of the friends who made my years at the University of Florida such an enjoyable chapter of my life.

I am grateful to my parents and parents in law for their unceasing love and dedication. Finally, I thank my wife, Seon-Kyung Kim, whose endless love and encouragement were most valuable to me. Most importantly, I would like to thank God for guiding me everyday.

TABLE OF CONTENTS

LIST OF TABLES

LIST OF FIGURES

Abstract of Dissertation Presented to the Graduate School
of the University of Florida in Partial Fulfillment of the
Requirements for the Degree of Doctor of Philosophy

RF CIRCUIT NONLINEARITY CHARACTERIZATION AND
MODELING FOR EMBEDDED TEST

By

Choongeol Cho

December 2005

Chair: William R. Eisenstadt
Major Department: Electrical and Computer Engineering

This dissertation presents a fitting algorithm useful for characterizing nonlinearities of RF circuits, and is specifically designed to estimate the third-order intercept point (IP_3) by extracting the nonlinear coefficients from the one-tone measurement. And the dissertation proposes a method to predict the 1 dB gain compression point ($P_{1\text{-}dB}$) from a two-tone measurement. The fitting algorithm is valuable for reducing production IC test time ans cost. A new relationship between the 1 dB gain compression point and the third-order intercept point has been derived. It follows that the difference between $IP_{1\text{-}dB}$ and IIP_3 is not fixed, and the discrepancy is explained by the new proposed equation which includes the relevant nonlinear coefficients. The new fitting algorithm has been verified through application to the simulation of a common-source amplifier. The best fitting range has been identified through the minimization of the standard errors of the nonlinear coefficients and of the sum of squares of the residuals. A robust algorithm to predict IIP_3 has been developed for wideband RF amplifiers, an application that is of particular

interest. The proposed fitting algorithm was successfully verified in experiments done on commercial RF power amplifiers. The estimated IIP_3 values obtained from one-tone measurement data was close to the experimently measured values. The method proposed to predict $IP_{1\text{-}dB}$ from a two-tone measurement was also applied successfully to the same commercial RF power amplifiers.

A simple embedded test using a direct conversion mixer can be realized to estimate the nonlinear characteristics of an amplifier based upon the estimate IIP_3 from the one-tone data. In this thesis, the nonlinear characteristics of a mixer is researched and a mixer embedded test technique is suggested. The effects of the mismatches and phase offset will be researched for mixer test in the future.

The methods developed in this thesis are useful tools in the context for typical RF/Mixed-signal production test. The advantage is that these methods avoid the difficulty of two-tone measurements or remove one-tone measurement test step. By developing the relationship between the 1 dB gain compression point and the third-order intercept point, a simpler embedded test model can be adopted avoiding the cost and time of a two-tone measurement.

CHAPTER 1
INTRODUCTION

1.1 Motivation

In the near future, RF microwave circuits will be embedded in highly integrated "Systems-on-a-Chip" (SoCs). These RF SoCs will need to be debugged in the design phase and will require expensive automated test equipment (ATE) with microwave test capability when tested in production. RF/mixed-signal portions of a SoC must be verified with high-frequency parametric tests. Currently, the ATE performs a production test on package parts with the assistance of an expensive and elaborate device interface board (DIB) or load board. Alternative methods of on-chip RF test should be explored to lower test cost [Eis01].

Another merit of the embedded test is to minimize test time. Current measurement is performed in the last stage of production. A parameter test of an RF circuit can be executed using the embedded circuit before packaging and even sorting.

The 1 dB gain compression point and the third-order intercept point are important nonlinear parameters of the RF/mixed-signal circuit and provide good verification of a circuit or device's linearity and dynamic range. The parameters can be connected to adjacent channel power ratio and error vector magnitude (EVM) in amplifiers and must be kept under control. Gain compression is a relatively simple microwave measurement since it requires a variable power single tone source and an output power detector. IIP_3 characterization is more complicated and more costly since two separate tones closely spaced in frequency must be generated and applied to the circuit under test (CUT) and

the CUT's fundamental and third order distortion term power must be measured. Thus, measurement of IIP_3 requires high Q filters to select first and third order distortion frequencies in the detector circuit [Eis02].

By developing an accurate relationship between gain compression and IIP_3, the production testing of the manufactured IC can be greatly simplified. Although the accuracy of this approach may not be as great as direct IIP_3 measurement, it has great appeal in test cost reduction and may be sufficient for production IC test.

1.2 Research Goals

The first goal in this research is to derive the relationship between 1 dB gain compression point and third-order intercept point. The published difference between 1 dB gain compression point and IIP_3 is roughly 10 dB; this relationship is derived using first-order and third-order nonlinear coefficients of transistor amplifier circuits. This calculation assumes that higher-order nonlinear coefficients do not affect the 1 dB gain compression. The simulation using 0.25 μm MOSFETs, 0.4 μm MOSFETs and Si-Ge BJTs models in Table 1-1 shows that this classical relationship does not work in simple transistor circuits. The difference between 1 dB gain compression and IIP_3 shows a variation of 8 dB to 13.7 dB. All the circuits (common-source amplifier, differential amplifier with resistive load, and common-emitter amplifier except for a differential amplifier with an active load) show that the difference between IIP_3 and $IP_{1\text{-}dB}$ is no longer constant. To simplify the embedded test, a more reliable relationship between these two parameters is required.

The second goal is to verify the relationship between two parameters that is derived in the first goal. This dissertation examines the general types of amplifiers,

Table 1-1 The 1 dB gain compression point and IIP_3 of various circuits

Model	Circuit	$IP_{1\text{-}dB}$* (dBm)	IIP_3** (dBm)	IIP_3 -$IP_{1\text{-}dB}$ (dB)
TSMC 0.25μm MOSFET	Common-Source Amplifier	-2.2	10.0	12.2
	Differential Amplifier (Resistive Load)	3.0	16.0	13.0
	Differential Amplifier (Active Load)	-13.0	-5.0	8.0
Si-Ge IBM6HP MOSFET	Common-Source Amplifier	-1.75	10.25	12.0
	Differential Amplifier (Resistive Load)	2.65	15.25	12.6
Si-Ge IBM6HP BJT	Common-Source Amplifier	-20.25	-6.5	13.75

*One-tone test : Source frequency = 100 MHz
**Two-tone test : frequencies = 100 MHz, 120 MHz

commercial wideband RF amplifiers and commercial RF power amplifiers. In this dissertation, the fitting approach is developed to estimate IIP_3 from a gain compression curve using higher-order nonlinear coefficients.

Finally, a simple embedded test using a mixer is considered and suggested to measure IIP_3 and $IP_{1\text{-}dB}$. Through developing the relationship between IIP_3 and $IP_{1\text{-}dB}$, the embedded test for IIP_3 requires only a one-tone source.

1.3 Overview of Dissertation

This Ph.D. dissertation consists of seven chapters. An overview of the research is given in this current chapter (Chapter 1), including the motivation, research goals, and the scope of this work. Chapter 2 reviews some background knowledge on this research. Basic concepts of both nonlinear systems and nonlinear analysis are described.

In chapter 3, a new relationship between the 1 dB gain compression point and the third-order intercept point is derived. First, this relationship between IIP3 and $IP_{1\text{-}dB}$ is

reviewed in classical prior analysis. The new relationship is derived by nonlinear analysis on the gain compression curve. The fitting algorithm to estimate IIP_3 from a one-tone measurement and the calculation method to predict $IP_{1\text{-}dB}$ from a two-tone measurement are developed. The linear regression theory required for the fitting algorithm is reviewed and modified for the application of the devised algorithm.

In chapter 4, the proposed fitting algorithm is verified through the application of the algorithm to the simulation of a common-source amplifier. The best fitting range is chosen through the standard errors of nonlinear coefficients and the sum of squares of the residuals. The effects of measurement errors at high frequency are researched. Through the Voletrra series analysis, the load effect on the algorithm is studied.

In chapter 5, a robust algorithm to predict IIP3 is developed for wideband RF amplifiers. The $IP_{1\text{-}dB}$ prediction from two-tone measurement has been applied to these wideband amplifiers. Through several steps of simple calculation using the third-order intercept point and the gain compression at the fundamental frequency, $IP_{1\text{-}dB}$ is estimated under 1 dB error.

In chapter 6, the fitting algorithm is applied to commercial RF power amplifiers. Through the inspection of the standard errors of fitting parameters, the best fitting range is chosen for the extraction of nonlinear coefficients used for the calculation of the third-order intercept point. The chosen fitting range is confirmed by the quantity, sum of squares of the residuals. Another method to predict $IP_{1\text{-}dB}$ from a two-tone measurement is applied to the commercial RF power amplifiers.

Lastly, in chapter 7, the primary contributions of this dissertation are summarized and future work is suggested.

CHAPTER 2
BACKGROUND

2.1 Classifications of Distortions

All physical components and devices are intrinsically nonlinear. Nevertheless, the most circuit and system theory deal almost exclusively with linear analysis. The reason is because linear systems are characterized in terms of linear algebraic, differential, integral, and difference equations that are relatively easy to solve, most nonlinear systems can be adequately approximated by equivalent linear systems for suitably small inputs, and closed-form analytical solutions of nonlinear equations are not normally possible. However, linear models are incapable of explaining important nonlinear phenomena [Wei80]. This section reviews types of distortions and nonlinearities for understanding nonlinear characteristics of a system.

Distortion actually refers to the distortion of a voltage or current waveform as it is displayed versus time [San99]. Any difference between the shape of the output waveform and that of the input waveform is called distortion except for scaling a waveform in amplitude. In a circuit, the type of distortion is classified as one of two classes. First, linear distortion is caused by the application of a linear circuit with frequency-varying amplitude or phase characteristics. For example, when a square-wave input is applied to a high-pass filter, the output waveform undergoes linear distortion. Second, nonlinear distortion is caused by nonlinear transfer function characteristics. For example, the application of a large sinusoidal waveform to the exponential transfer function

characteristic of a bipolar transistor based amplifier can cause a sharpening of one hump of the waveform and flattening of the other one.

Nonlinear distortion is classified finely in two categories : weak and hard distortion. In the case of weak distortion, the harmonics gradually shrink as the signal amplitude becomes smaller. However, the harmonics are never zero. The harmonic amplitudes can easily be calculated from a Taylor series expansion around the quiescent or operating point. In weakly nonlinear distortion, the Volterra series can be used for estimating the nonlinear behavior of a circuit.

Hard distortion, on the other hand, can be seen in Class AB, B, and C amplifiers. In these cases, a part of the sinusoidal waveform is simply cut off, leaving two sharp corners. These corners generate a large number of high-frequency harmonics. They are the sources of hard distortion. Hard distortion harmonics suddenly disappear when the amplitude of the sinusoidal waveform falls below the threshold, i.e., the edge of the transfer characteristic. The class C amplifier is considered below as an example of a circuit with hard distortion. Figure 2-1 shows the output current of an ideal class C

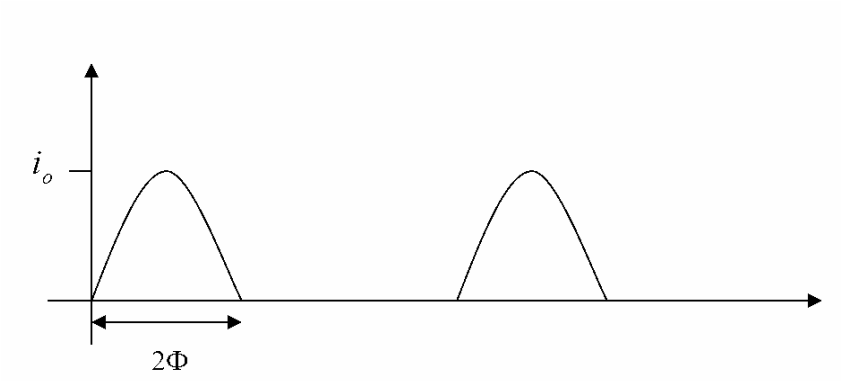

Figure 2-1 The output current of an ideal class C amplifier for a sine-wave input amplifier. The output current amplitude at a fundamental frequency is in the form of a nonlinear function which shown in equation (2-1).

$$i_{fund} = \frac{i_o}{2\pi}(2\Phi - \sin 2\Phi) \tag{2-1}$$

where 2Φ is a conduction angle and is a nonlinear function of output amplitude i_o.

2.2 Taylor's Series Expansion

Let be $f(x)$ continuous on a real interval I containing x_0 (and x), and let $f^{(n)}(x)$ exist at x and $f^{(n+1)}(\xi)$ be continuous for all $\xi \in I$. Then we have the following Taylor series expansion:

$$\begin{aligned} f(x) = f(x_0) &+ \frac{1}{1} f'(x_0)(x-x_0) + \frac{1}{1\cdot 2} f''(x_0)(x-x_0)^2 \\ &+ \frac{1}{1\cdot 2\cdot 3} f'''(x_0)(x-x_0)^3 + \ldots \\ &+ \frac{1}{n!} f^{(n)}(x_0)(x-x_0)^n + R_{n+1}(x) \end{aligned} \tag{2-2}$$

where $R_{n+1}(x)$ is called the *remainder term*. Then, Taylor's theorem provides that there exists some ξ between x and x_0 such that

$$R_{n+1}(x) = \frac{f^{(n+1)}(\xi)}{(n+1)!}(x-x_0)^{n+1} \tag{2-3}$$

In particular, if $\left|f^{(n+1)}\right| \le M$ in I , then

$$R_{n+1}(x) \le \frac{M}{(n+1)!}\left|x-x_0\right|^{n+1} \tag{2-4}$$

which is normally small when x is close to x_0 [Ros98].

For a nonlinear conductance, the current through the element, $\boldsymbol{i_{out}(t)}$, is a nonlinear function f of the controlling voltage, $\boldsymbol{v_{CONTR}(t)}$. This function can be expanded into a power series around the quiescent point $\boldsymbol{I_{OUT} = f(V_{CONTR})}$ [Wam98].

$$\boldsymbol{i_{OUT}(t) = f(v_{CONTR}(t)) = f(V_{CONTR} + v_{contr}(t))}$$

$$= f(V_{CONTR}) + \sum_{k=1}^{\infty} \frac{1}{k!} \frac{\partial^k f(v(t))}{(\partial v)^k}\bigg|_{v=V_{CONTR}} \bullet v_{contr}^k(t) \tag{2-5}$$

Nonlinear coefficients are defined as follows

$$K_n = \frac{1}{k!} \frac{\partial^k f(v(t))}{(\partial v)^k}\bigg|_{v=V_{CONTR}} \tag{2-6}$$

The expression of the AC current through the conductance is in equation (2-7).

$$i_{out}(t) = K_1 v_{contr}(t) + K_2 v_{contr}^2(t) + K_3 v_{contr}^3(t) + \ldots \tag{2-7}$$

2.3 Measurement of Nonlinear System

A single-tone test is used for the measurement of harmonic distortion, gain compression/expansion, large-signal impedances and root-locus analysis. The configuration of a single-tone test can be seen in Figure 2-2. When the input power sweeps a wide range, the output power at the same frequency as the input is measured in the sweep range. The cable and other interconnection components that transfer power should be calibrated since these components have power loss.

For the analysis of intermodulation, cross-modulation and desensitization, the two-tone test is used. Figure 2-3 shows the configuration of a two-tone harmonic test. In this test, the power combiner is used for combining two powers at different frequencies. Through this test, a third-order intercept point is determined.

The next chapter develops the relationship between 1 dB gain compression point and third-order intercept point. Taylor series analysis above is essential for performing that analysis.

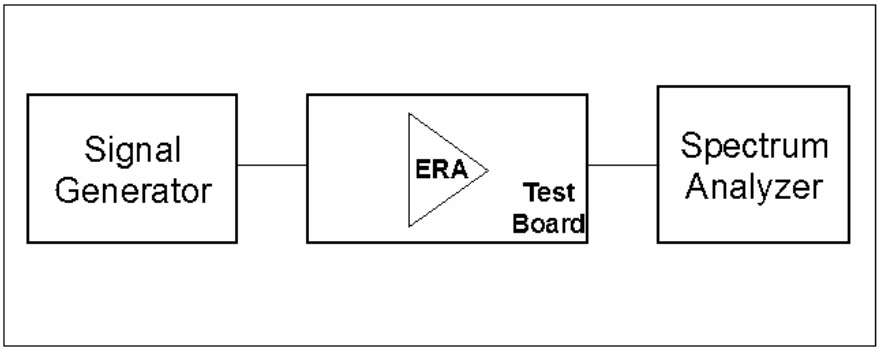

Figure 2-2 The configuration of a single-tone test. ERA is a commercial amplifier.

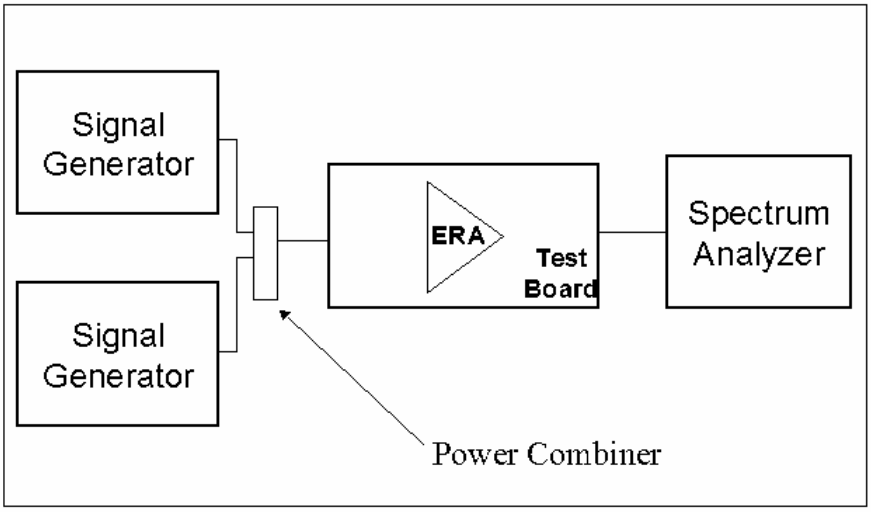

Figure 2-3 The configuration of a two-tone test. ERA is a commercial amplifier.

CHAPTER 3
THE RELATIONSHIP BETWEEN THE 1 dB GAIN COMPRESSION POINT AND THE THIRD-ORDER INTERCEPT POINT

3.1 Definition of 1 dB Gain Compression and Third-order Intercept Point

The constant small-signal gain of a circuit is usually obtained with the assumption that the harmonics are negligible. However, as the signal amplitude increases, the gain begins to vary with input power. In most circuits of interest, the output at high power is a compressive or saturating function of the input. In analog, RF and microwave circuits, these effects are quantified by the 1-dB gain compression point [Raz98]. Figure 3-1 shows the definition of the 1 dB gain compression point. The real gain curve, C is plotted on a log-log scale as a function of the input power level. The output level falls below its ideal value since the compression of the real gain curve is caused by the

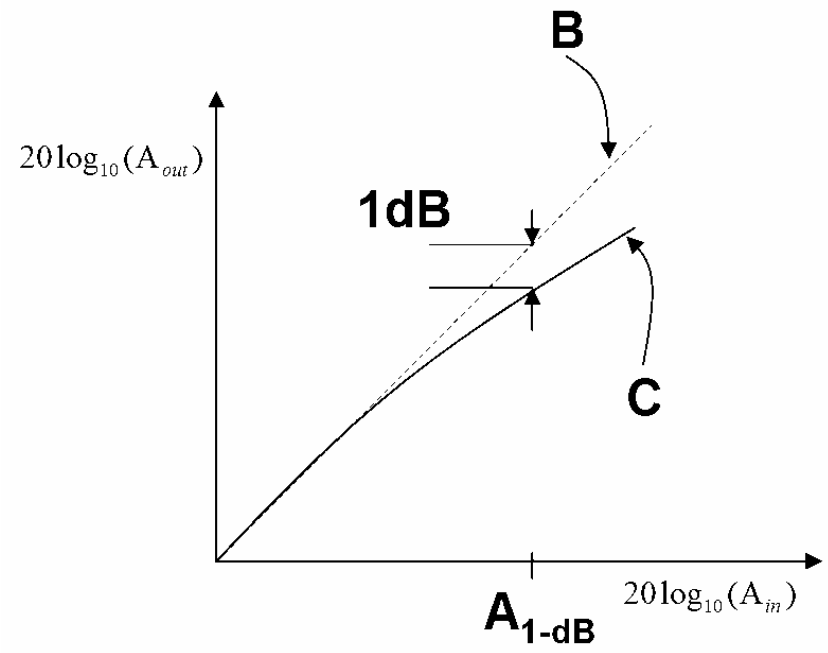

Figure 3-1 Definition of 1-dB gain compression point

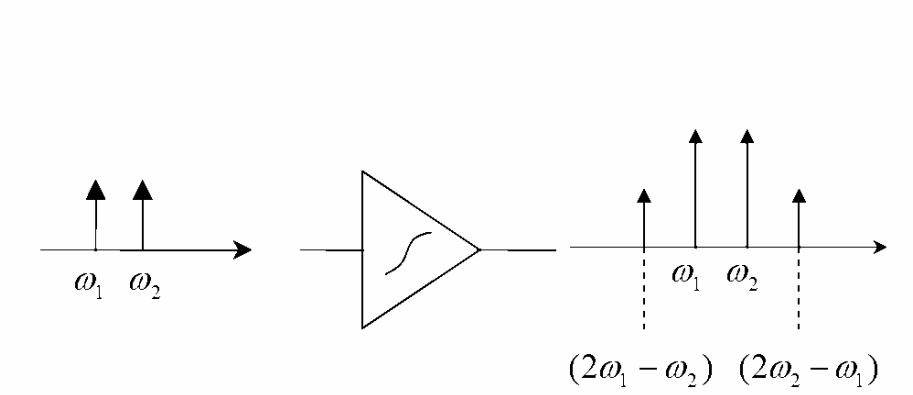

Figure 3-2 Intermodulation in a nonlinear system

nonlinear transfer characteristics of the circuit. Point $A_{1\text{-dB}}$ is defined as the input signal level in which the difference between the ideal linear gain curve B and the real gain curve C is 1 dB.

Another important nonlinear characteristic is the intermodulation distortion in a two-tone test. When two signals with different frequencies, ω_1 and ω_2, are applied to a nonlinear system, the large signal output exhibits some components that are not harmonics of the input frequencies. Of particular interest are the third-order intermodulation products at $(2\omega_1 - \omega_2)$ and $(2\omega_2 - \omega_1)$, as illustrated in Figure 3-2. In this figure, two large signals at the left are inputs into an amplifier in the center. The output is shown on the right of the figure as the two fundamental signals plus the intermodulation frequencies $(2\omega_1 - \omega_2)$ and $(2\omega_2 - \omega_1)$.

The corruption of signals due to third-order intermodulation of two nearby interferers is so common and so critical that a performance metric has been defined to characterize this behavior. The third-order intercept points IIP_3 and OIP_3 are used for characterizing this effect. These terms are defined at the intersection of two lines shown in Figure 3-3. The first line has a slope of one on the log-log plot (20 log (amplitude at

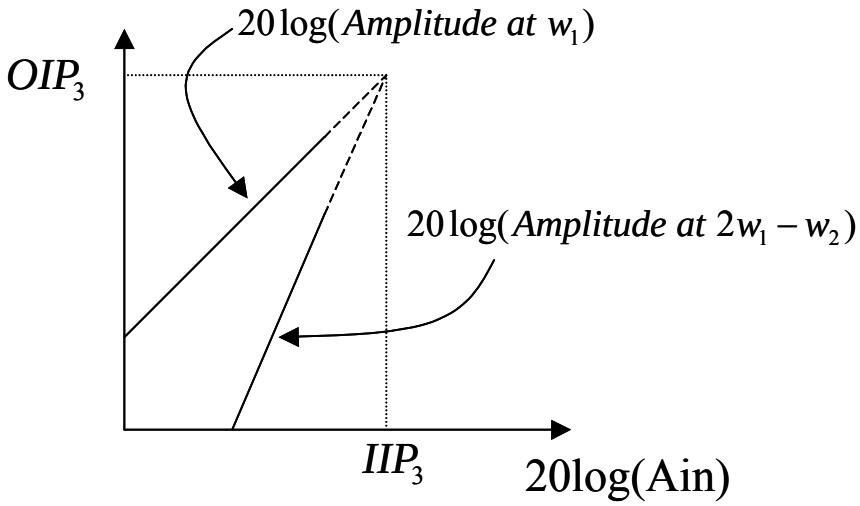

Figure 3-3 Definition of third-order intercept point

w1)) and represents the input and output power of the fundamental frequency. The second line represents the growth of the $(2\omega_1 - \omega_2)$ intermodulation harmonic with input power, it has a slope of three. OIP_3 is the output power at the intercept point and IIP_3 is the input power at the intercept point, IP_3.

3.2 Classical Approach to Model IIP_3

In a nonlinear system without memory such as an amplifier at low frequency, the output can be modeled by a power series of the input in section 2.2. If the input of the nonlinear system is $x(t)$, the output $y(t)$ of this system is as follows,

$$y(t) = K_1 x(t) + K_2 x(t)^2 + K_3 x(t)^3 + \ldots \quad (3\text{-}1)$$

where K_i is nonlinear coefficients of this system. This example is explained in equation (2-6) in section 2.2. The classical analysis of the nonlinear system uses the assumption that the fourth-order and higher-order terms in equation (3-1) are negligible. In the classical analysis, the nonlinear system is modeled as follows [Raz98][Gon97],

$$y(t) = K_1 x(t) + K_2 x(t)^2 + K_3 x(t)^3 \quad (3\text{-}2)$$

If a sinusoidal input with a fundamental frequency is applied to this nonlinear system

$$x(t) = A\cos(\omega t) \tag{3-3}$$

then the output of this system is represented by using the equation (3-2),

$$\begin{aligned} y(t) = \frac{K_2 A^2}{2} + \left(K_1 A + \frac{3K_3 A^3}{4} \right) \cos(\omega t) + \frac{K_2 A^2}{2} \cos(2\omega t) \\ + \frac{3K_3 A^3}{4} \cos(3\omega t) \end{aligned} \tag{3-4}$$

At the fundamental frequency ω, the gain is defined as a function of the input signal amplitude,

$$Gain(at\ \omega) = K_1 A + \frac{3K_3 A^3}{4} \tag{3-5}$$

If K_3 has the opposite sign of K_1, the gain is a decreasing function of the input amplitude.

The 1-dB gain compression point is defined in Figure 3-1, the equation at this point is

$$20\log\left| K_1 A_{1dB} + \frac{3K_3 {A_{1dB}}^3}{4} \right| = 20\log\left| K_1 A_{1dB} \right| - 1dB \tag{3-6}$$

where A_{1dB} is the input amplitude at the 1 dB gain compression point. The solution of equation (3-6) is

$$A_{1dB} = \sqrt{0.145 \left| \frac{K_1}{K_3} \right|} \tag{3-7}$$

In summary, the input amplitude referred to the 1 dB gain compression point is found using only two nonlinear coefficients K_1 and K_3.

The classical analysis is considered in a two-tone test. The input signal in the two-tone test is composed of two signals with the same input amplitude and different frequencies.

$$x(t) = A\cos(\omega_1 t) + A\cos(\omega_2 t) \tag{3-8}$$

When this input signal is applied to the nonlinear system represented by the equation (3-2), the output is,

$$\begin{aligned} y(t) = &\left(K_1 A + \frac{9K_3 A^3}{4} \right)\cos(\omega_1 t) + \left(K_1 A + \frac{9K_3 A^3}{4} \right)\cos(\omega_1 t) \\ &+ \left(\frac{3K_3 A^3}{4} \right)\cos((2\omega_1 - \omega_2)t) + \left(\frac{3K_3 A^3}{4} \right)\cos((2\omega_2 - \omega_1)t) + \ldots \end{aligned} \tag{3-9}$$

The third-order intercept point is defined in Figure 3-3. At this point, the output amplitude at a fundamental frequency is the same as that at an intermodulation frequency. The input signal level satisfying the above condition is represented by,

$$\left| K_1 A_{IP3} \right| = \left| \frac{3K_3 {A_{IP3}}^3}{4} \right| \tag{3-10}$$

where A_{IP3} is the input amplitude at the third-order intercept point. The solution of above equation (3-10) is

$$A_{IP3} = \sqrt{\frac{4}{3}\left| \frac{K_1}{K_3} \right|} \tag{3-11}$$

The input signal level at the third-order intercept point is also found using two nonlinear coefficients K_1 and K_3. From equation (3-7) and equation (3-10), the relationship between the input signal levels at the 1 dB gain compression point and the third-order intercept point can be derived,

$$\frac{A_{1dB}}{A_{IP3}} = \frac{\sqrt{0.145}}{\sqrt{4/3}} \approx -9.6dB \tag{3-12}$$

The classical analysis shows that the relationship between two nonlinear characteristics is represented by equation (3-12).

3.3 New Approach to Model Gain Compression Curve

For simplicity, the analysis is limited to memoryless, time-invariant nonlinear systems. Prior classical analysis limits the output to the third-order nonlinearity coefficient. For the more exact analysis, the relaxation of this limitation is required. The nonlinear system in this analysis is represented by,

$$y(t) = K_1 x(t) + K_2 x(t)^2 + K_3 x(t)^3 + K_4 x(t)^4 + K_5 x(t)^5 \tag{3-13}$$

If a sinusoidal input such as equation (3-2) is applied to this system, then the output amplitudes at each odd-frequency are as follows,

$$y(t;\omega) = \left(K_1 A + \frac{3}{4} K_3 A^3 + \frac{5}{8} K_5 A^5 \right) \cos(\omega t) \tag{3-14}$$

$$y(t;3\omega) = \left(\frac{1}{4} K_3 A^3 + \frac{5}{16} K_5 A^5 \right) \cos(3\omega t) \tag{3-15}$$

$$y(t;5\omega) = \left(\frac{1}{16} K_5 A^5 \right) \cos(5\omega t) \tag{3-16}$$

If a low input signal level is considered in equation (3-14), the following condition is satisfied,

$$\left| K_1 A \right| >> \left| \frac{3}{4} K_3 A^3 + \frac{5}{8} K_5 A^5 \right| \tag{3-17}$$

then the output amplitude at the fundamental frequency is $K_1 A$. From equation (3-15), the output amplitude at frequency 3ω is $\frac{1}{4} K_3 A^3$ if ,

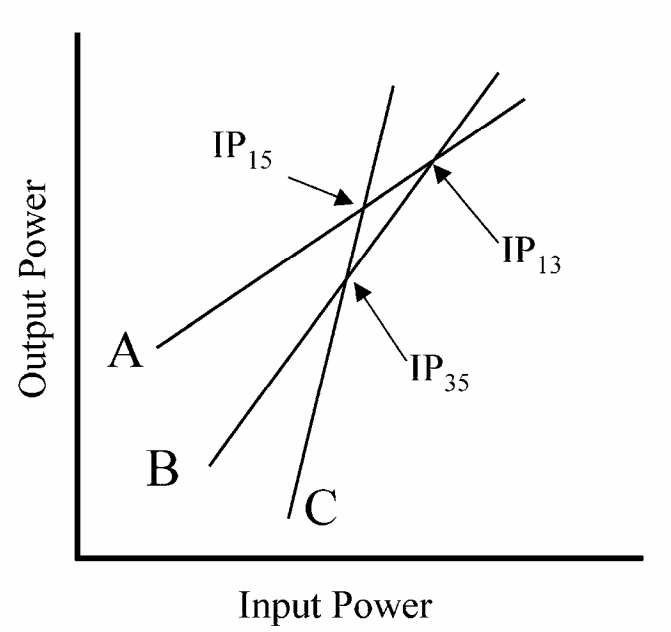

Figure 3-4 The definition of Intercept points in one-tone test. A= 20 log (K_1A), B=20 log ($K_3A^3/4$) and C=20 log ($K_5A^5/16$)

$$\left|\frac{1}{4}K_3A^3\right| >> \left|\frac{5}{16}K_5A^5\right| \tag{3-18}$$

As stated in the previous section, it is possible to define the intercept points shown in Figure 3-4 in one-tone test. In Figure 3-4, Line A represents the output amplitude at the fundamental frequency and has a slope of one in the log-log scale graph. This line is extrapolated from linear small-signal area in equation (3-14) from equation (3-17). Line B is the output amplitude at triple fundamental frequency and has a slope of three. This line is also extrapolated from equation (3-15) under the condition of equation (3-18). Line C with a slope of five is the output amplitude at frequency 5ω and is drawn from equation (3-16). The intercept points between three lines in this figure are denoted by IP_{15}, IP_{13} and IP_{35}. At the point IP_{13}, which is the interception point between Line A, and Line B, the input signal level A_{13} can be found from,

$$\left|K_1 A_{13}\right| = \left|\frac{1}{4} K_3 {A_{13}}^3\right| \tag{3-19}$$

where the value of Line A is the same as that of Line B at the input level A_{13}. From this equation (3-19), the input signal level can be represented by using two nonlinear coefficients K_1 and K_3 such as,

$$A_{13} = 2\left|\frac{K_1}{K_3}\right|^{\frac{1}{2}} \tag{3-20}$$

At the intercept point IP_{15} between Line A and Line C, the input signal level A_{15} is found by solving the following equation,

$$\left|K_1 A_{15}\right| = \left|\frac{1}{16} K_5 {A_{15}}^4\right| \tag{3-21}$$

$$A_{15} = 2\left|\frac{K_1}{K_5}\right|^{\frac{1}{4}} \tag{3-22}$$

The signal level A_{35}, which is the input value at the intercept point IP_{35}, can be described by,

$$\left|\frac{1}{4} K_3 {A_{35}}^3\right| = \left|\frac{1}{16} K_5 {A_{35}}^4\right| \tag{3-23}$$

$$A_{35} = 2\left|\frac{K_3}{K_5}\right|^{\frac{1}{2}} \tag{3-24}$$

The relationship between the input signal levels at the intercept points can be derived from the equation (3-20), (3-22) and (3-24),

$$A_{13} A_{35} = {A_{15}}^2 \tag{3-25}$$

The equation (3-25) can be expressed differently by using logarithm,

$$20\log(A_{13}) + 20\log(A_{35}) = 2 \times 20\log(A_{15}) \tag{3-26}$$

In addition, this relationship can be designated by,

$$IP_{13} + IP_{35} = 2 \times IP_{15} \tag{3-27}$$

where IP_{ij} is the input-referred power at the interception point IP_{ij}.

The 1 dB gain compression is considered in this approach. The input signal level A_{1dB} at this point can be represented by the equation

$$20\log\left|K_1 A_{1dB} + \frac{3}{4}K_3 {A_{1dB}}^3 + \frac{5}{8}K_5 {A_{1dB}}^5\right| = 20\log\left|K_1 A_{1dB}\right| - 1dB \tag{3-28}$$

From the above equation, one can see that fifth order nonlinear coefficient makes the gain compression change from equation (3-6) in the previous section. Generally, gain compression arises when K_3 has the opposite sign of K_1. From equation (3-28), the gain compression curve is affected by K_5. The simple equation is derived from equation (3-28).

$$\frac{5}{8}\left(\frac{K_5}{K_1}\right){A_{1dB}}^4 + \frac{3}{4}\left(\frac{K_3}{K_1}\right){A_{1dB}}^2 + 0.109 = 0 \tag{3-29}$$

Using intercept points as defined above, this equation is represented (K_1>0, K_3<0 and K_5<0) by,

$$10\left(\frac{A_{1dB}}{A_{15}}\right)^4 + 3\left(\frac{A_{1dB}}{A_{13}}\right)^2 - 0.109 = 0 \tag{3-30}$$

If K_5 is positive then,

$$10\left(\frac{A_{1dB}}{A_{15}}\right)^4 - 3\left(\frac{A_{1dB}}{A_{13}}\right)^2 - 0.109 = 0 \tag{3-31}$$

Therefore, if A_{13}, A_{15} and A_{35} nonlinear coefficients are known, it is possible to evaluate A_{1dB}.

Equation (3-8) takes the form of the input signal in a two-tone test. If this input is applied to the system described by equation (3-13), the output has a more complicated form than that in the one-tone test. The output at fundamental frequency is described by,

$$y(t;\omega_i)=\left(K_1A+\frac{9}{4}K_3A^3+\frac{25}{4}K_5A^5\right)\cos(\omega_i t) \tag{3-32}$$

where ω_i represents the fundamental frequency which is one of two frequencies ω_1 and ω_2. The amplitude of the output, $|y(t;\omega_i)|$ in equation (3-32) is different from that of the output $y(t;\omega)$ in the equation (3-14) of the one-tone test. This difference is called as the term desensitization [Wam98]. This term is originated from communication circuits in which a weak signal is affected by an adjacent strong unwanted signal through a nonlinear transfer characteristic. The output amplitude at the intermodulation frequency $(2\omega_1-\omega_2)$ is represented by the following equation,

$$y(t;2\omega_1-\omega_2)=\left(\frac{3}{4}K_3A^3+\frac{25}{8}K_5A^5\right)\cos((2\omega_1-\omega_2)t) \tag{3-33}$$

The third-order intercept point is defined in the small-signal area of a gain plot. The input signal level at the third-order intercept point is the same as that in the classical analysis. Equation (3-11) shows the input signal level at this intercept point.

In this analysis, it is possible to estimate IIP_3 and 1 dB gain compression points from the knowledge of the nonlinear coefficients since IIP_3 and 1 dB gain compression point are represented by functions of nonlinear coefficients. The gain compression curve in the result of a one-tone test is a function of the nonlinear coefficients represented by

equation (3-14). It is possible to extract the nonlinear coefficients from the gain compression curve by applying a fitting method that will be explained in the next section. If the nonlinear coefficients are extracted from the gain compression curve in a one-tone test, it is possible to estimate IIP_3 without the two-tone test. In the results of the two-tone test, the gain curve at each frequencies ω_1 and ω_2 is a function of the nonlinear coefficients described by equation (3-32). Even though the equation (3-32) includes the desensitization factor, this factor is also a function of the nonlinear coefficients. It is possible to extract the nonlinear coefficients from these gain curves by using a numerical fitting method. In addition, the IIP_3 measurement contains the nonlinear coefficients effects. It is possible to predict 1 dB gain compression points and estimate the gain curve without the one-tone test by using the nonlinear coefficients extracted from two-tone test results.

3.4 Fitting Polynomials Data by Using Linear Regression Theory

If a model has n sets of observations and is fitted with a series of linear parameters $b_0, b_1, b_2, \ldots, b_m$, by the method of least squares, the model is represented by the following matrix form [Dra95],

$$\overline{Y} = \overline{X} \bullet \overline{b} + \overline{E} \tag{3-34}$$

where $\overline{Y}, \overline{X}, \overline{b}$ and $\overline{E}$ are $n \times 1, n \times m, m \times 1$ and $n \times 1$ matrices respectively. In this equation (3-34), $\overline{Y}$ is a measured result, $\overline{X}$ is an input data, $\overline{b}$ is a set of linear parameters and $\overline{E}$ represents the error between a fitting model and a real model.

The above linear regression model has three basic assumptions. First, the average of the errors in the observations is zero and the variance of these errors is σ^2. Second, E_i and E_j are uncorrelated if i is different from j. Third, the error follows the normal

random variable distribution. These three basic assumptions are included intrinsically or extrinsically in the statistical approach of linear regression analysis.

The sum of squares of deviations or errors is,

$$SS(E_i) = \overline{E}^T \bullet \overline{E} = \left(\overline{Y} - \overline{X} \bullet \overline{b}\right)^T \bullet \left(\overline{Y} - \overline{X} \bullet \overline{b}\right) \tag{3-35}$$

To find the sum of square of errors the least quantity, $\overline{b}$ can be found as follows,

$$\overline{b} = \left(\overline{X}^T \bullet \overline{X}\right)^{-1} \bullet \left(\overline{X}^T \bullet \overline{Y}\right) \tag{3-36}$$

After finding $\overline{b}$ using above equation (3-36), the variance of $\overline{b}$ is,

$$V\left(\overline{b}\right) = \left(\overline{X}^T \bullet \overline{X}\right)^{-1} \bullet \sigma^2 \tag{3-37}$$

where the diagonal terms of the above variance represent the variance of the parameter b_i and the off-diagonal terms stand for the covariance of the pair b_i and b_j. The variance of errors, σ^2, is calculated through the analysis of the residual. The residual is defined as the difference between a fitting model and a real model. The sum of square of the residuals is represented by the equation (3-35). The mean square of the residual is defined as the sum of square of the residuals divided by the degree of freedom of the residual. If the number of the observations is n and the degree of freedom of the regression parameter is m, the degree of freedom of the residual is n-m. The mean square of the residual is used as the estimate of the variance of errors, σ^2. The mean square of the residual is,

$$MS_E = \sigma^2 = \left(\overline{Y} - \overline{X} \bullet \overline{b}\right)^T \bullet \left(\overline{Y} - \overline{X} \bullet \overline{b}\right) \div \frac{1}{n-m} = \frac{\left(\overline{Y}^T \overline{Y} - \overline{b}^T \overline{X}^T \overline{Y}\right)}{n-m} \tag{3-38}$$

In this research, the fitting model for the gain curve is the odd-order polynomial equation,

$$\overline{\overline{y}}_i = K_1 \bullet x_i + K_3 \bullet x_i^{\,3} + K_5 \bullet x_i^{\,5} \tag{3-39}$$

where $\overline{\overline{y}}_i$ is the estimate value of the fitting model. The residual is,

$$E_i = y_i - \overline{\overline{y}}_i \tag{3-40}$$

The matrices in the equation (3-34) can be formed as follows,

$$\overline{Y} = \begin{bmatrix} y_1 \\ y_2 \\ \cdots \end{bmatrix} \tag{3-41}$$

$$\overline{\overline{X}} = \begin{bmatrix} x_1 & x_1^{\,3} & x_1^{\,5} \\ x_2 & x_2^{\,3} & x_2^{\,5} \\ \cdots & \cdots & \cdots \end{bmatrix} \tag{3-42}$$

$$\overline{b} = \begin{bmatrix} K_1 \\ K_3 \\ K_5 \end{bmatrix} \tag{3-43}$$

$$\overline{E} = \begin{bmatrix} E_1 \\ E_2 \\ \cdots \end{bmatrix} \tag{3-44}$$

The degree of freedom of the parameter $\overline{b}$ is three. If the number of the data points is n, the degree of freedom of the residual is n-3. Using the degree of freedom of the residual, the variance of the errors can be calculated in equation (3-37). The standard error of the parameters is defined as the square root of the variance of the parameter. The standard errors of the parameters or nonlinear coefficients can be calculated using the equation (3-37). The sum of square of the residual also can be calculated using equation (3-35). These two analyses, the standard errors of the nonlinear coefficients and the sum of square of the residual are used in determining the fitting range in this research.

3.5 Summary

In this chapter, the new relationship between the 1 dB gain compression point and the third-order intercept point has been derived. First, this relationship between IIP_3 and $IP_{1\text{-}dB}$ was reviewed in classical analysis. The difference between two nonlinear characteristics was 9.6 dB and constant. The classical analysis included only third-order nonlinear coefficients. The new relationship was derived by expanding nonlinear analysis on the gain compression curve up to the fifth-order nonlinear coefficients. The difference between $IP_{1\text{-}dB}$ and IIP_3 is not fixed and is explained by the equation including nonlinear coefficients. The fitting algorithm to estimate IIP_3 from one-tone measurement and the calculation method to predict $IP_{1\text{-}dB}$ from two-tone measurement are devised. The linear regression theory required for the fitting algorithm has been reviewed and modified for the application of the algorithm.

CHAPTER 4
SIMULATION

4.1 A MOSFET Common-Source Amplifier

The modeling approach developed in a previous chapter is applied to the simulation of a weakly nonlinear system. A common source amplifier is considered as a weakly nonlinear system. There are two methods that can estimate 1 dB gain compression point and IIP_3 from one-tone test. The first method uses the ratio of nonlinear coefficients. These ratios are found from the harmonic power intercept points, which are explained in Chapter 3. For determining gain compression, measurement of the overall device or amplifier power is needed but for IIP_3 estimation, the measurement of the third and fifth harmonic frequency magnitudes is required. The second method to estimate IIP_3 is fitting the gain curve at the fundamental frequency for the extraction of the nonlinear coefficients. The gain curve is fitted via a Matlab program developed in this research. The second IIP_3 determination technique is more useful than the first since the second technique does not need the third and fifth harmonic frequency amplitude coefficients to the measured.

To demonstrate the fitting technique, a common-source amplifier with TSMC 0.25 μm n-MOSFET is considered. Figure 4-1 shows the schematic for a common-source amplifier. In this amplifier design, supply voltage V_{DD} is 3.3 V and the load resistor R_D is 10 KΩ. The size of the transistor M1 is a minimum size (W/L=1.18 μm/0.25 μm) and BSIM3 model of this transistor is listed in the Appendix A. The gate bias voltage is set to produce the weakly nonlinear behavior in the amplifier. This bias point was found by an

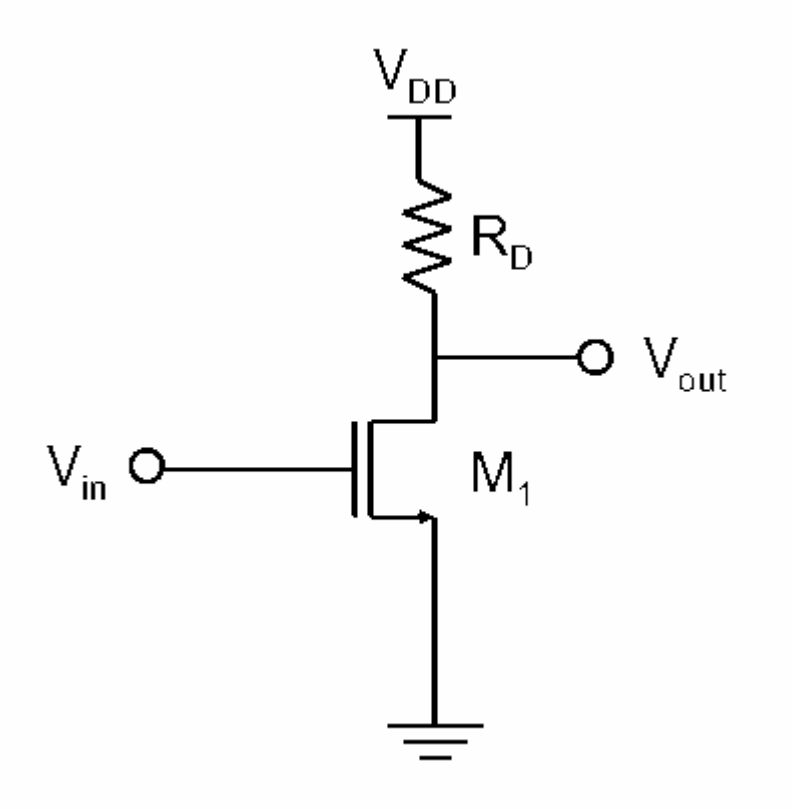

Figure 4-1 A schematic of a common-source amplifier

analysis of the DC characteristic of this amplifier using the Agilent ADS2002 software. The I-V characteristic curve and transfer characteristic curve are shown in Figure 4-2. For a weakly nonlinear simulation, a gate bias is chosen near the center point that is shown as point P in both Figure 4-2.A and Figure 4-2.B. At the gate bias, 1.1 V, an AC simulation was performed. Figure 4-3 shows the result of AC simulation. When the frequency increases above 1 GHz, the voltage gain decreases significantly. This indicates that the parasitic capacitance of the n-MOSFET needs to be considered in the gain calculation and cannot be ignored above 1 GHz. As a result, the fitting algorithm in the frequency-domain has some errors related to the transistor parasitic capacitances (gate and drain) since the power series does not include the phase information caused by these parasitic capacitors.

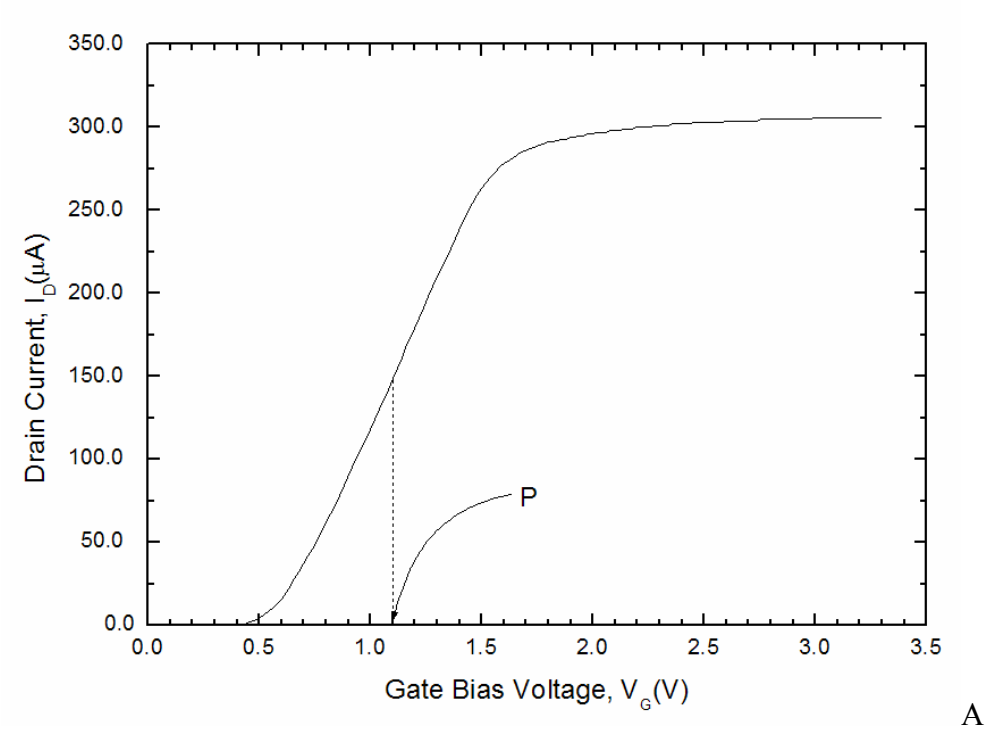

A

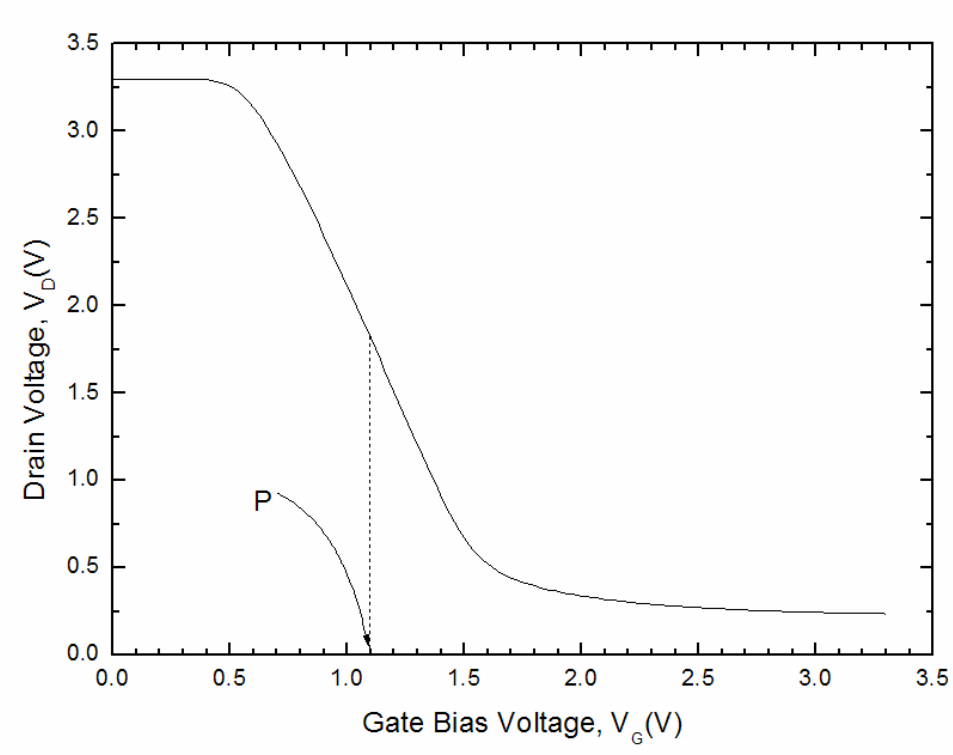

B

Figure 4-2 DC characteristic of a common-source amplifier. A) shows the drain current and B) shows the drain voltage.

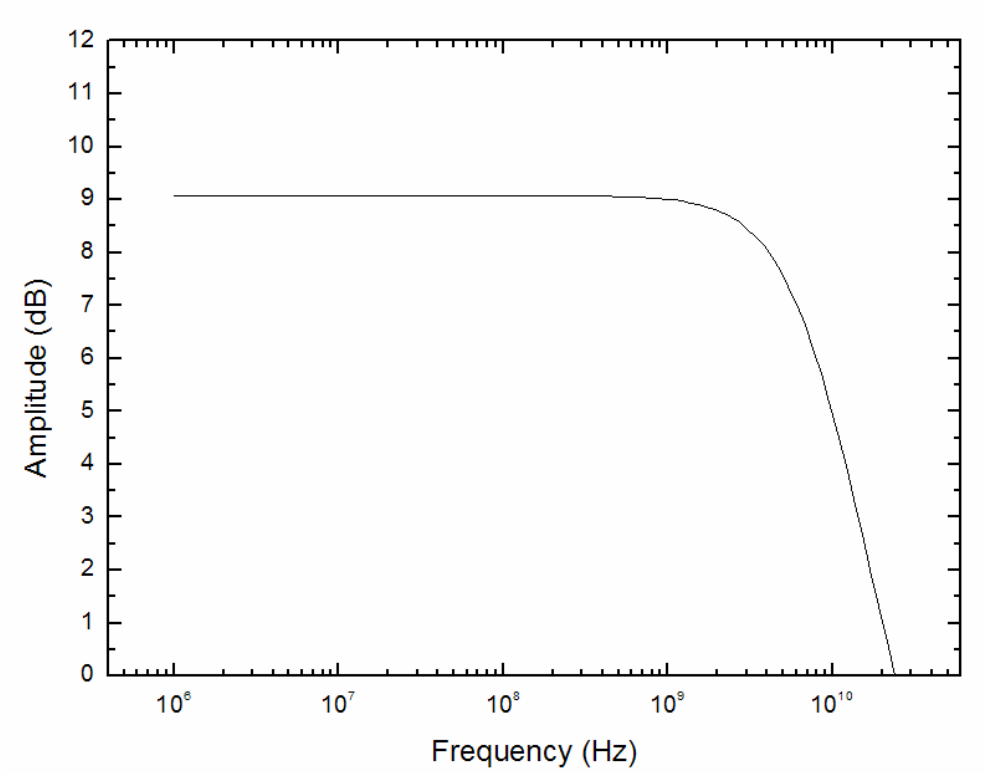

Figure 4-3 The AC simulation of a common-source amplifier

At the same gate bias as the AC simulation, a one-tone test and a two-tone test were simulated using the harmonic-balance simulator in the ADS2002 software. Figure 4-4 and Figure 4-5 show the simulation results of one-tone and two-tone voltage gain transfer function described in Chapter 2. Voltage gain curves are made by observing the amplifier output amplitude or power while sweeping the input voltage or power at a fixed frequency. In Figure 4-4, the amplitude of the input voltage is swept from 0.01 V to 2 V at the fundamental frequency of 100 MHz. Curve A is the voltage gain curve which is the output amplitude measured at the drain node of M1 in Figure 4-1 of the common-source amplifier. Line B represents the ideal gain curve under the assumption that there are no harmonics at any amplifier power level. GC denotes the 1 dB compression point that shows an 1 dB difference between Curve A and Line B. At the voltage amplitude gain

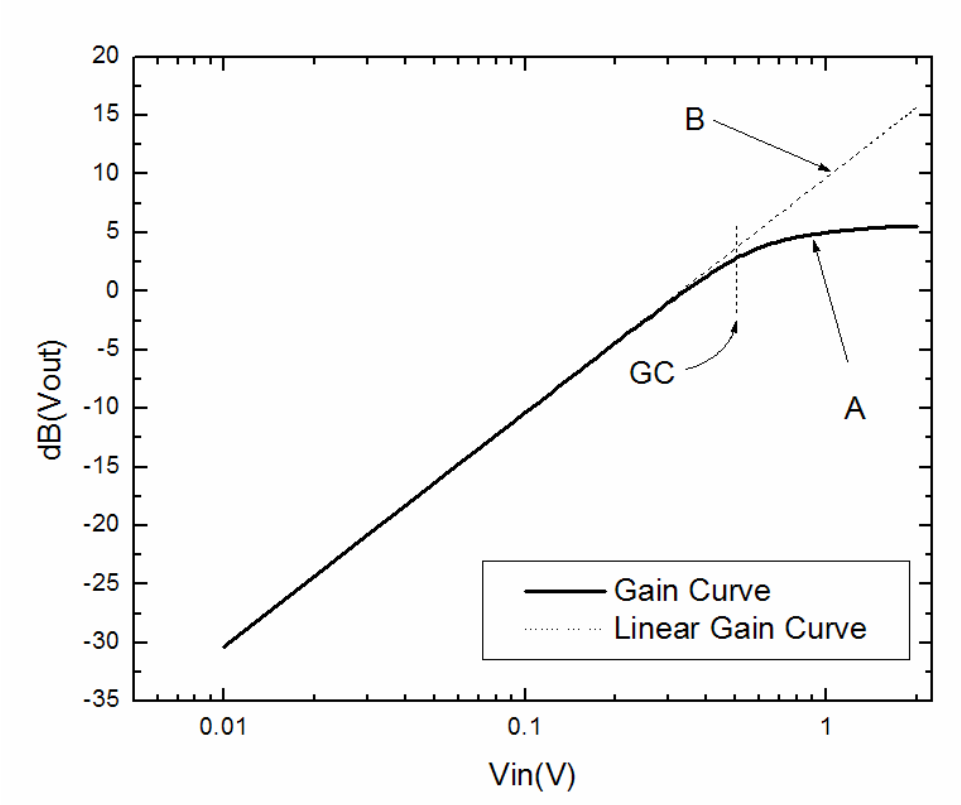

Figure 4-4 The results of one-tone simulation

compression of 1 dB, the input voltage is 0.52 V in Figure 4-4. The applied frequencies in the two-tone test are 100 MHz and 110 MHz. In Figure 4-5, Curve A and B represent the amplifier output signal amplitudes at 100 MHz and at 90 MHz separately. Curve A is the fundamental frequency of 100 MHz, Curve B indicates the amplitude at intermodulation frequency of 90 MHz (2×100 MHz – 110 MHz). Line C and D indicate the ideal harmonic response of the amplifier if no other harmonics are present. A real amplifier introduces an increasing number of harmonic components as gain compression is increased. The point of intersection of the two ideal harmonic lines, denoted by point TOI, indicates the intermodulation intercept point that has a value of 2.05V. This intermodulation intercept point has the same definition as that of the third-order-intercept point in a 50 Ω system such as an RF system. In two-tone test, the amplitudes at two

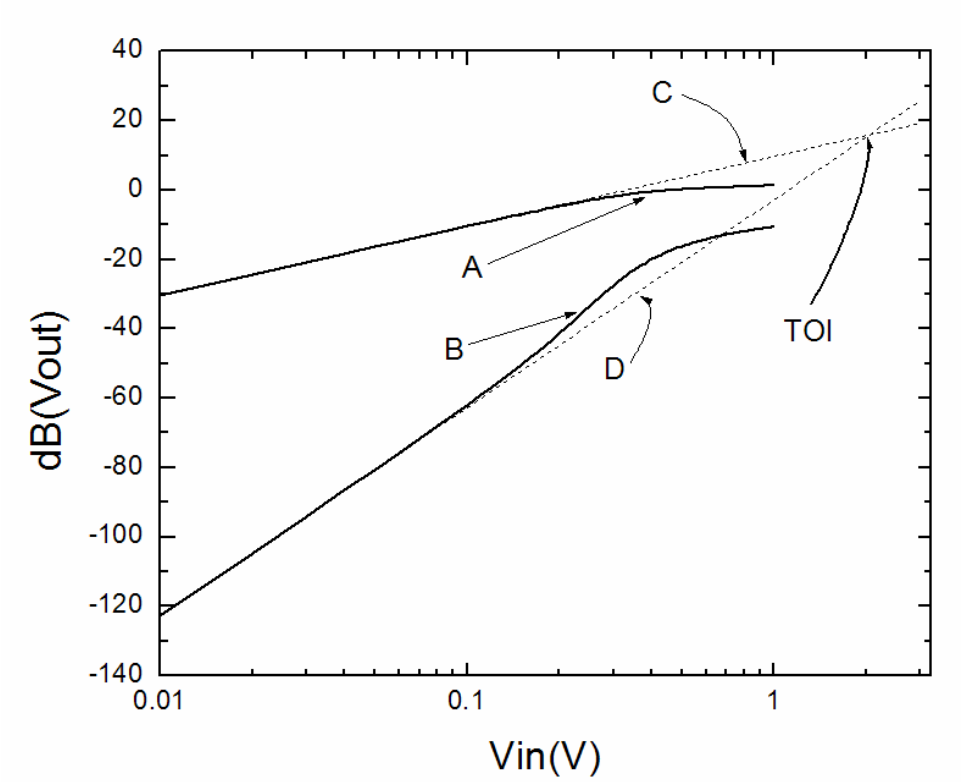

Figure 4-5 The results of a two-tone simulation

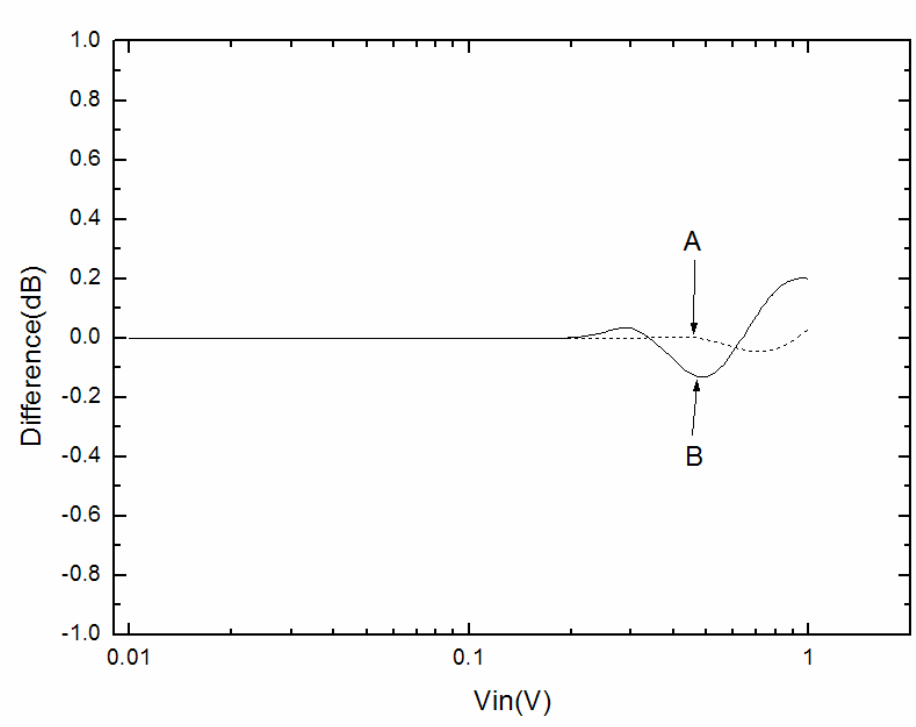

Figure 4-6 The difference between amplitudes at two frequencies. A: Input frequency (100 MHz, 110 MHz) B: Intermodulation frequency (90 MHz, 120 MHz)

frequencies and two intermodulation frequencies should be considered. These amplitudes are compared in Figure 4-6. In this figure, Curve A shows the difference between the amplitudes at two fundamental frequencies (100 MHz and 110 MHz). Curve B is the difference between the amplitudes at two intermodulation frequencies (90 MHz and 120 MHz). Up to 0.2 V, the difference of amplitudes at two intermodulation frequencies is under 0.001 dB. In the case of two fundamental frequencies, the difference is under 0.001 dB up to 0.34 V. Since the third-order intercept point is defined in the small-signal area explained in Chapter 3, the third-order intercept point between two curves at 110 MHz and 120 MHz is the same as that between 2 curves at 100 MHz and 90 MHz. In view of the CMOS amplifier simulations, the difference between 1 dB gain compression point and third order intercept point is 12 dB. This outcome differs with 10 dB that is shown in the classical nonlinear calculations for amplifiers [Raz98].

Nonlinear coefficients can be derived from the least-square polynomial fitting of the gain compression curve A of Figure 4-4. The polynomial model used in this fitting is as the power series that follows,

$$y = K_1 \bullet x + \frac{3}{4} K_3 \bullet x^3 + \frac{5}{8} K_5 \bullet x^5 \qquad (4\text{-}1)$$

where K_i is a nonlinear coefficient representing the output signal amplitude at harmonic i. According to linear regression theory, the standard error can be analyzed on the individual coefficient, K_i, fitting outcomes. In addition, the difference between the fitting model and the actual gain curve produces a fitting residual, a curve fitting error. Therefore, the best fitting range can be selected by analyzing the fitting error and standard error of each fitting coefficient. When the input amplitude decreases, the output amplitude includes more information of lower-order harmonics in the polynomials.

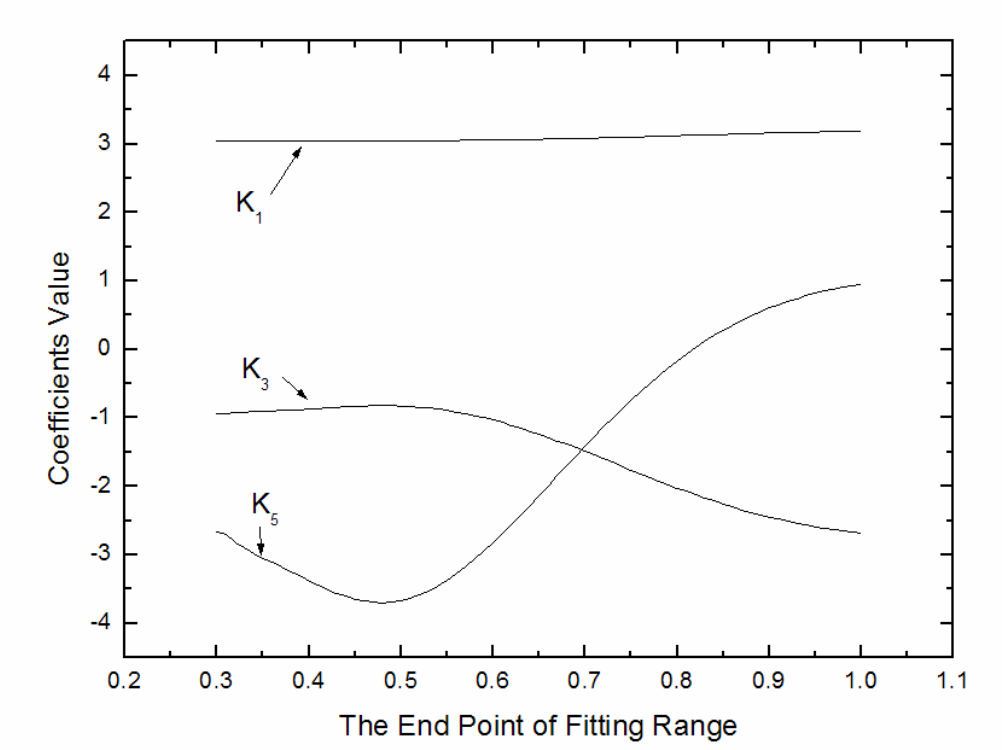

Figure 4-7 Extracted nonlinear coefficients

Selecting a range with a small input voltage should be the first consideration during the fitting process. The fitting algorithm extracts the nonlinear coefficients from the lowest-order harmonic to 5th-order harmonic or the highest-order harmonic. A small area is chosen in the small input signal region of the gain curve data as the first fitting range. In this fitting range, each of the nonlinear coefficients, the standard error of each nonlinear coefficients and residuals are extracted in the fitting process by using the polynomial model, equation (4-1). After finding the information in this range, the fitting process continues in a wider range than the first fitting range. The respective coefficients and the change of the fitting range are shown in Figure 4-7. The first fitting range in the gain compression curve is from 0.01 V to 0.3 V in a small input amplitude area. In Figure 4-7, K_1 at the point that x-axis is 0.3 V represents the value of the first-order nonlinear coefficient extracted from this first fitting region. In addition, K_3 and K_5 indicate the

third-order and the fifth-order nonlinear coefficients correspondingly. A horizontal axis defines the width of the fitting range in Figure 4-7 since the starting point of the fitting range is fixed at 0.01 V to include the small input amplitudes. The x-axis represents the end point of the fitting range in volts. This graph shows us that individual coefficients K_1, K_3 and K_5 vary based on the widths of the fitting range. It is important to define the best fitting range to choose the extracted nonlinear coefficients as shown in Figure 4-7 since the nonlinear coefficients vary with the width of the data fitting range.

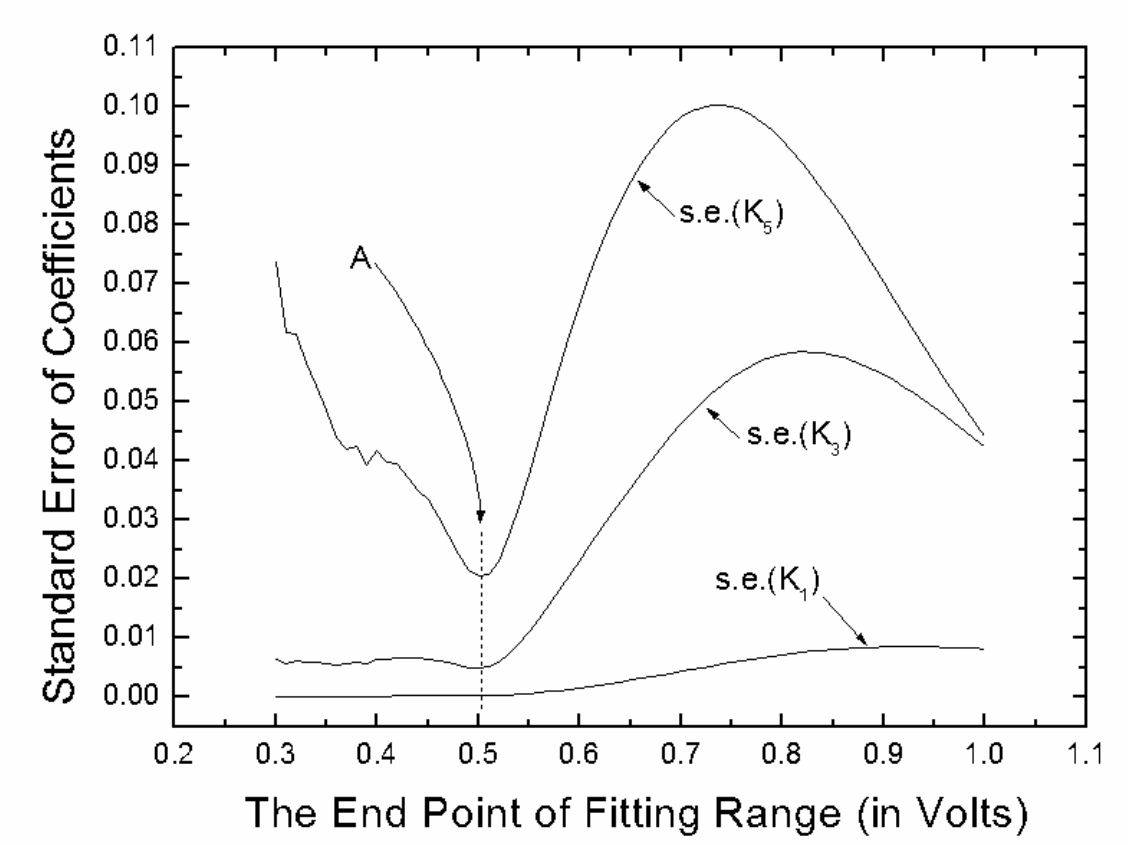

Figure 4-8 Standard errors of nonlinear coefficients

The standard errors of the separate coefficients in their fitting ranges are calculated by using the following equations that were presented in chapter 3.

$$s.e.(K_i) = \sqrt{V(\bar{b})_{ii}} \tag{4-2}$$

where $s.e.(K_i)$ is the standard error of the K_i coefficient and $V(\bar{b})_{ii}$ is the diagonal term of the variance of the parameters or nonlinear coefficients which are calculated by equation (3-28). Figure 4-8 shows the standard error of nonlinear coefficients according to the width of the fitting range. In this graph, $s.e.(K_i)$ points to the standard error of the nonlinear coefficient K_i. The lowest values for the standard errors of K_1, K_3 and K_5 are shown by Point A in Figure 4-8. This point is about 0.5 V that is near 1 dB gain compression point, 0.52 V. The sum of square of the residual, $SS(E_i)$ between the fitting model and the actual gain curve can be found using equation (4-3),

$$SS(E_i) = \overline{E}^T \bullet \overline{E} = \overline{Y}^T \overline{Y} - \bar{b}^T \overline{X}^T \overline{Y} \qquad (4\text{-}3)$$

where the calculation is the same as equation (3-26). This quantity shows the total error

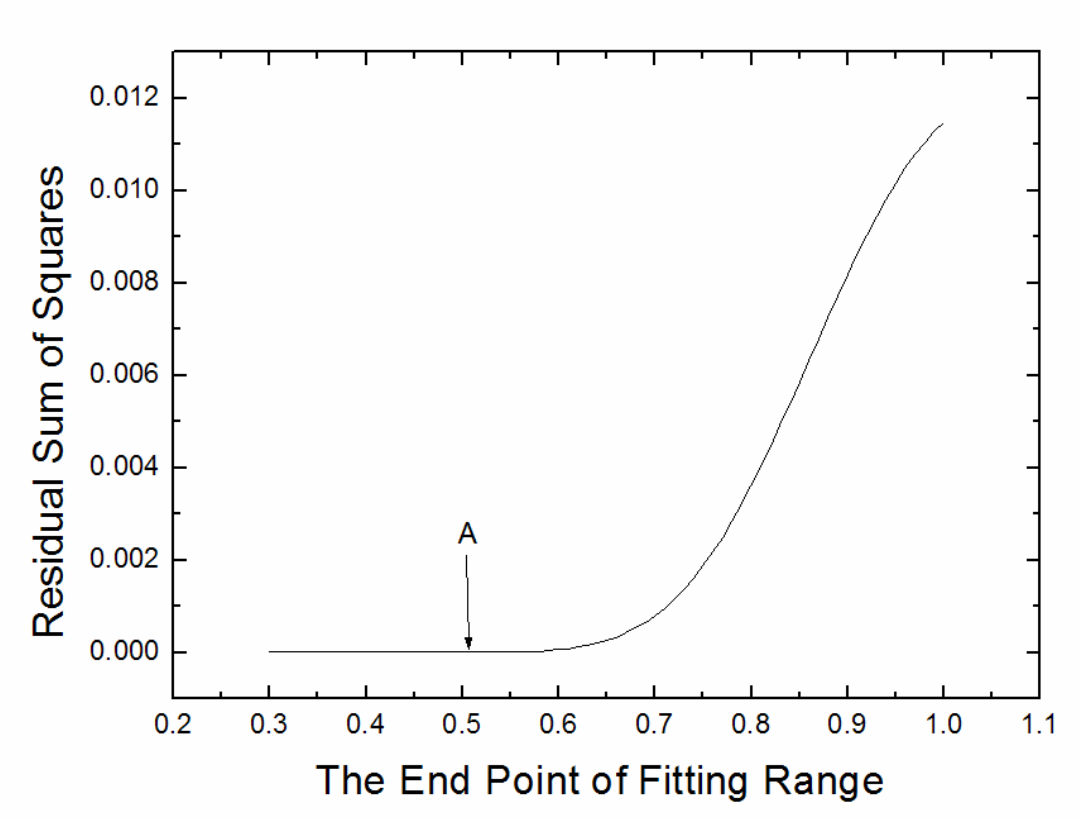

Figure 4-9 The sum of squares of the residual

caused by the difference between the fitting model and the actual model. Figure 4-9 shows the sum of square of the residual, $SS(E_i)$. In this graph, the total error quantity is significantly lower under the 0.6 V fitting range. Point A represents the lowest value found in Figure 4-8. From this graph, it is shown that the width of the fitting range from 0.01 V to point A of Figure 4-8 has small $SS(E_i)$. Therefore, the fitting range that has the minimum standard error and the small total residuals can be defined through Figure 4-8 and Figure 4-9. The fitting outcome for this set of prospective ranges is summarized in Table 4-1. At the third-order-intercept point IIP_3, the input voltage is 2.21 V or 6.9 dB input voltage with the resulting harmonic coefficients. This measured input value shows about 0.7 dB difference in comparison with the simulated value of 6.24 dB. This error may be created by the phase information that is missing from the fitting model and is caused by errors in the calculation of the power measurements with no phase information. In general, Volterra series are used to model the case of weakly nonlinear behavior. However, the one tone measurement is not sufficient to implement both phase-information detection and phase analysis that are required for Volterra-series parameters. In spite of these errors, 1 dB or less difference for the third-order-intercept point simulation and measurement is a good result.

Table 4-1 The summary of fitting results

Parameters	Values
Coefficient K_1	3.05
Coefficient K_3	-0.83
Coefficient K_5	-3.67
Calculated V(IIP_3)	2.21V(6.9 dB)
Simulated V(IIP_3)	2.05V(6.24 dB)

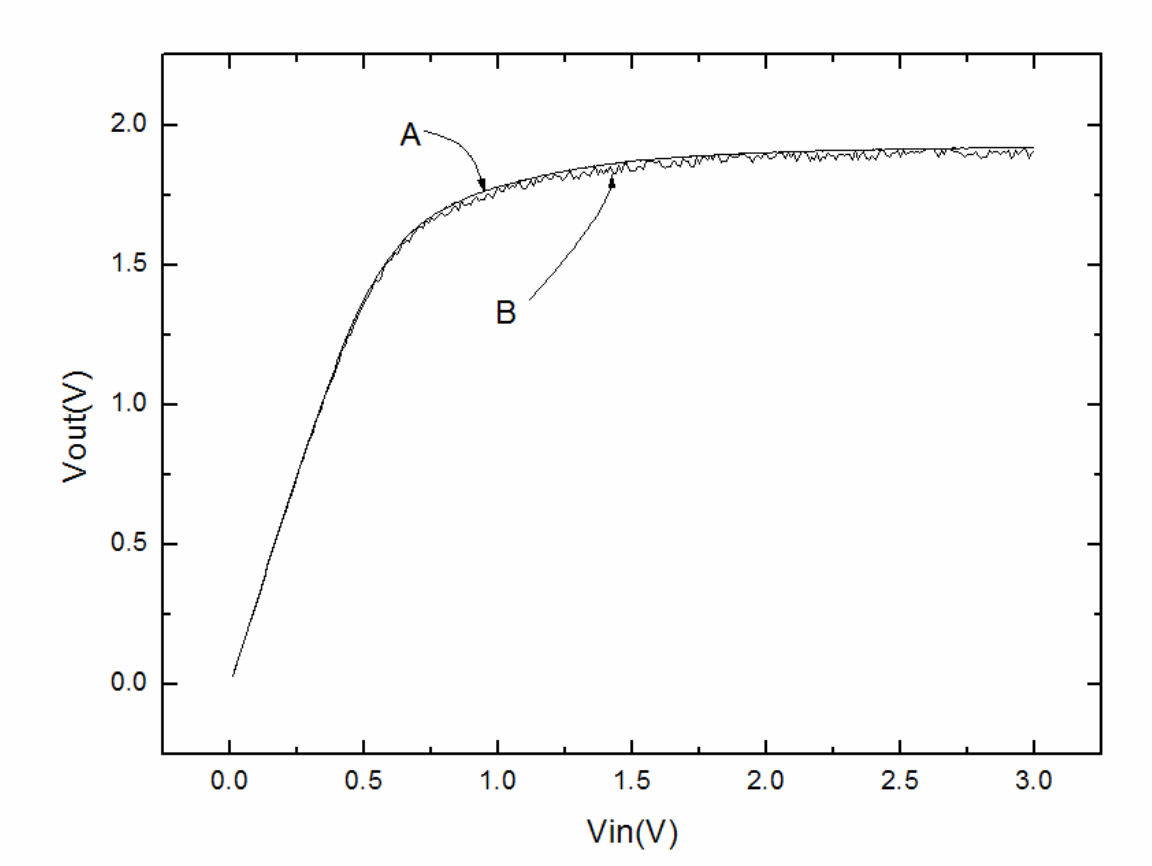

Figure 4-10 Gain curves with 0.1% and 2% random noise

4.2 Measurement Error Consideration

Measurement error needs to be considered in the actual data measurement with the algorithm presented in Section 4.1. The effect of additional random noise upon the simulated data is analyzed in this section for the determination of the measurement error. In addition, the error boundaries are studied in order to produce satisfactory results with the proposed algorithm.

To analyze the effect of random noise, random noise is created by using random number generation in Matlab software and is added to the each one-tone data point used in the previous section.

$$z_i = y_i + y_i \times (P\%) \times n_i \tag{4-4}$$

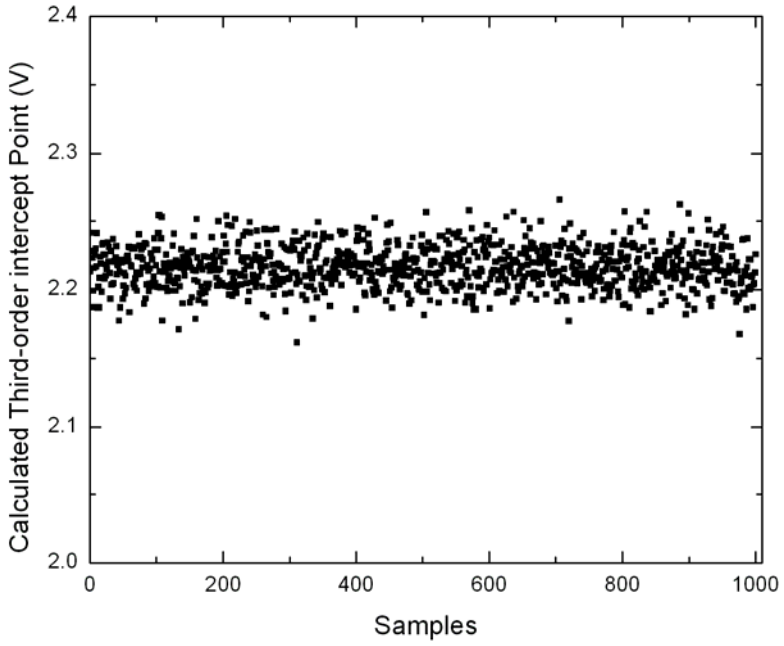

Figure 4-11 Calculated third-order intercept point with 0.1 percent added random noise

where y_i is the voltage output amplitude of the individual data point, n_i is the real number that is chosen randomly from -1 to 1, P is the percentage of added random noise, and z_i is a new data point that includes the output amplitude and random noise. Figure 4-10 shows two gain curves with 0.1 % and 2 % additional random noise. Curve A is the gain curve with 0.1 % additional random noise and Curve B represents the gain curve including 2% additional random noise. In this section, the fitting range from 0.01V to 0.52 V that was defined in Section 4.1 is used for fitting the gain curve data including random noise. The gain curve data with 0.1 % added random noise is fitted in the fixed fitting range. The same procedure is repeated one thousand times averaging in the gain data with different 0.1 % random noise. The calculated third-order intercept points over one thousand samples are shown in Figure 4-11. The average value over one thousand

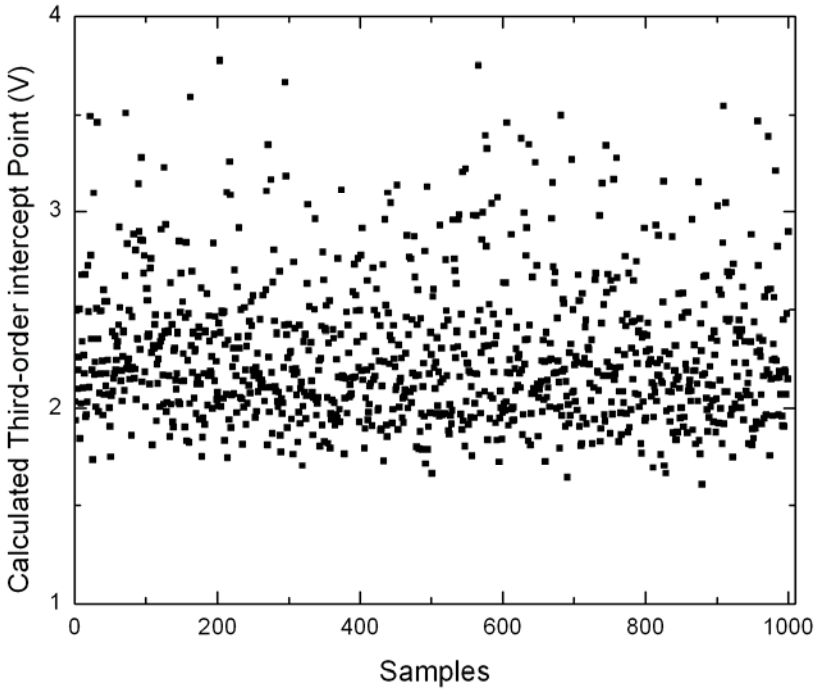

Figure 4-12 Calculated third-order intercept point with 2.0 percent added random noise

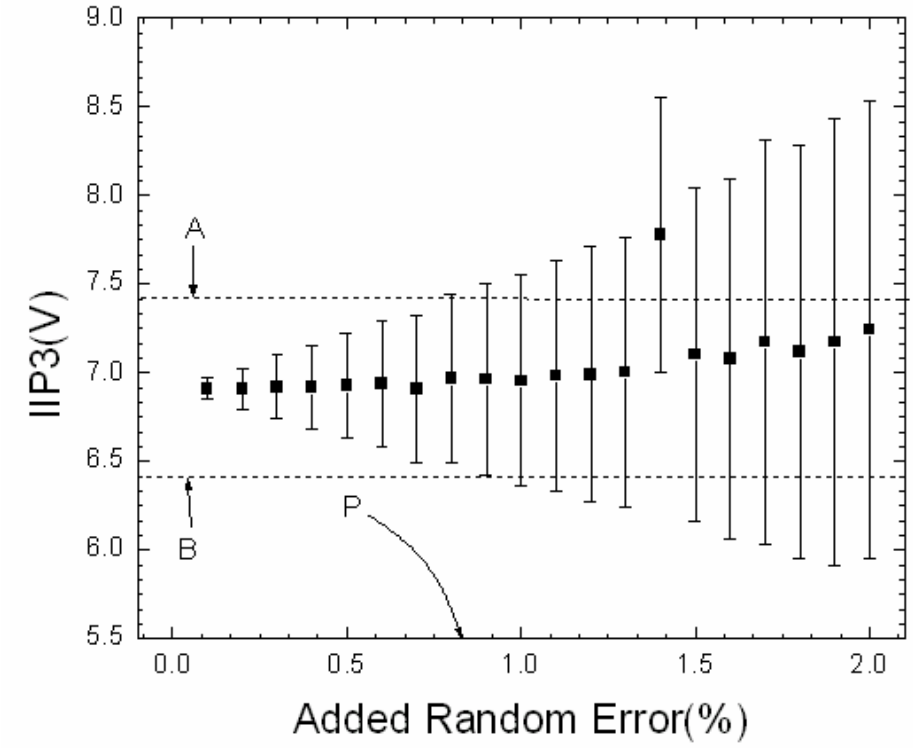

Figure 4-13 The influence of added random error on the fitting results

samples is 2.216 V and the standard deviation of these samples is 0.0149 V. Figure 4-12 shows the calculated third-order intercept point with 2 percent added random noise over one thousand samples. In this graph, the distribution of third-order intercept point calculated from the gain data added 2% random noise is wider than that added 0.1 % random data. The average value of these samples is 2.3023 V and the standard deviation is 0.3692 V. Fitting results on the each additional random error amount and the associated standard deviation are shown in the Figure 4-13. In this graph, added random error increases by 0.1% increments from 0.1% to 2.0%. As the additional amount of random error increases, standard deviation grows. Two dotted lines A and B show 0.5 dB as an acceptable range of third-order intercept point error for the center value of 6.9 dB. Each bar represents the standard deviation for one thousand samples. If the fitting results from random errors are limited within ± 0.5 dB, the additional random error amounts are within 0.8%. In other words, if measurement error is in 0.8% of the correct measurement value, the applied result through the fitting algorithm makes an IIP_3 estimation with ±0.5 dB accuracy possible. However, if more than 1% random errors are added to this data, it becomes difficult to predict the IIP_3 from a single measurement of the gain curve and produce an accurate value. Data averaging with multiple data point measurements to reduce average error must be used.

4.3 Frequency Effect on the Fitting Algorithm

What kind nonlinearity effects can higher frequencies produce? Frequency becomes higher for recent wireless circuits. In addition, the high frequency region of operation needs to be measured to analyze the nonlinearity of RF components. The extraction algorithm is applied to frequencies up to 30 GHz in the circuits used in the previous sections. The results are shown in the Table 4-2. According to Table 4-2, the

difference between the extracted third-order intercept point and simulated value grows when the frequency increases from 100 MHz to 5 GHz. There is an evident difference between the simulation and the power series model used for the fitting algorithm. In order to analyze that difference, the gain compression curve is represented by Volterra-series components. Appendix B shows Volterra-kernels of a common-source amplifier. When the input is

$$V_{in} = V\cos(\omega_1 t) \tag{4-5}$$

the output amplitude at the fundamental frequency is as follows,

$$\begin{aligned} V_{out}(t;\omega_1) = \mathrm{Re}\{&V\mathrm{H}_1(\omega_1)\exp(j\omega_1 t) + \frac{3}{4}V^3\mathrm{H}_3(\omega_1,\omega_1,-\omega_1)\exp(j\omega_1 t) \\ &+ \frac{5}{8}V^5\mathrm{H}_5(\omega_1,\omega_1,\omega_1,-\omega_1,-\omega_1)\exp(j\omega_1 t) + ...\} \end{aligned} \tag{4-6}$$

Table 4-2 Frequency effect on the fitting algorithm

Frequency	$V_{1\text{-dB}}$(dB)	$VIIP_3$(dB)	Estimated $VIIP_3$(dB)	Difference (dB)
100 MHz	0.52 V (-5.68 dB)	2.05 V (6.24 dB)	2.21 V (6.89 dB)	0.65 dB
900 MHz	0.52 V (-5.68 dB)	2.05 V (6.24 dB)	2.23 V (6.97 dB)	0.73 dB
2 GHz	0.53 V (-5.68 dB)	2.06 V (6.28 dB)	2.29 V (7.20 dB)	0.92 dB
5 GHz	0.57 V (-5.51 dB)	2.07 V (6.32 dB)	2.43 V (7.71 dB)	1.39 dB
10 GHz	0.61 V (-4.88 dB)	2.04 V (6.19 dB)	2.21 V (7.00 dB)	0.70 dB
20 GHz	0.64 V (-4.29 dB)	2.05 V (6.24 dB)	2.24 V (6.24 dB)	0.77 dB
30 GHz	0.67 V (-3.88 dB)	2.12 V (6.53 dB)	2.41 V (7.64 dB)	1.11 dB

At low frequency, the parasitic capacitance between gate and drain, Cgd, can be ignored. Using the calculated Volterra-series kernel in Appendix B, the output amplitude is,

$$V_{out}(t;\omega_1) = \mathrm{Re}\{-\frac{K_1 V}{G_L + j\omega_1 C_L}\exp(j\omega_1 t) - \frac{3}{4}\frac{K_3 V^3}{G_L + j\omega_1 C_L}\exp(j\omega_1 t) - \frac{5}{8}\frac{K_5 V^5}{G_L + j\omega_1 C_L}\exp(j\omega_1 t) + ...\} \quad (4\text{-}7)$$

From equation (4-7), each coefficient has same phase if C_{gd} is disregarded and C_{db} is a linear parasitic capacitor. At low frequency, Volterra-series coefficients are similar to Power-series coefficients. The output amplitude at the fundamental frequency is in equation (4-8).

$$V_{out}(\omega_1) = K_1' \bullet V + \frac{3}{4}K_3' \bullet V^3 + \frac{5}{8}K_5' \bullet V^5 \quad (4\text{-}8)$$

where $K_i' = -K_i \bullet \left(G_L{}^2 + \omega_1{}^2 C_L{}^2\right)^{-1/2}$.

At high frequency, C_{gd} should be regarded in the calculation of Volterra-kernels. If C_{gd} is included in Volterra-kernels, the output amplitude is

$$V_{out}(t;\omega_1) = \mathrm{Re}\{-\frac{(K_1 - j\omega_1 C_{gd})V}{G_L + j\omega_1 C_L}\exp(j\omega_1 t) - \frac{3}{4}\frac{K_3 V^3}{G_L + j\omega_1 C_L}\exp(j\omega_1 t) - \frac{5}{8}\frac{K_5 V^5}{G_L + j\omega_1 C_L}\exp(j\omega_1 t) + ...\} \quad (4\text{-}9)$$

Apart from disregarded C_{gd} in the previous analysis, each coefficient has different phase. Due to the phase discrepancy, each coefficient needs to be described by a complex number. Therefore, another effect on the frequency exists when the result of one-tone test is modeled as a Volterra series. According to Table 4-2, the estimated deviation value by 5 GHz increases up to 1.4 dB. After that, the deviation does not increase with frequency.

Frequency has a greater effect on phase than amplitude at more than 5 GHz. In addition, the gain of the amplifier reduces drastically . Though the deviation of the estimate grows the increased frequency, the deviation is limited by within 1.5 dB at any frequency.

4.4 Load Effect on the Fitting Algorithm

The nonlinear characteristics of an amplifier is affected by the load of the amplifier. In this section, the effect of loads on the nonlinear characteristic is studied and the effect on the fitting algorithm is researched. Two types of loads are considered for affecting the nonlinear characteristics. A passive load is composed of passive components such as resistors, capacitors and inductors. An active load is a current mirror that is made by an active device such as transistor. First, the passive load effects on a single transistor amplifier are studied. The equivalent circuit of a general single transistor amplifier is shown in Figure 4-14. In this figure, Z_L represents the passive load, Z_{in} is an input impedance, V_1 and V_2 are an input node and an output node respectively, i represents the input-voltage-controlled-current source. The passive components used in the passive load

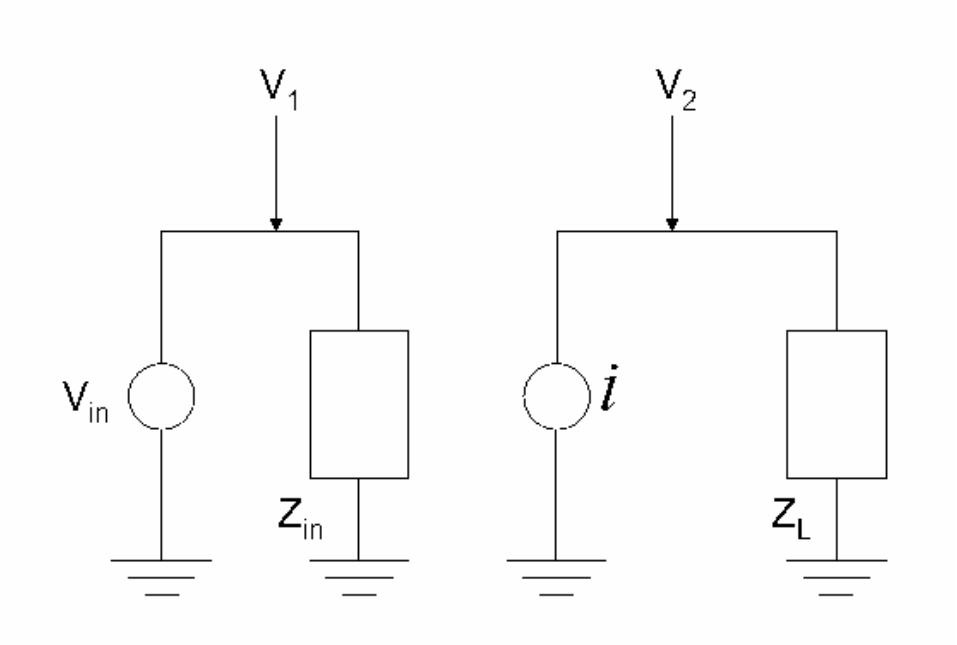

Figure 4-14 An equivalent circuit

are assumed to be linear components to simplify calculation. Under a given bias condition, the voltage-controlled-current source can be described by Taylor series at the quiescent point in equation (2-6) in chapter 2.

$$i = K_1 \mathrm{v} + K_2 \mathrm{v}^2 + K_3 \mathrm{v}^3 + \ldots \tag{4-10}$$

The passive load is a function of s in the s-domain,

$$Z_L = Z_L(s) \tag{4-11}$$

Volterra-kernel at the output node in the equivalent circuit can be described by

$$\mathrm{H}_i(s_1, s_2, \ldots, s_i) = -K_i Z_L\left(\sum_{n=1}^{i} s_n\right) \tag{4-12}$$

The nonlinear characteristic of an amplifier is determined by the above Volterra-kernels. The output amplitude at a fundamental frequency in one-tone test of this circuit is found by combining Volterra-kernels. If the input is

$$V_{in} = V\cos(\omega_1 t) \tag{4-13}$$

then the output at fundamental frequency ω_1 is

$$\begin{aligned} V_{out}(t;\omega_1) = \mathrm{Re}\{ & V\mathrm{H}_1(\omega_1)\exp(j\omega_1 t) + \frac{3}{4}V^3\mathrm{H}_3(\omega_1,\omega_1,-\omega_1)\exp(j\omega_1 t) \\ & + \frac{5}{8}V^5\mathrm{H}_5(\omega_1,\omega_1,\omega_1,-\omega_1,-\omega_1)\exp(j\omega_1 t) + \ldots\} \end{aligned} \tag{4-14}$$

The load impedance used in odd-order Volterra-kernels is

$$\sum_{n=1}^{i} s_i = s_1 = j\omega_1 \tag{4-15}$$

$$Z_L\left(\sum_{n=1}^{i} s_n\right) = Z_L(j\omega_1) \tag{4-16}$$

Therefore, the odd-order Volterra-kernel at the fundamental frequency is

$$\mathrm{H}_i = -K_i Z_L(j\omega_1) \tag{4-17}$$

The passive load is used to the change of each odd-order Volterra-kernel. This change includes frequency effects. In the model used in this analysis, the change of Volterra-kernel yields only frequency effects in the passive load. The fitting algorithm is not affect by the passive load except for the change caused by the operating frequency. The effect of the operating frequency on the amplifier was researched in the previous section.

The effect of the active load on the nonlinear characteristic of a single transistor amplifier is studied. Figure 4-15 shows an example of a single transistor amplifier with an active load. BSIM3 models of PMOS and NMOS FETs are listed in Appendix A. The current mirror consisted of two PMOS devices, M_2 and M_3, which act as an active load and the sizes of these two devices are the minimum width and length (W/L=1.18 μm / 0.25 μm). In this schematic, supply bias voltage V_{DD} is 3.3 V, R_1 is 10 kΩ. V_1 is the gate

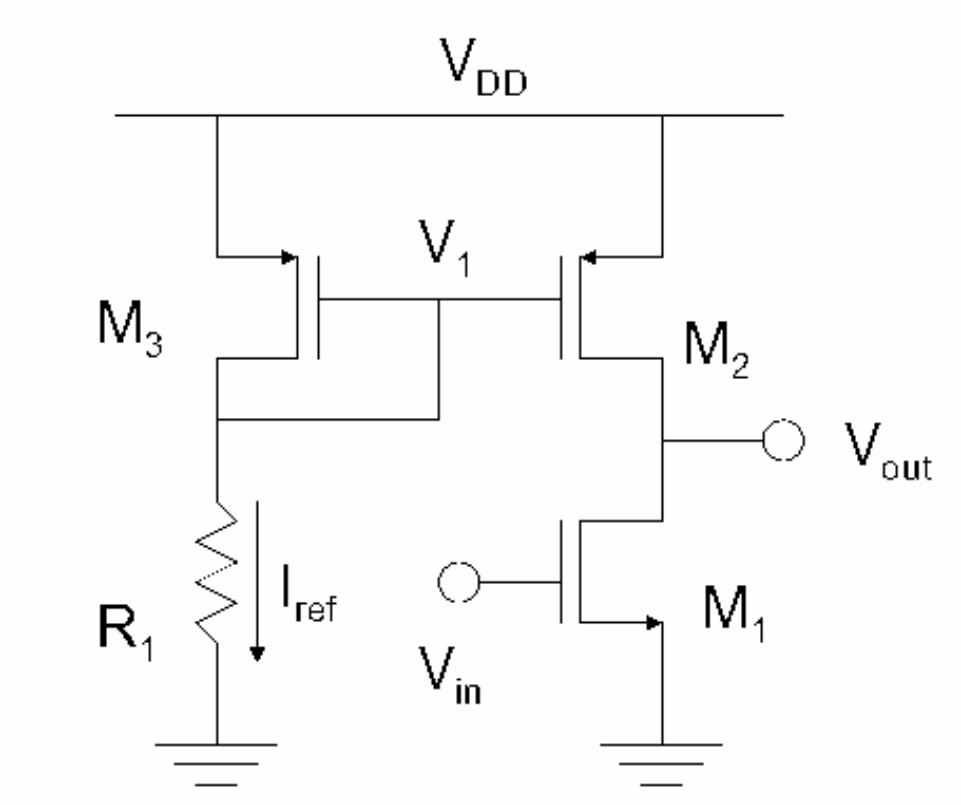

Figure 4-15 A schematic of a common-source amplifier with an active load

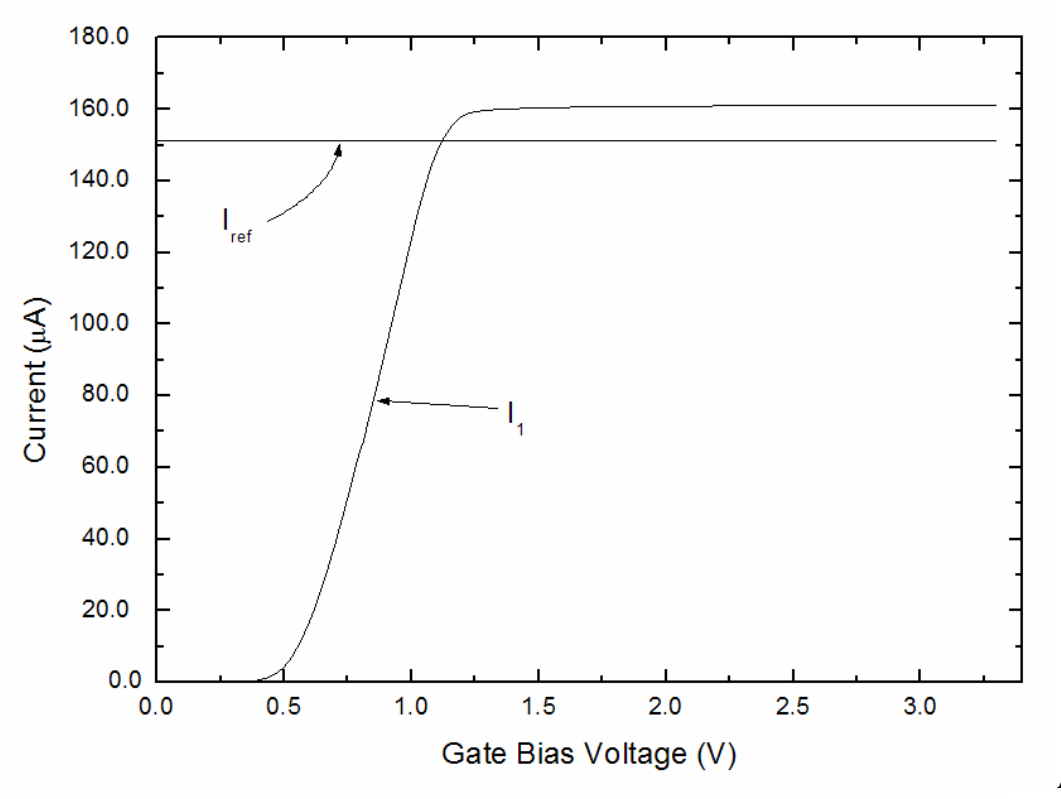

A

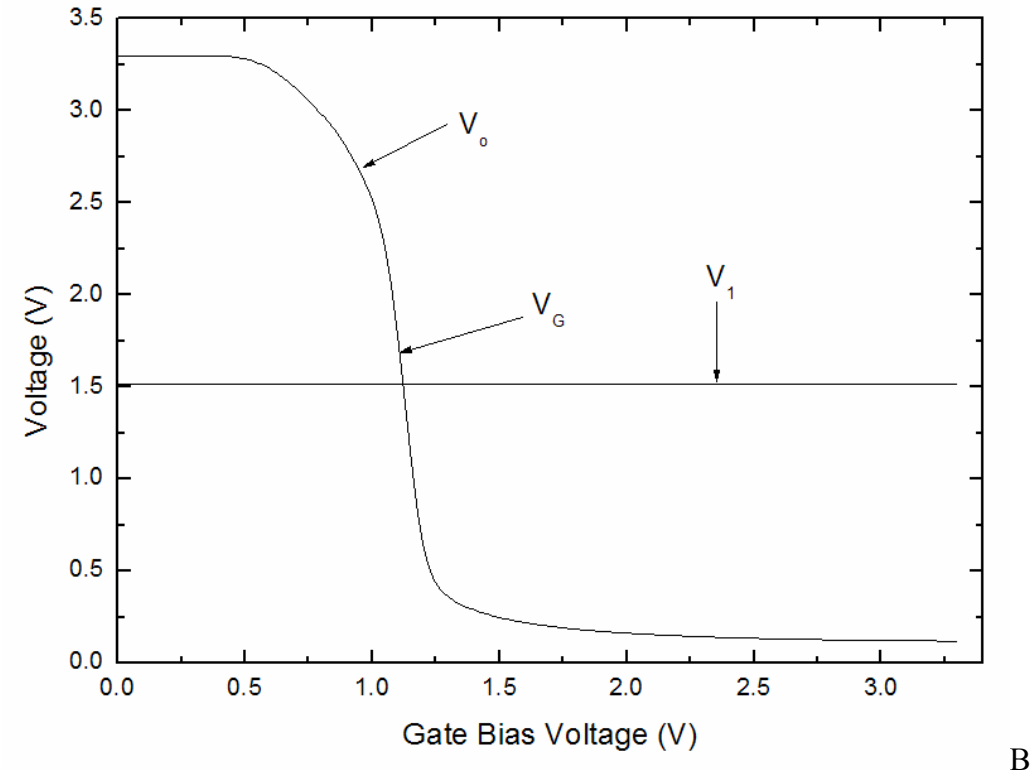

B

Figure 4-16 DC Characteristics of a common-source amplifier with an active load. A) is current and B) is voltage.

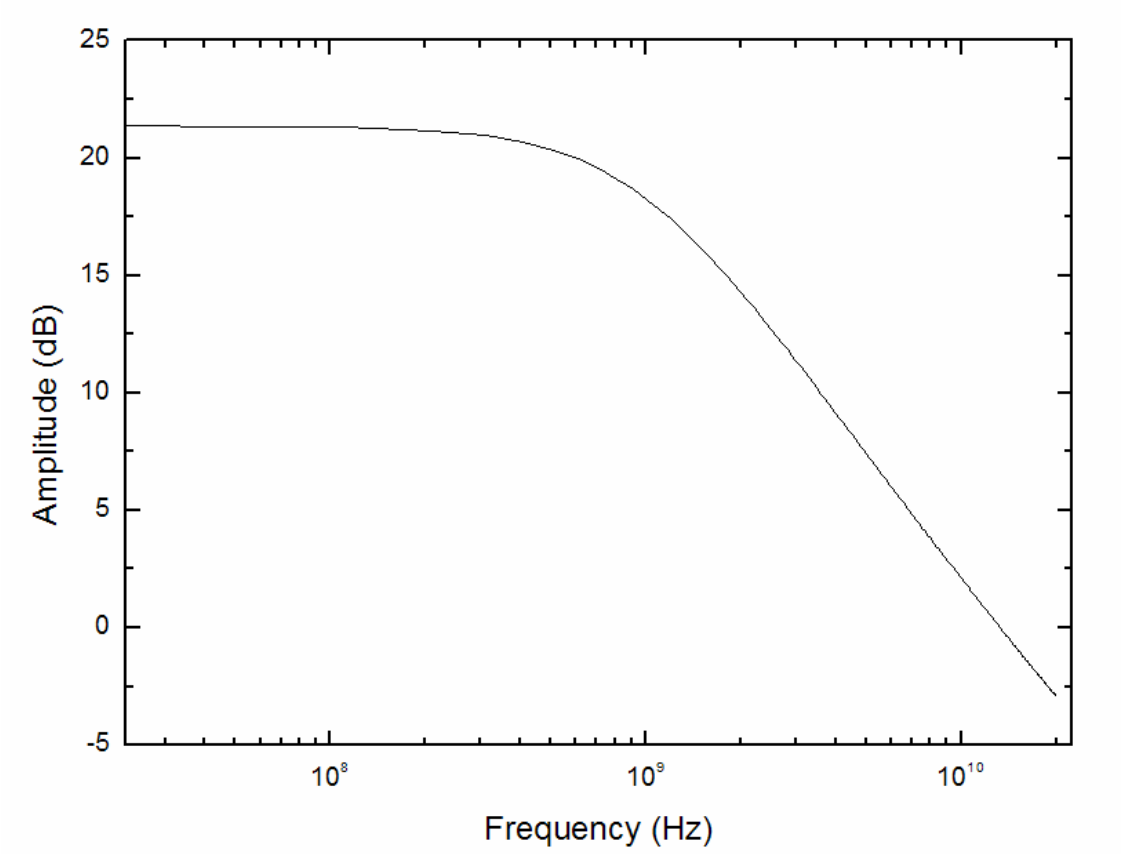

Figure 4-17 The AC simulation of a common-source amplifier with an active load

bias voltage of the current mirror. The I-V characteristic curve and transfer characteristic curve are shown in Figure 4-16. In Figure 4-16.A, I_{ref} is the current of the resistor R_1 whose value is 151.2 μA. I_1 is the drain current of the transistor M_1. In Figure 4-16.B, V_1 is the gate bias of transistors M_2 and M_3 which construct current mirror, the value of V_1 is 1.51 V. V_o is the drain voltage of transistor M_1. For the simulation of AC, one-tone and two-tone test, the gate bias voltage is chosen at the point V_G in which all MOS transistors are in saturation mode. The result of AC simulation of this amplifier is shown in Figure 4-17. The 3-dB bandwidth of this amplifier is about 1 GHz. For applying the fitting algorithm to the common-source amplifier with active load, one-tone and two-tone tests are simulated in this schematic at the gate bias voltage V_G. The result of the one-tone test

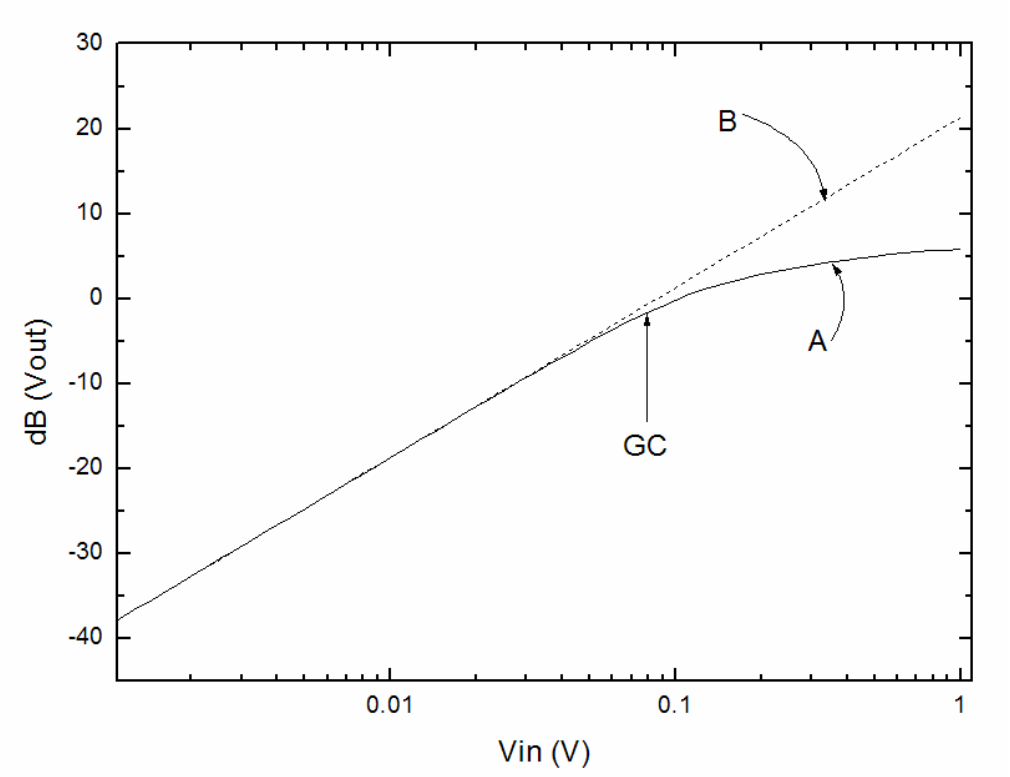

Figure 4-18 The results of one-tone simulation

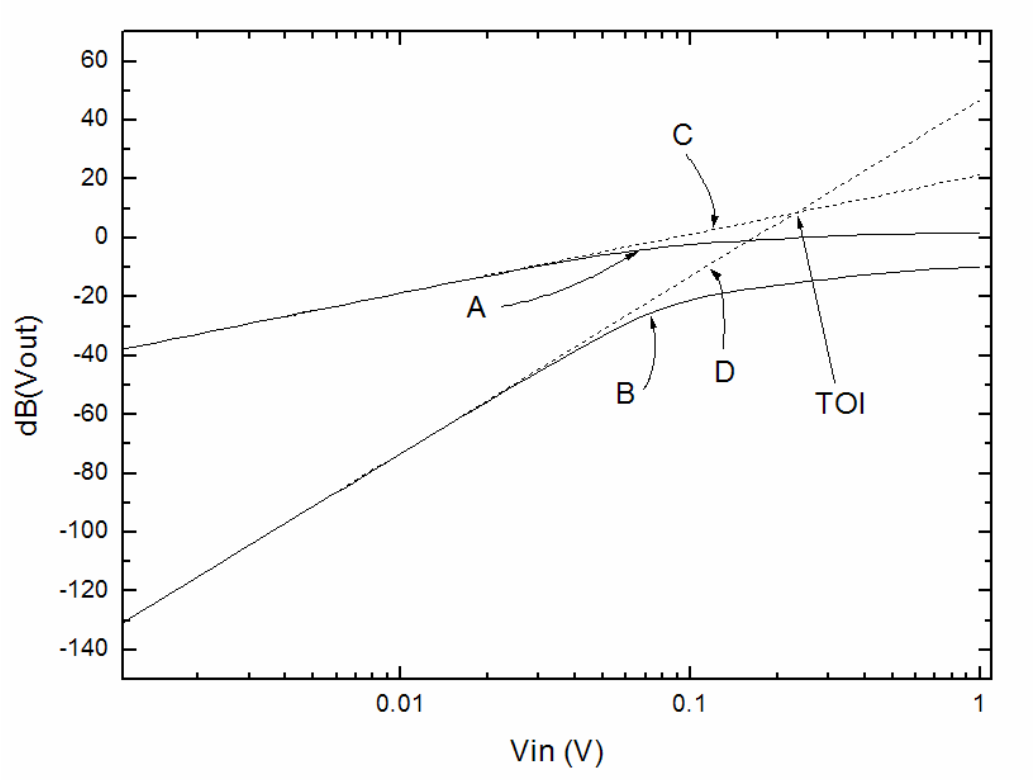

Figure 4-19 The results of two-tone simulation

is shown in Figure 4-18. In this test, the amplitude of the input voltage is swept from 0.001 V to 1 V at the fundamental frequency 100 MHz. Curve A is the gain curve and Line B represents the ideal gain curve under the assumption that there are no harmonics. The 1 dB gain compression point is denoted by GC in this graph. The value of input-referred 1 dB compression point is 0.08V. Figure 4-19 shows the result of two-tone simulation. The applied frequencies in the two-tone test are 100 MHz and 110 MHz. Curve A and B represent the output voltages at 100 MHz and at 90 MHz separately. Curve A is the fundamental frequency of 100 MHz, Curve B indicates the amplitude at intermodulation frequency of 90 MHz. Line C and D indicate the ideal harmonic response. The point of intersection of the two ideal harmonic lines, denoted by point TOI, indicates the third order interception point that has a value of 0.25V. The fitting algorithm that extracts nonlinear coefficients from a gain compression curve is explained previously in Section 4-1. The same algorithm is applied to this single transistor amplifier

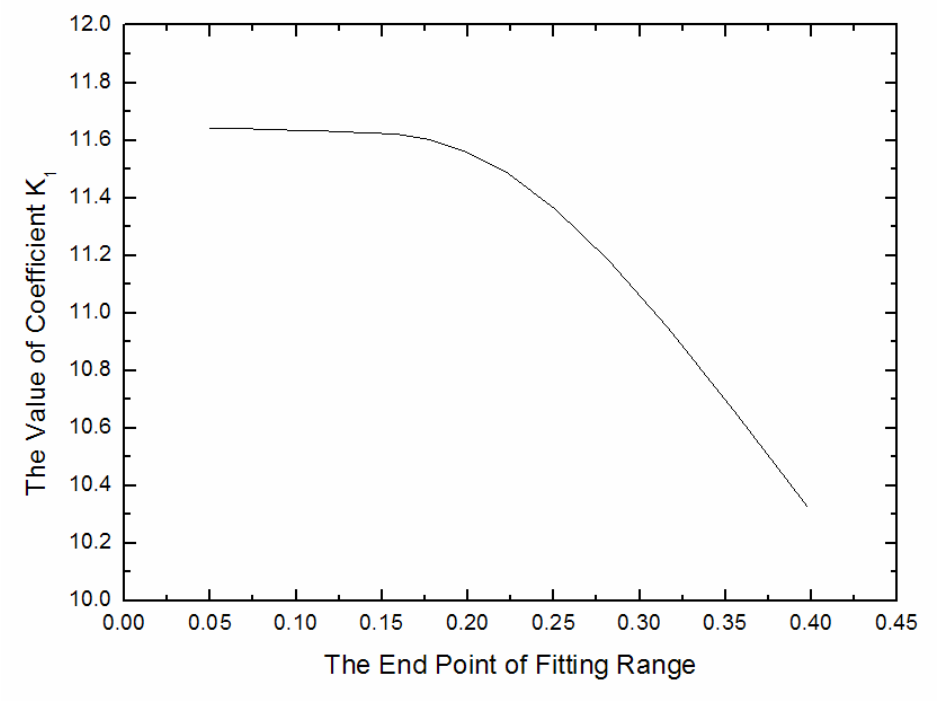

Figure 4-20 Extracted nonlinear coefficient K_1

with an active load. Figure 4-20 shows the value of coefficient K_1 though this fitting algorithm. In this figure, the value of K_1 is extracted by the fitting method through the fitting range from 0.001 V to the end point of the fitting range. The voltage gain of this amplifier is greater than that of a common source amplifier in Section 4-1 since the value of K_1 in this figure is greater than that of K_1 in Figure 4-7. The value of K_3 is shown in Figure 4-21. The negative sign of K_3 causes the gain compression on

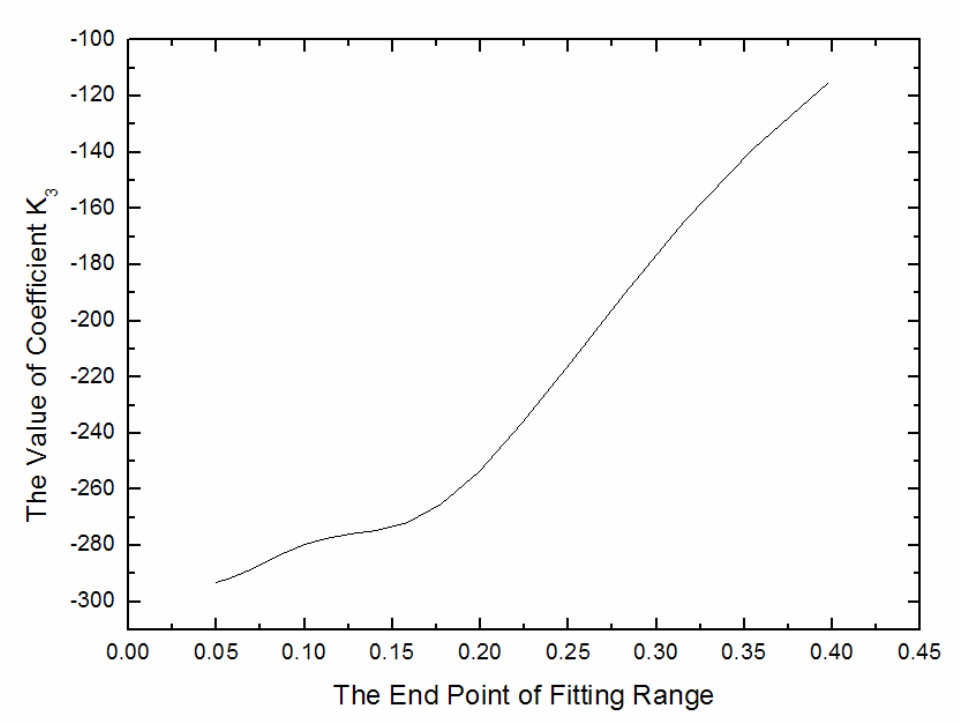

Figure 4-21 Extracted nonlinear coefficient K_3

the gain curve since the sign of K_3 is opposite to the sign of K_1. The extracted value of K_5 is shown in Figure 4-22. The value of this coefficient decreases rapidly when the width of the fitting range increases. Through these three graphs, the extracted values of nonlinear coefficients change according to the width of the fitting range. This result is the same as that in the previous section. Figure 4-23 shows the standard errors of nonlinear coefficients according to the width of the fitting range. In this graph, K_i represents the

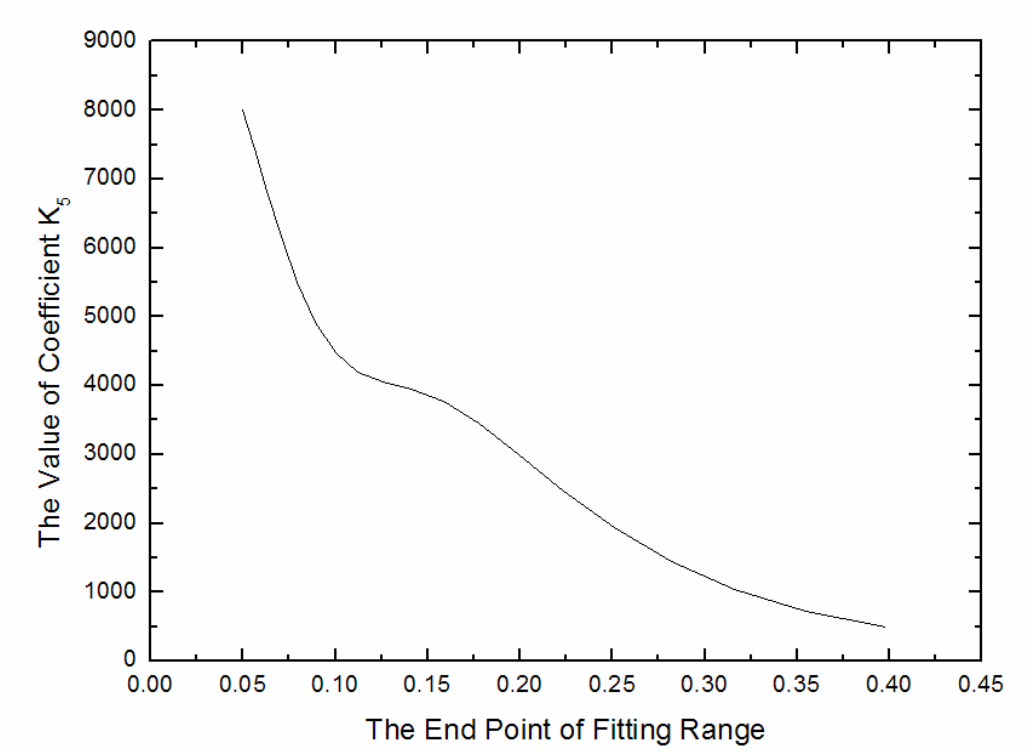

Figure 4-22 Extracted nonlinear coefficient K_5

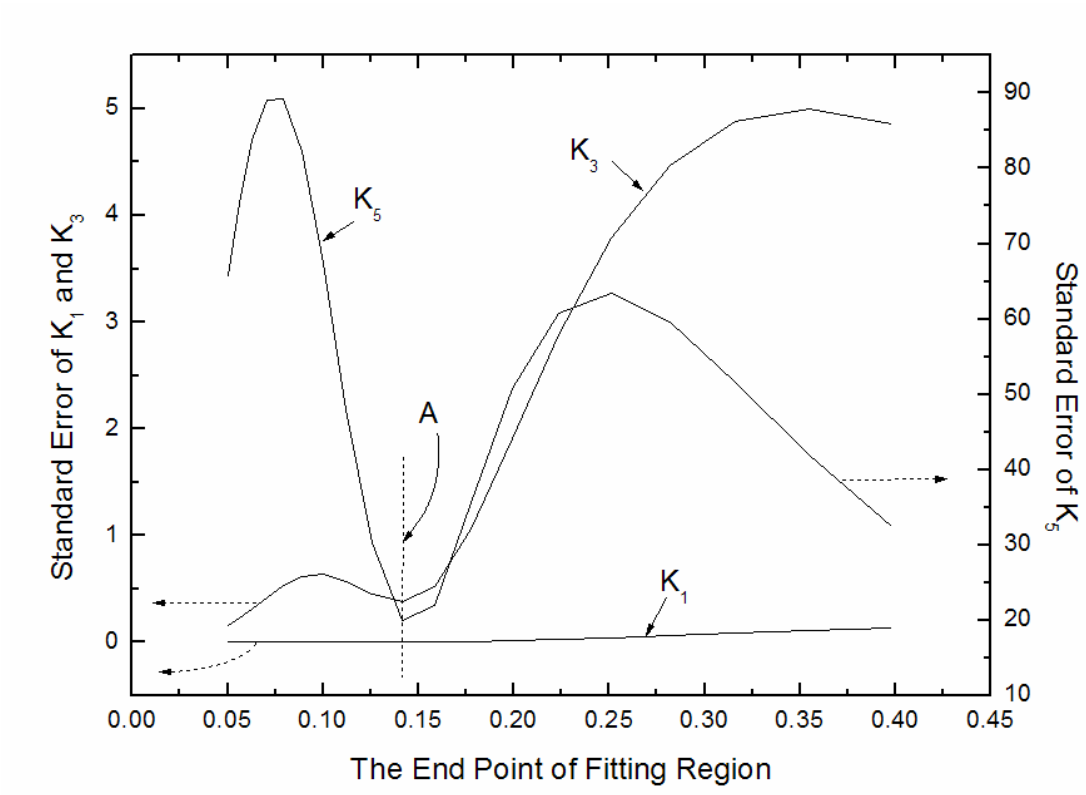

Figure 4-23 Standard errors of nonlinear coefficients

standard error of the nonlinear coefficient K_i, curve K_1 and K_3 follows the left y-axis and curve K_5 is represented by the right y-axis. The lowest values for the standard errors of each coefficients are shown by Point A in Figure 4-23. This point is about 0.14 V. This is greater than the 1 dB gain compression point, 0.08 V. The best fitting range of this circuit is different from that of a common-source amplifier discussed in Section 4-1. Figure 4-24 shows the sum of square of the residual. In this graph, the total error quantity is significantly lower at point A in the standard error graph. Therefore, the fitting range that has the minimum standard error and the small total residuals can be defined through these two graphs. The fitting outcome for this set of prospective ranges is summarized in Table 4-3. At the 3rd order intercept point, the input voltage is 0.238 V and -12.48 dB. This value shows about a 0.44 dB difference in comparison with the simulated value -12.04 dB. The estimated third-order intercept point is close to the simulated third-order intercept point. The applied fitting algorithm works well in this example. The equivalent circuit of an amplifier with an active load can be modeled by the passive component at the quiescent point. The Volterra analysis researched in the previous part of this section is applied to this amplifier with an active load by replacing the active load with the passive components. The fitting algorithm is not affect by the active load except for the change caused by the operating frequency.

Table 4-3 Fitting results

Parameters	Values
Coefficient K_1	11.63
Coefficient K_3	-274.7
Coefficient K_5	3957
Calculated V(IIP_3)	0.238 V (-12.48 dB)
Simulated V(IIP_3)	0.25 V (-12.04 dB)

4.5 Summary

In this chapter, the proposed fitting algorithm has been verified through the application of the algorithm to the simulation of a common-source amplifier. The best fitting range has been chosen through the standard errors of nonlinear coefficients and the sum of squares of the residuals. The effect of measurement error was explored by adding random noise to the simulation data. Frequency effects on the fitting algorithm was examined up to 30 GHz. The IIP_3 estimation error is less than 2 dB up to 30 GHz. Through the Volterra series analysis, the effect of loads on the algorithm was investigated and there were no differences except for the changes in operating frequency.

CHAPTER 5
COMMERCIAL RF WIDEBAND AMPLIFIER

5.1 Nonlinearity Test

Commercial amplifiers and test boards (ERA-series, MiniCircuit, Co.) shown in Figure 5-1 were used for the measurement of one-tone and two-tone tests. It is difficult to extract the nonlinear power coefficients for these ERA amplifiers due to noise sources in the measurement system. One of the noise sources is the signal generator. Even though this signal generator is designed to give a pure signal source with elaborate internal units, it still has harmonics in the frequency-domain. A low pass filter is used to decrease the harmonics in the signal generator. Figure 5-2 shows the spectrum in the signal source with and without a low pass filter. In Figure 5-2.A, Curve A represents the power at fundamental frequency, Curve B corresponds to the power at second harmonic frequency, and Curve C stands for the power at third harmonic frequency. In this graph, the power at second harmonic and third harmonic frequencies exist in the signal generator. Figure 5-2(b) shows that the harmonic components decrease when the low pass filter is used.

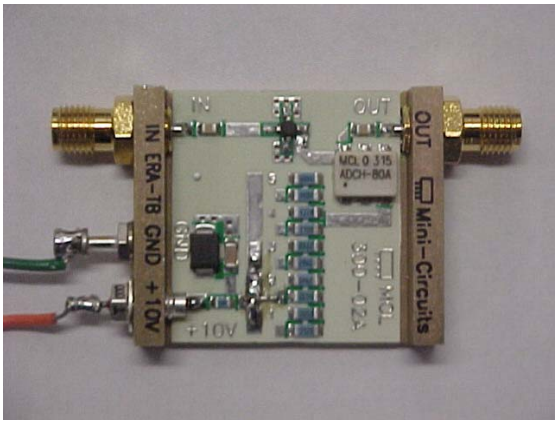

Figure 5-1 ERA1 amplifier in a test board

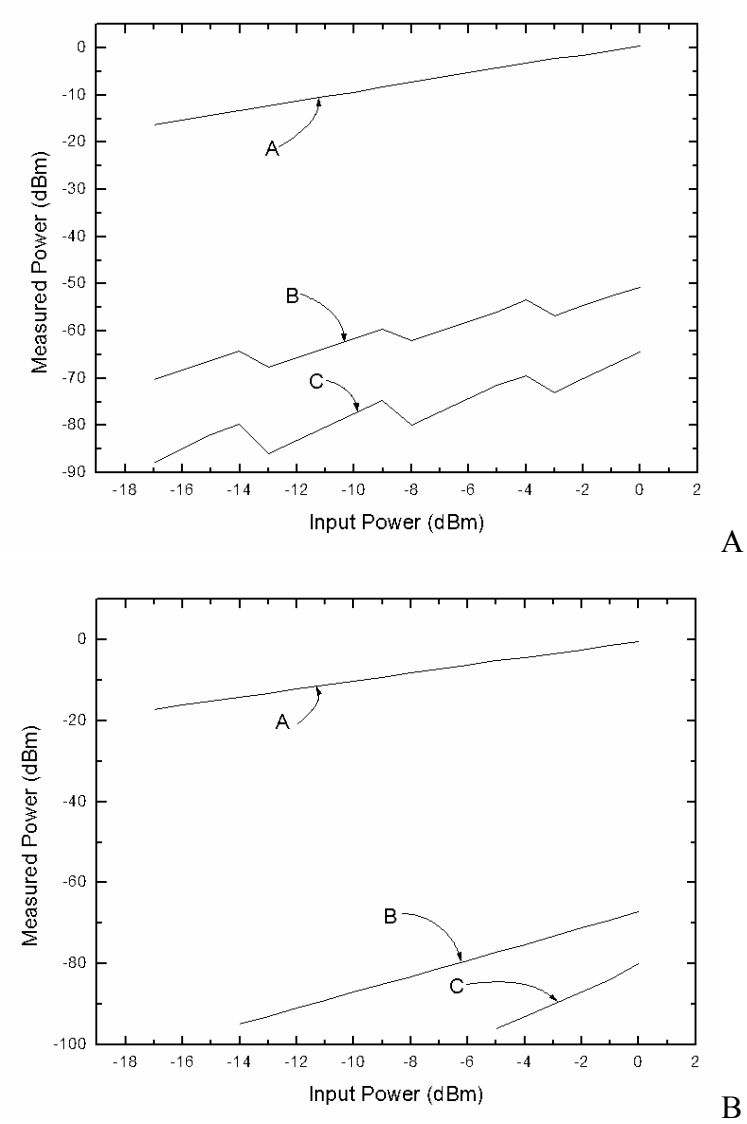

Figure 5-2 The spectrum from the signal source. A) shows the spectrum without a low pass filter and B) shows the spectrum with a low pass filter.

The ERA1 amplifier is measured in a one-tone test. The test scheme is shown in Figure 5-3. The fundamental frequency used for this test is 100 MHz. Figure 5-4 shows the result of the one-tone measurement. In this graph, the input referred 1 dB compression point, $IP_{1\text{-}dB}$ is 1.7 dBm and is denoted by GC. In this figure, Curve A represents the measured compression curve and Line B is the ideal linear curve. Here, the gain compression curve at the fundamental frequency, Curve A is used for the extraction of nonlinear coefficients. The application of a fitting method on this curve will be

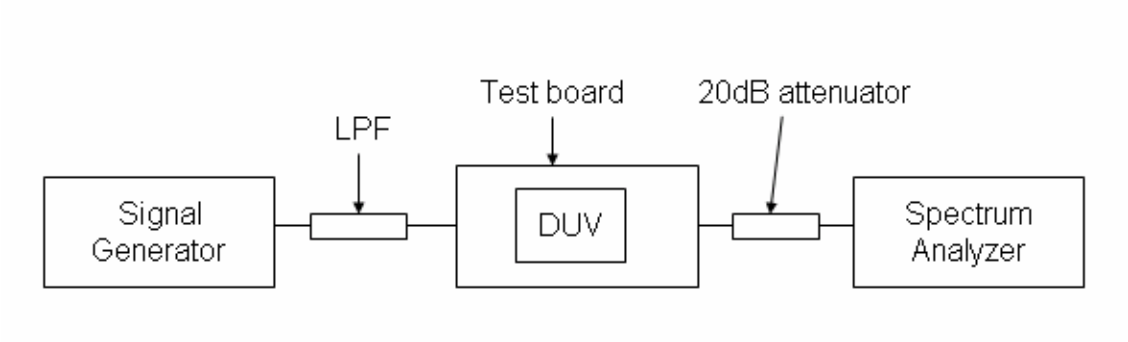

Figure 5-3 One-tone test scheme

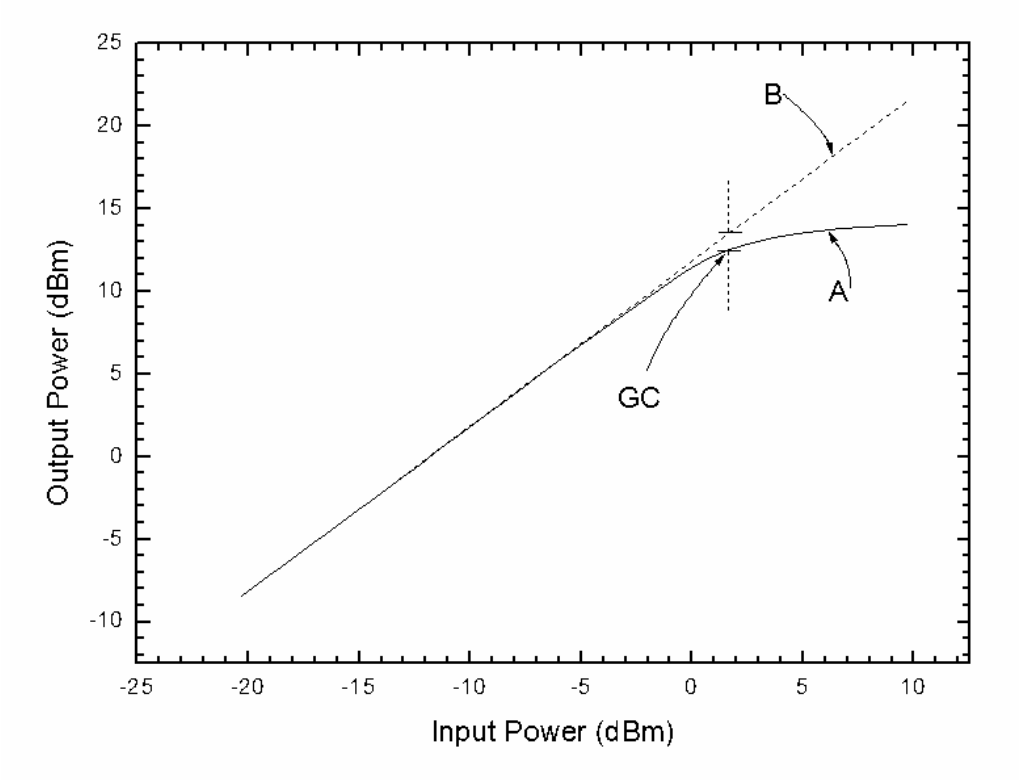

Figure 5-4 The measurement data of one-tone test (ERA1 amplifier)

explained in next section. Figure 5-5 shows the test scheme for the two-tone test. Source frequencies in this two-tone test are 100 MHz and 120 MHz. The result of the two-tone test is shown in Figure 5-6. In this figure, Curve A and B represent the amplifier output signal amplitudes at 100 MHz and at 80 MHz separately. Curve A represents the output power at fundamental frequency of 100 MHz, Curve B indicates the output power at

intermodulation frequency of 80 MHz (2×100 MHz – 120 MHz). The point of intersection of the two dotted lines, IP_3 indicates the third-order intercept point. The input-referred third-order intercept point, IIP_3 is 16.3 dBm. GC denotes 1 dB gain compression point that has a value of -2.5 dBm. The 1 dB compression point in two-tone test is explained in section 3.3.

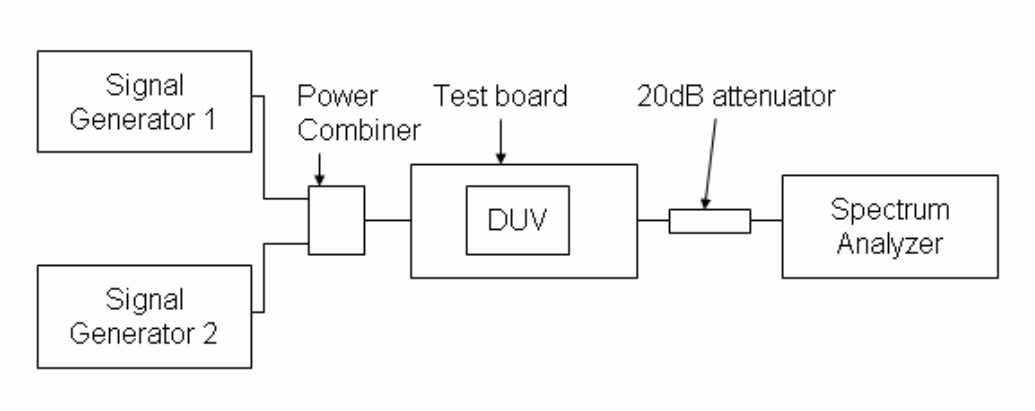

Figure 5-5 Two-tone test scheme

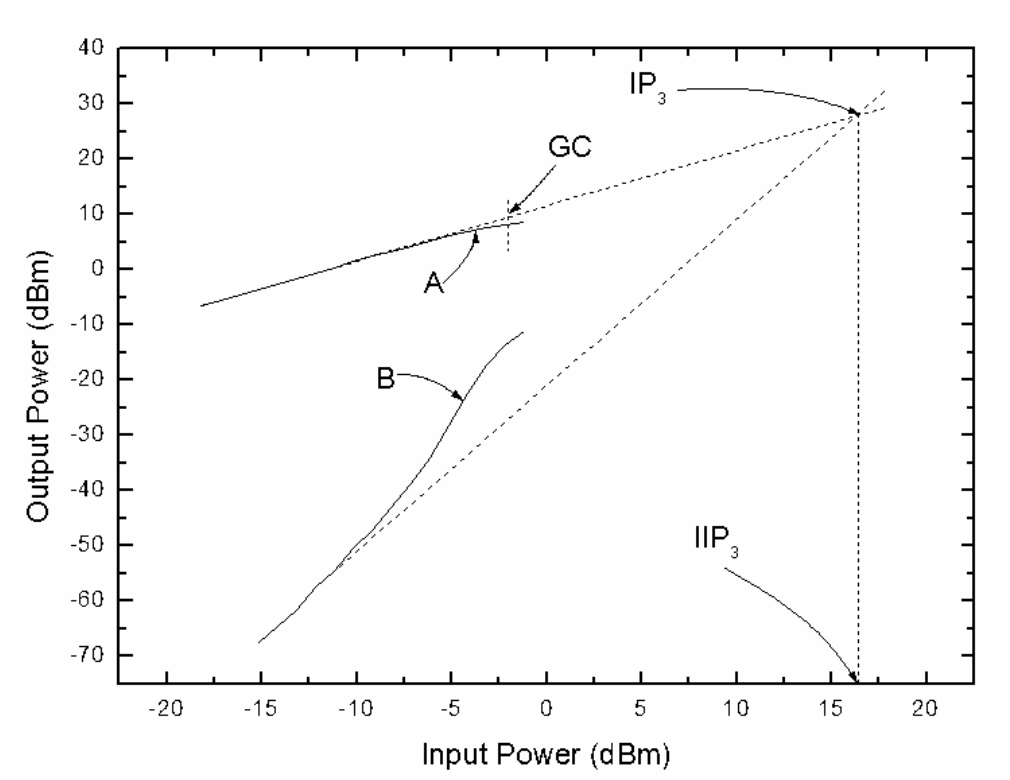

Figure 5-6 The measurement data of two-tone test (ERA1 amplifier)

ERA2 and ERA3 amplifiers are also tested in the same bias condition as ERA1 amplifier to verify the proposed algorithm to predict third-order intercept point using extraction of nonlinear coefficients from the gain compression curve. The one-tone test data of ERA2 is shown in Figure 5-7. Input-referred 1 dB gain compression point denoted by GC is -0.8 dBm. Figure 5-8 shows two-tone data of ERA2. Like Figure 5-6,

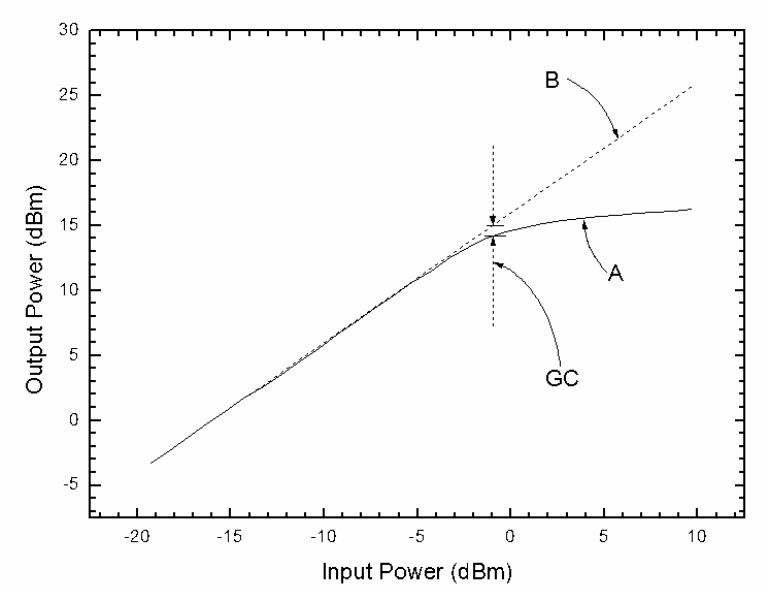

Figure 5-7 The measurement data of one-tone test (ERA2 amplifier)

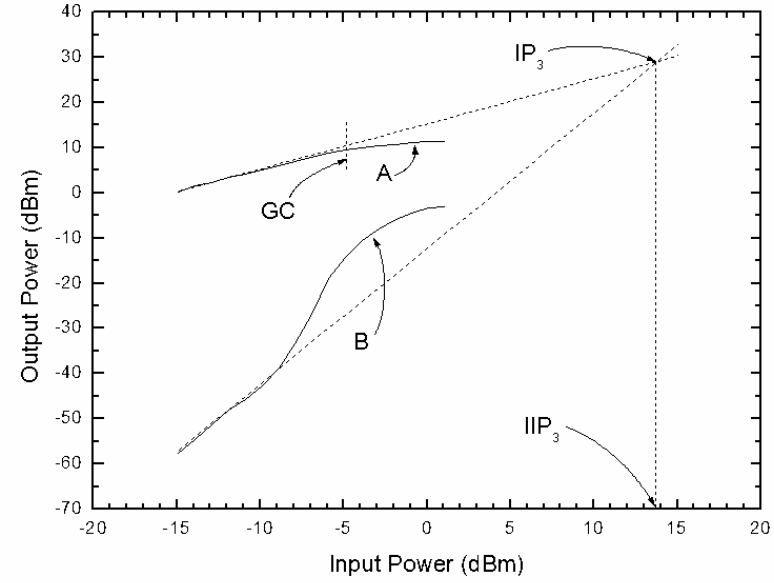

Figure 5-8 The measurement data of two-tone test (ERA2 amplifier)

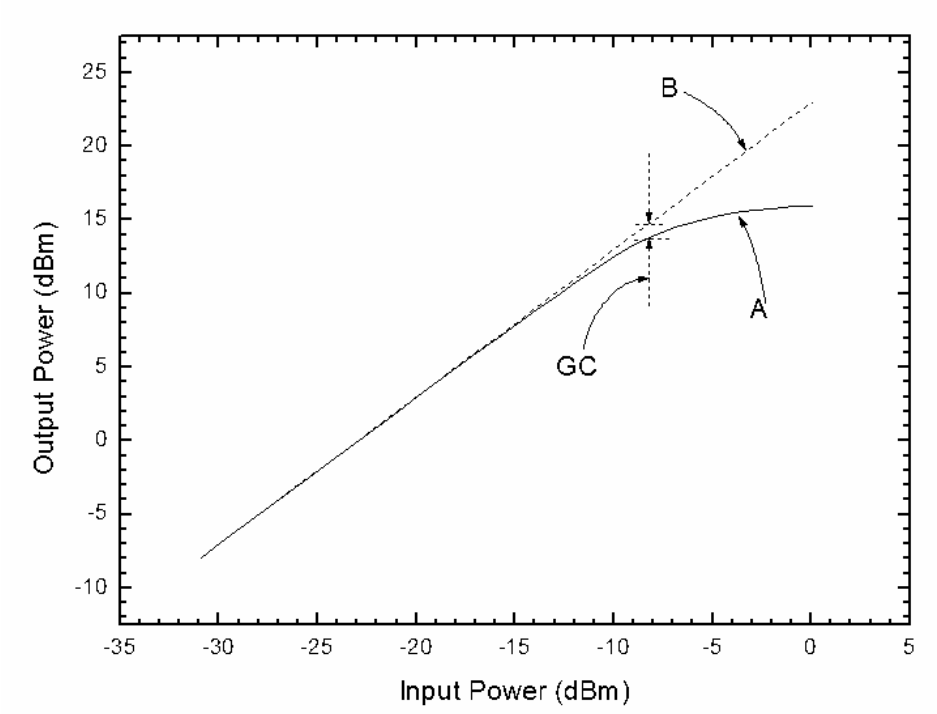

Figure 5-9 The measurement data of one-tone test (ERA3 amplifier)

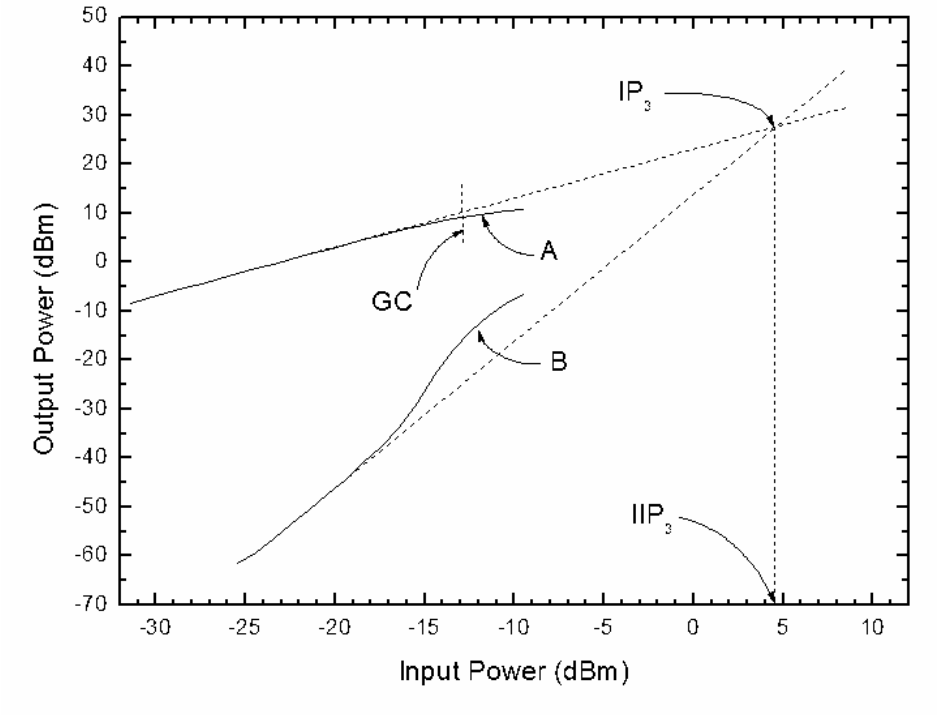

Figure 5-10 The measurement data of two-tone test (ERA3 amplifier)

Table 5-1 The summary of the measurement results of commercial amplifiers

Device	$IP_{1\text{-}dB}$*	$IP_{1\text{-}dB,2}$**	IIP_3**	IIP_3-$IP_{1\text{-}dB}$
ERA1	1.7	-2.5	16.3	14.6
ERA2	-0.8	-5	13.8	14.6
ERA3	-8	-13	4.5	12.5

*One-tone test : Source frequency = 100 MHz
**Two-tone test : frequencies = 100 MHz, 120 MHz

Curve A and Curve B represent the output power at 100 MHz and at 80 MHz separately. The input-referred third-order intercept point is 13.8 dBm. The input-referred 1 dB gain compression point denoted by GC is -5 dBm. The 1 dB gain compression point of the ERA3 amplifier is -8 dBm denoted by GC in Figure 5-9. The result of the two-tone test is shown in Figure 5-10. The 1 dB compression point is -13 dBm and the input-referred third-order intercept point is 4.5 dBm in Figure 5-10. The measurement data of these amplifiers are summarized in Table 5-1. In this table, the difference between 1 dB gain compression point and third-order intercept point is not constant. Through real measurements, the relationship between two nonlinear characteristics can be constructed.

5.2 IIP_3 Prediction from the Gain Compression Curve

The application of the technique to manufacturing test LNA measurements required substantial modification. IIP3 extraction from LNA gain simulation data has the benefit of many decibel places of accuracy (high S/N) and an ideal (no loss) test system. Real measurements from spectrum analyzers can exhibit roughly 1% accuracy in the data and substantial power loss due to cables and fixtures in the test setup. Even after using power magnitude calibration techniques on spectrum analyzer data, significant uncertainty can exist due to phase errors. In addition, it was found that to extract properly IIP_3 parameters the data has to be measured on one power range of the spectrum analyzer.

Using multiple spectrum analyzer power ranges introduced offset errors in the measured data. In summary, the simulated LNA data had remarkably high S/N across the entire data set while the measured LNA gain data had a mediocre S/N at high-power which decreased as power decreased.

Given the situation, a global extraction of the LNA power series expansion coefficients was not stable with small changes in the data set. Adding a few more data points at the high-power range would create large changes in the K_3 and K_5 extracted coefficients. To counteract this problem, which could be seen in ATE systems doing manufacturing test, a new parameter extraction methodology had to be created. After experimenting with many ways of performing this parameter extraction, a regional parameter extraction methodology was devised.

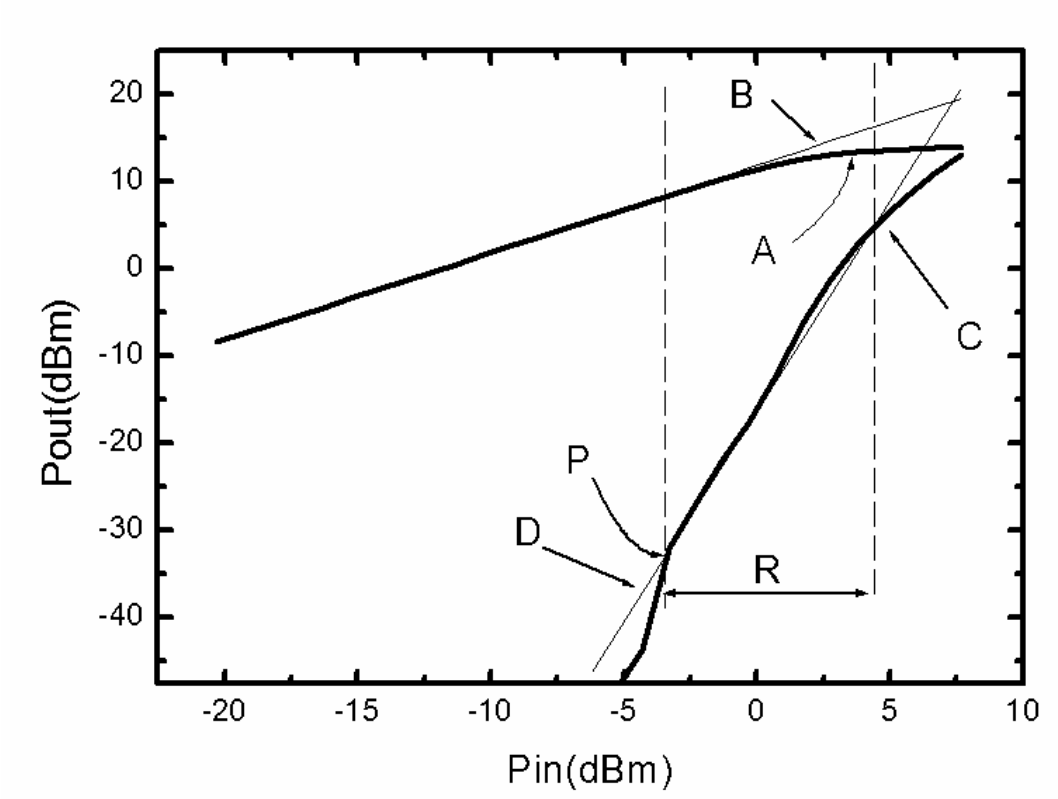

Figure 5-11 One-tone data and extraction from ERA1 device at 100 MHz

A new robust measurement extraction algorithm is developed for one-tone gain data as graphed in Figure 5-11 for ERA1 amplifier. In this new algorithm, the nonlinear power coefficients are extracted regionally. To help understanding how to interpret this graph, the procedure is explained step by step in Figure 5-12. First, the entire one-tone

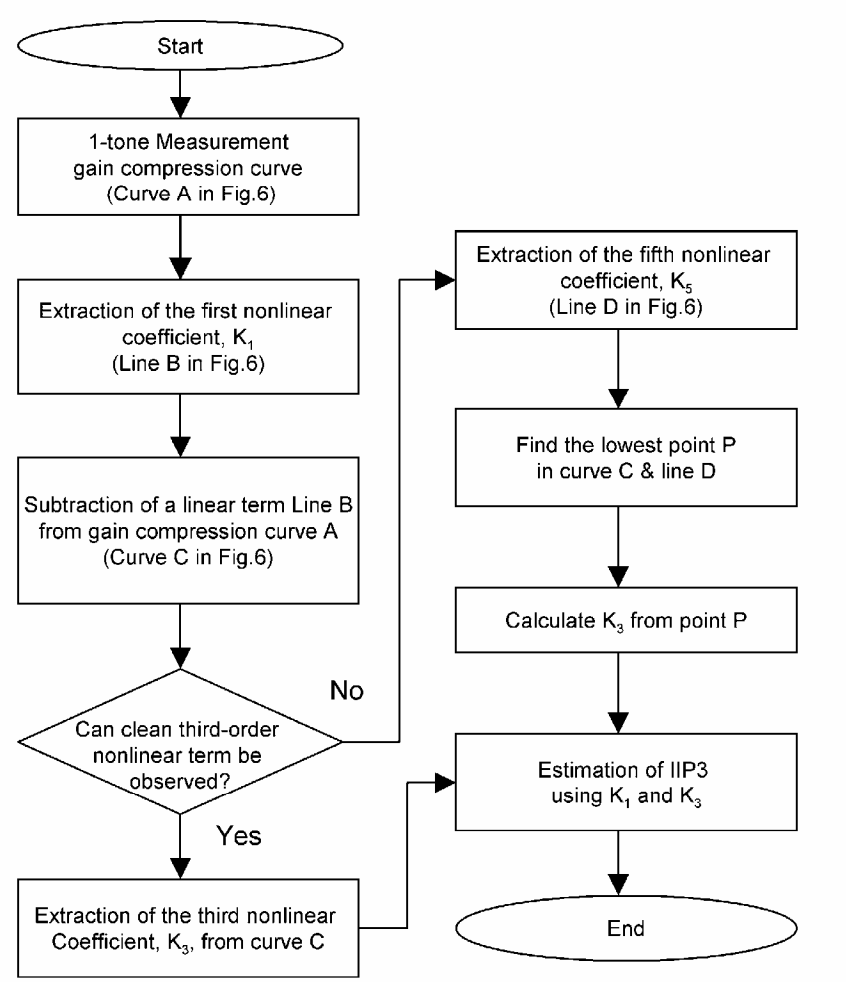

Figure 5-12 A flow chart for estimation of IIP3 from one-tone measurement

power compression curve is measured as shown by curve B in Figure 5-11. Line B is a straight-line that can be fitted to the low-power amplifier data. From this line B, the K_1 factor is determined. The effects of the K_1 factor are subtracted from the original gain compression curve A (slope 1/1). Curve C shows the remaining terms on the gain compression curve. From this curve C, it is easy to see that the K_3 extraction region

below point P of region R has very high noise. Instead of K_3, the K_5 factor is extracted from the compression region R of Figure 5-11. This is easily verified because the slope of line D is 5/1. Fortunately, it is not necessary to know the slope of the K_3 factor, since it is, idealy, 3/1. To determine the value K_3, one need to know where it intercepts line D and that is at point P. Point P is at the intercept between the K_3 line and the K_5 line. Point P is also the highest S/N point in the measured K_3 factor data. The calculated IIP_3 from this point is 16.82 dBm is very close to the measured IIP_3, 16.3 dBm. Figure 5-13 shows the application of the algorithm to ERA2 amplifier. The explanation of this graph is the same

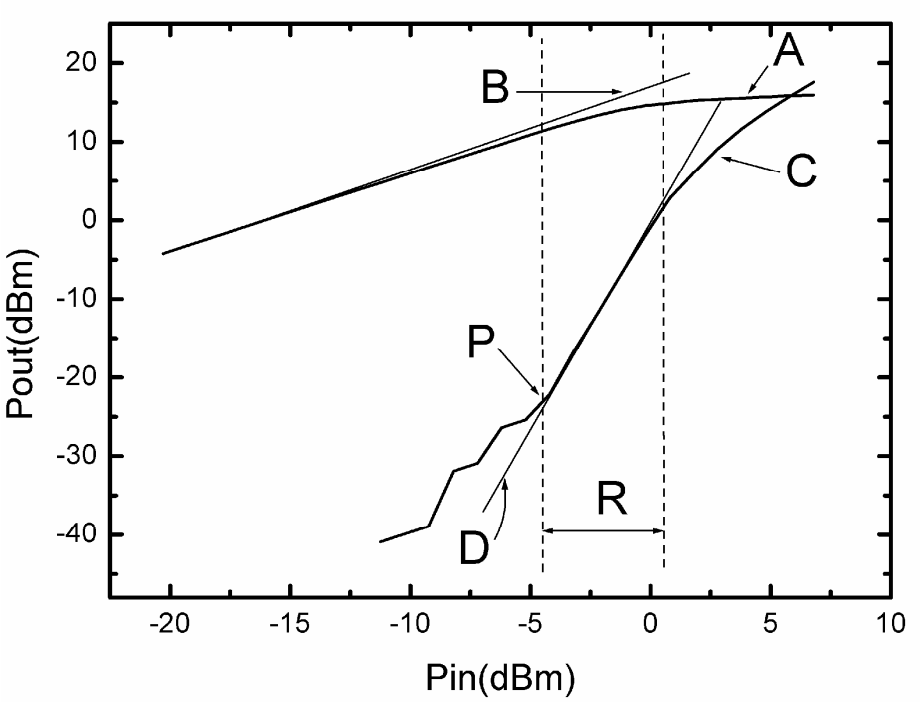

Figure 5-13 One-tone data and extraction from ERA2 device at 100 MHz

Table 5-2 The summary of the estimated IIP_3 of commercial amplifiers

Device	Measured IIP3	Estimated IIP3
ERA1	16.3	16.82
ERA2	13.8	12.81
ERA3	4.5	3.71

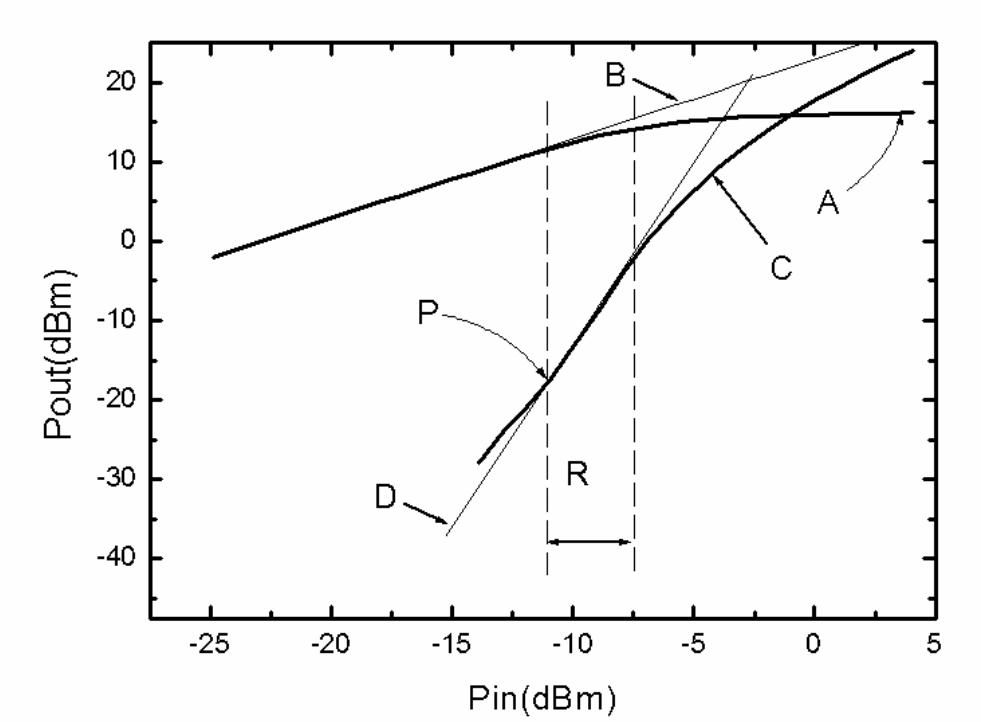

Figure 5-14 One-tone data and extraction from ERA3 device at 100 MHz

as that of Figure 5-11. The same analysis is applied to ERA3 amplifier in Figure 5-14. Table 5-2 shows the measured characteristics and estimated IIP_3 of the ERA devices (ERA1, ERA2 and ERA3). From the table, the difference between the measured IIP_3 and the estimated IIP_3 is less than 2 dB in all cases and less than or equal to 0.41 dB for most cases. Through these experiments a method for predicting IIP3 using a one-tone LNA gain measurement was developed.

5.3 The Application of the Proposed Algorithm at High Frequency

The ERA2 amplifier is retested at a relatively high frequency 2.4 GHz in Figure 5-15. Fig 5-15 shows the new robust extraction algorithm at high frequency. The result in Table 5-3 shows that this algorithm is working in microwave frequencies. Through these experiments a method for predicting IIP_3 using a one-tone LNA gain measurement was developed.

Table 5-3 The measurement data and calculated IIP_3 of a commercial amplifier

Device	$IP_{1\text{-}dB}$*	IIP_3**	IIP_3***
ERA2	-0.4	12.1	12.08

*One-tone test : Source frequency = 2.4 GHz
**Two-tone test : frequencies = 2.4 GHz, 2.475 GHz
*** Calculated from the extracted nonlinear coefficients

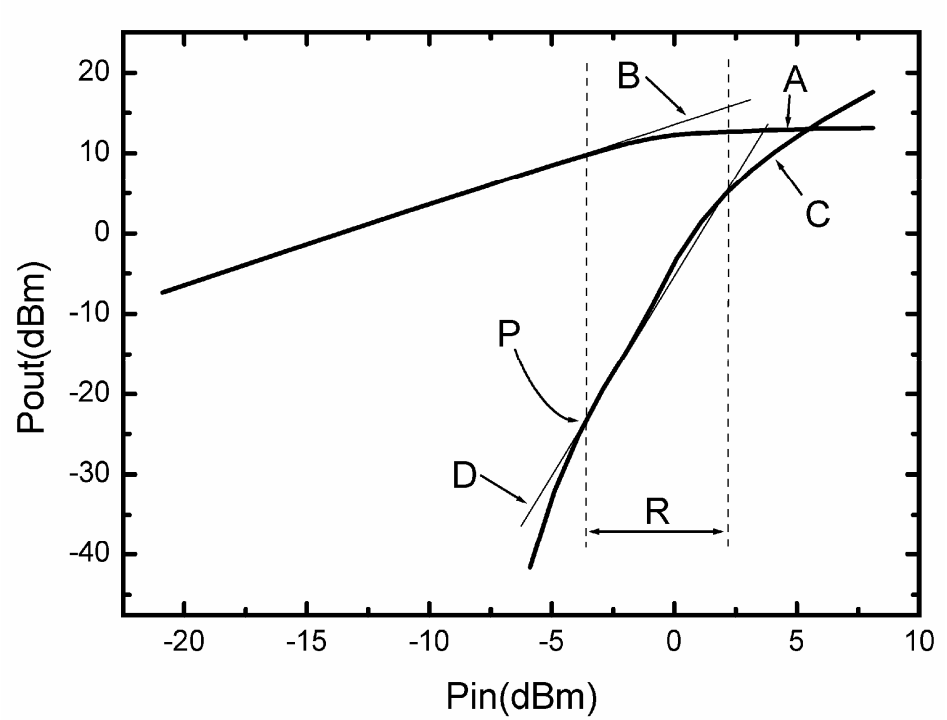

Figure 5-15 One-tone data and extraction from ERA2 device at 2.4 GHz

5.4 $IP_{1\text{-}dB}$ Estimation from Two-tone Data

The algorithm in section 5.2 estimates IIP_3 from the one-tone data. In this section, the estimation of the 1 dB gain compression point is investigated on the basis of the two-tone measurement data. Let the input amplitude at the 1 dB compression point be $A_{1\text{-}dB}$. From equation (3-24), The 1 dB compression point in the one-tone test is found in equation (3-24).

$$\frac{5}{8}\left(\frac{K_5}{K_1}\right)A_{1-dB}{}^4+\frac{3}{4}\left(\frac{K_3}{K_1}\right)A_{1-dB}{}^2+0.109=0 \tag{5-1}$$

Two ratios, $\left(\frac{K_5}{K_1}\right)$ and $\left(\frac{K_3}{K_1}\right)$ are needed to solve above equation (5-1). These ratios are found in the two-tone measurement data. From equation (3-9), the ratio $\left(\frac{K_3}{K_1}\right)$ is determined using following equation,

$$\left|\frac{K_3}{K_1}\right|=\frac{4}{3}\times\frac{1}{A_{IP3}{}^2} \tag{5-2}$$

where A_{IP3} is the input amplitude at the third-order intercept point. The sign of this ratio should be decided by inspecting the gain curve at the fundamental frequency in the two-tone measurement. For example, the sign of $\left|\frac{K_3}{K_1}\right|$ is negative in Figure 5-6 since Curve A shows the compression in the gain curve. The 1 dB gain compression point in the two-tone test is explained by equation (5-3),

$$\frac{25}{4}\left(\frac{K_5}{K_1}\right)A_{1-dB,2}{}^4+\frac{9}{4}\left(\frac{K_3}{K_1}\right)A_{1-dB,2}{}^2+0.109=0 \tag{5-3}$$

where $A_{1-dB,2}$ is the input amplitude at the 1 dB compression point of the two-tone test that is denoted by GC in Figure 5-6. From above equation, the ratio $\left(\frac{K_5}{K_1}\right)$ can be found by

$$\left(\frac{K_5}{K_1}\right)=\left(-\frac{4}{25}A_{1-dB,2}{}^{-4}\right)\left(\frac{9}{4}\left(\frac{K_3}{K_1}\right)A_{1-dB,2}{}^2+0.109\right) \tag{5-4}$$

Inserting two ratios $\left(\frac{K_5}{K_1}\right)$ and $\left(\frac{K_3}{K_1}\right)$ to equation (5-1), the input-referred 1 dB gain compression point, $IP_{1\text{-dB}}$ can be calculated. This method is applied to ERA amplifiers for verification.

First, the ERA1 amplifier is considered as the application example of this algorithm. IIP_3 of ERA1 amplifier is 16.3 dBm in Table 5-1. The input amplitude at this point is

$$A_{IP3} = 10^{(IIP_3 - 10)/20} = 2.065 \tag{5-5}$$

where the unit of A_{IP3} is volt (V) and the input resistor and the output resistor loads are 50 Ω. The absolute value of the ratio, $\left|\frac{K_3}{K_1}\right|$ can be found in equation (5-2).

$$\left|\frac{K_3}{K_1}\right| = \frac{4}{3} \times 2.065^{-2} = 0.3146 \tag{5-6}$$

The sign of above ratio $\left|\frac{K_3}{K_1}\right|$ is negative since the gain at the fundamental frequency compresses in Figure 5-6. The ratio $\left(\frac{K_3}{K_1}\right)$ is

$$\left(\frac{K_3}{K_1}\right) = -0.3146 \tag{5-7}$$

From table 5-1, the $IP_{1\text{-dB},2}$ is -2.5 dBm. The input amplitude at this 1 dB compression point in two-tone is

$$A_{1-dB,2} = 10^{(IP_{1-dB,2} - 10)/20} = 0.2371 \tag{5-8}$$

Using the value of $A_{1-dB,2}$ and the ratio $\left(\frac{K_3}{K_1}\right)$, the ratio $\left(\frac{K_5}{K_1}\right)$ is found in equation (5-4). The calculated value of $\left(\frac{K_5}{K_1}\right)$ is -3.5140. The 1 dB compression point in the one-tone test is now found by solving equation (5-1). The solution of this equation is 0.4192. The calculated IP_{1-dB} is 2.45 dBm and is very close to the measured value, 1.7 dBm. Through the application of the algorithm, two ratios $\left(\frac{K_5}{K_1}\right)$ and $\left(\frac{K_3}{K_1}\right)$ are found and 1 dB compression point is estimated. The difference between the measured value and the estimated value of 1 dB compression point is less than 1 dB.

The data of the ERA2 amplifier is used for another example to verify this algorithm. First, the input amplitude at third-order intercept point is

$$A_{IP3} = 1.5488 \tag{5-9}$$

since IIP_3 of ERA2 amplifier is 13.8 dBm in Table 5-1. From this value, the absolute value of the ratio $\left(\frac{K_3}{K_1}\right)$ is calculated. The sign of this ratio is negative since the gain curve compresses in Figure 5-8. The calculated value of $\left(\frac{K_3}{K_1}\right)$ is -0.5588. From $IP_{1-dB,2}$ in Table 5-1, the calculated value of $A_{1-dB,2}$ is 0.1778. Using the value of $A_{1-dB,2}$ and the ratio $\left(\frac{K_3}{K_1}\right)$, the calculated value of the ratio $\left(\frac{K_5}{K_1}\right)$ is -11.1224. Finally, the calculated value of A_{1-dB} from equation (5-1) is 0.5143. The estimated value of the 1 dB compression point in one-tone test is -0.05 dBm. Compared to the measured value of 1 dB compression point, -0.8 dBm, the estimation error is less than 1 dB.

Finally, the data of the ERA3 amplifier is used for the estimation of 1 dB compression point from two-tone data. In this amplifier, the input amplitude at third-order intercept point is

$$A_{IP3} = 0.5309 \tag{5-10}$$

since IIP_3 of ERA3 amplifier is 4.5 dBm in Table 5-1. The absolute value of the ratio $\left(\frac{K_3}{K_1}\right)$ is calculated by using equation (5-2). The sign of this ratio need to be negative since the gain curve compresses in Figure 5-10.

$$\left(\frac{K_3}{K_1}\right) = -4.7308 \tag{5-11}$$

From table 5-1, the $IP_{1\text{-}dB,2}$ is -13 dBm. The input amplitude at this 1 dB compression point in two-tone data is

$$A_{1-dB,2} = 0.0708 \tag{5-12}$$

Using the value of $A_{1-dB,2}$ and the ratio $\left(\frac{K_3}{K_1}\right)$, the calculated value of the ratio $\left(\frac{K_5}{K_1}\right)$ is

$$\left(\frac{K_5}{K_1}\right) = -354.5 \tag{5-13}$$

From equation (5-1), the calculated value of A_{1-dB} is 0.1248. The estimated value of the 1 dB compression point in one-tone test is -8.08 dBm and is very close to the measured value, -8 dBm. Table 5-4 summarize the results of these applications of three amplifiers.

Table 5-4 The summary of the application results of the $IP_{1\text{-}dB}$ estimation algorithm

Device	Measured $IP_{1\text{-}dB}$	Estimated IIP_3
ERA1	1.7	2.45
ERA2	-0.8	-0.05
ERA3	-8	-8.08

In this table, the difference between the measured $IP_{1\text{-}dB}$ and the estimated $IP_{1\text{-}dB}$ is less than 1 dB in all cases and less than or equal to 0.75 dB for most cases. Through these experiments a method for estimating $IP_{1\text{-}dB}$ using a two-tone LNA gain measurement was developed.

5.5 Summary

In this chapter, a robust algorithm to predict IIP_3 has been developed for the wideband RF amplifier. Given the noisy measurement situation, a global extraction of the LNA power series expansion coefficients was not stable with small changes in the data set. Adding a few more data points at the high-power range would create large changes in the K_3 and K_5 extracted coefficients. To counteract this problem, which would be seen in ATE systems doing manufacturing test, a new parameter extraction methodology had to be created. After experimenting with many ways of performing this parameter extraction, a regional parameter extraction methodology was devised. The $IP_{1\text{-}dB}$ prediction from two-tone measurement has been applied to these wideband amplifiers. Through several steps of simple calculation using the third-order intercept point and the gain compression at the fundamental frequency, $IP_{1\text{-}dB}$ has been estimated within less than 1 dB error.

CHAPTER 6
POWER AMPLIFIERS

6.1 Linear and Nonlinear Power Amplifiers

The final stage which gives signal to an antenna is apower amplifier. The characteristics of this power amplifier is specified by the communication scheme. Linearity and efficiency among these characteristics are important factors for determining power amplifiers in their circuit application. Nonlinear power amplifiers are preferred in constant envelope modulations and Linear power amplifiers are used in amplitude modulations and π/4-QPSK in digital modulations.

The issue of nonlinearity is directly related to the spectral regrowth in a communication system transmission. The standards for various communication protocals define the nonlinearity as adjacent channel power ratio (ACPR) or adjacent channel power (ACP). In the early stage of designing RF components, IIP_3 measured in two-tone test is used for the measure of nonlinearity instead of ACPR or ACP. IIP_3 is easily measured and reported the nonlinearity estimation even though IIP_3 is not exactly the same as ACPR or ACP.

Linear power amplifier operation is classified as “class A” operation. An ideal linear amplifier doesn’t have nonlinear terms. But in actual case the active devices used for the amplifiers do produce harmonics. In class A amplifier, nonlinear behavior is made be a weakly nonlinear behavior. The definition of this weakly nonlinear behavior is explained in chapter 2. This behavior can be analyzed by using the power series or

Volterra series. In this chapter, the power amplifiers are investigated for their nonlinear characteristics.

6.2 Measurement of Commercial Power Amplifiers

Four commercial RF power amplifiers are measured in one-tone and two-tone tests. To distinguish these amplifiers, amplifiers are named alphabetically. First, the result of one-tone test on the amplifier A is shown in Figure 6-1. The fundamental frequency used for this test is 2.45 GHz. In this figure, Curve A represents the measured output power and the dotted Line B is the ideal linear curve. The 1 dB gain compression point is denoted by GC in this figure. The input-referred 1 dB gain compression point, $IP_{1\text{-}dB}$ is -11 dBm. Figure 6-2 shows the result of a two-tone test. The two input frequencies are 2.45 GHz and 2.46 GHz. Curve A represents the amplifier output signal power at 2.45 GHz and dotted Line B is the ideal linear curve extrapolated from Curve A. Curve C indicates the output power at intermodulation frequency of 2.44 GHz (2×2.45 GHz – 2.46 GHz). The dotted Line D has slope of 3 and is extrapolated from the low input power region of Curve C. The point of intersection of the two dotted lines, TOI indicates the third-order intercept point. The input-referred third-order intercept point, IIP_3 is -4.4 dBm. GC2 denotes 1 dB gain compression point in two-tone test which has a value of -16 dBm. Figure 6-3 and Figure 6-4 show the results of nonlinear tests on amplifier B. The test condition of this amplifier is the same as that of the amplifier A. In Figure 6-3, the input-referred 1 dB gain compression point is -8 dBm. IIP_3 is 0 dBm and $IP_{1\text{-}dB,2}$, denoted by GC2, is -13 dBm. The test results of the amplifier C are shown in Figure 6-5 and Figure 6-6. The same test condition as that of the amplifier A is applied to this test of the amplifier C. $IP_{1\text{-}dB}$, denoted by GC, is -6 dBm from the result of one-tone test in Figure 6-5. IP1-dB,2 is -10 dBm and IIP3 is 3 dBm in Figure 6-6. Figure 6-7 shows the results

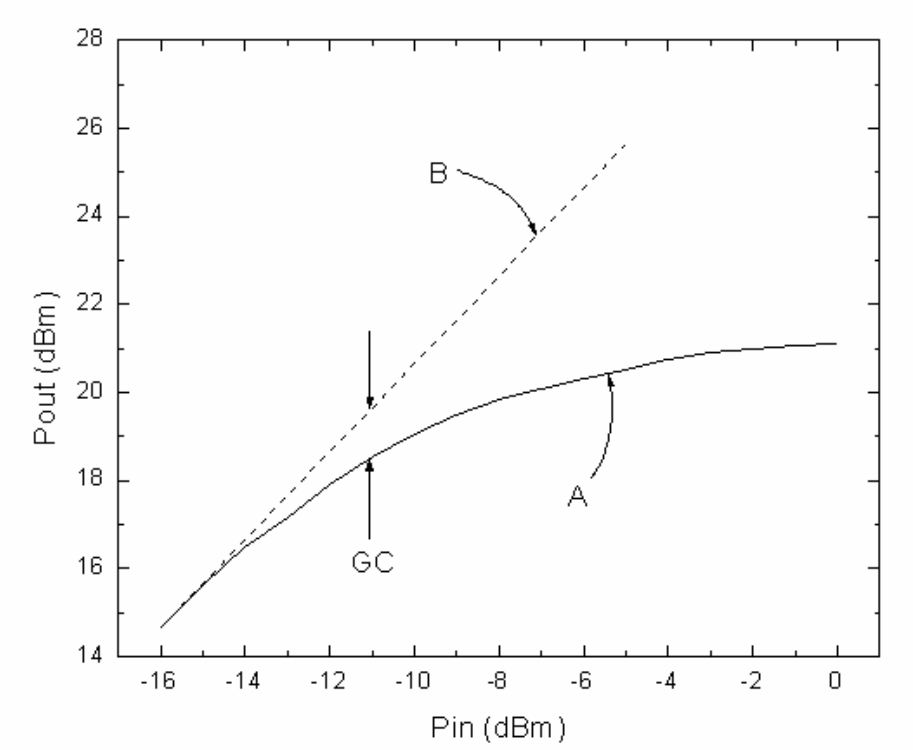

Figure 6-1 The measurement data of one-tone test of the amplifier A

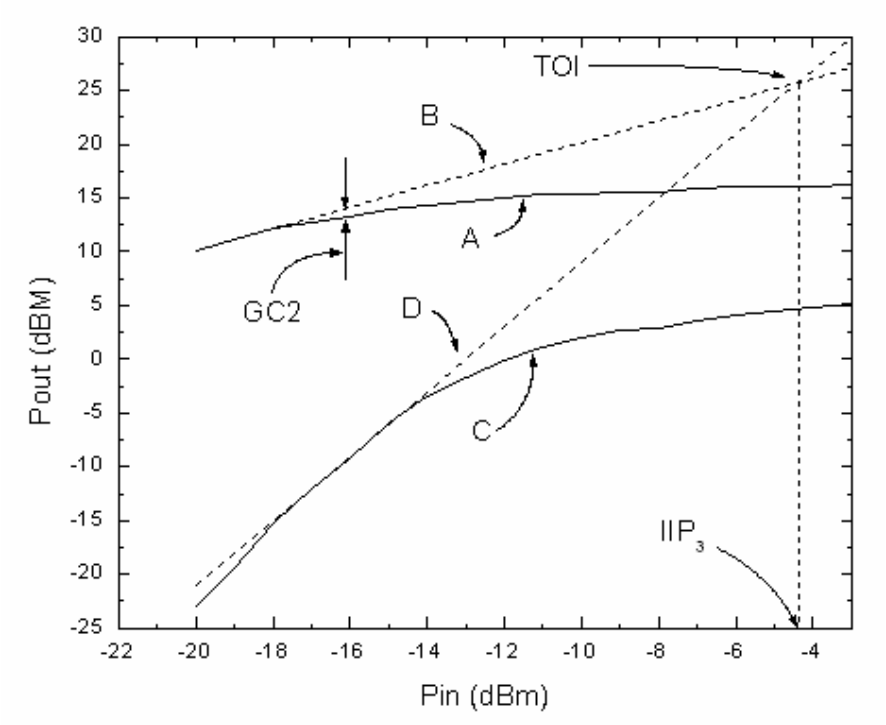

Figure 6-2 The measurement data of two-tone test of the amplifier A

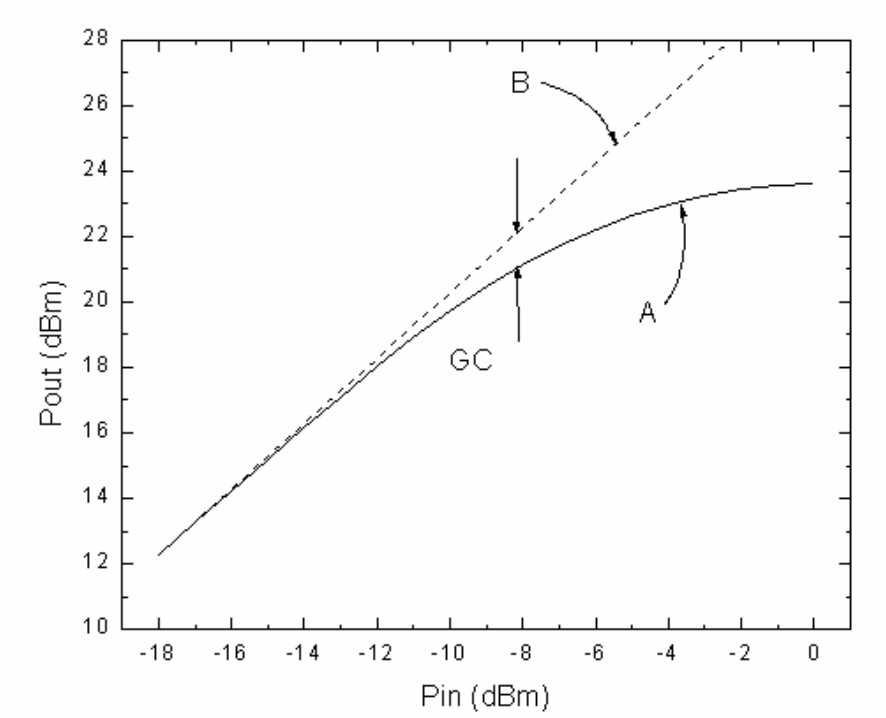

Figure 6-3 The measurement data of one-tone test of the amplifier B

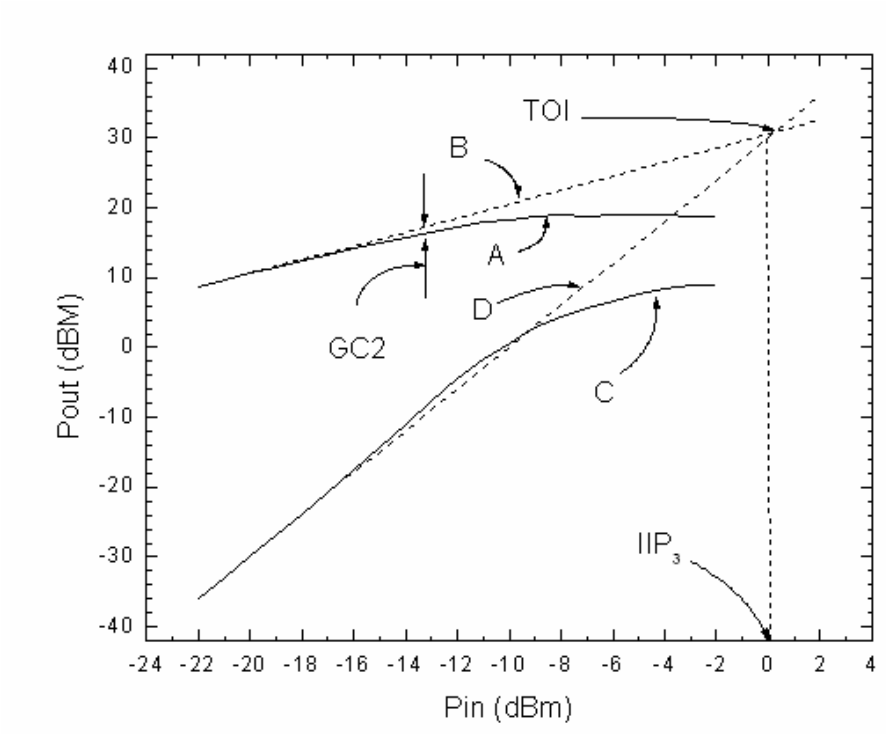

Figure 6-4 The measurement data of two-tone test of the amplifier B

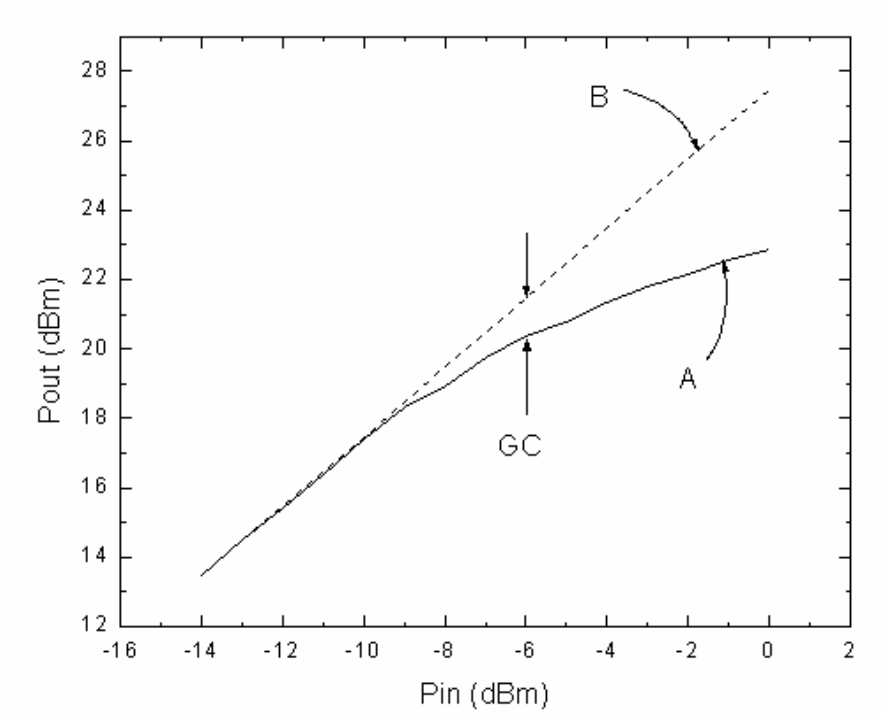

Figure 6-5 The measurement data of one-tone test of the amplifier C

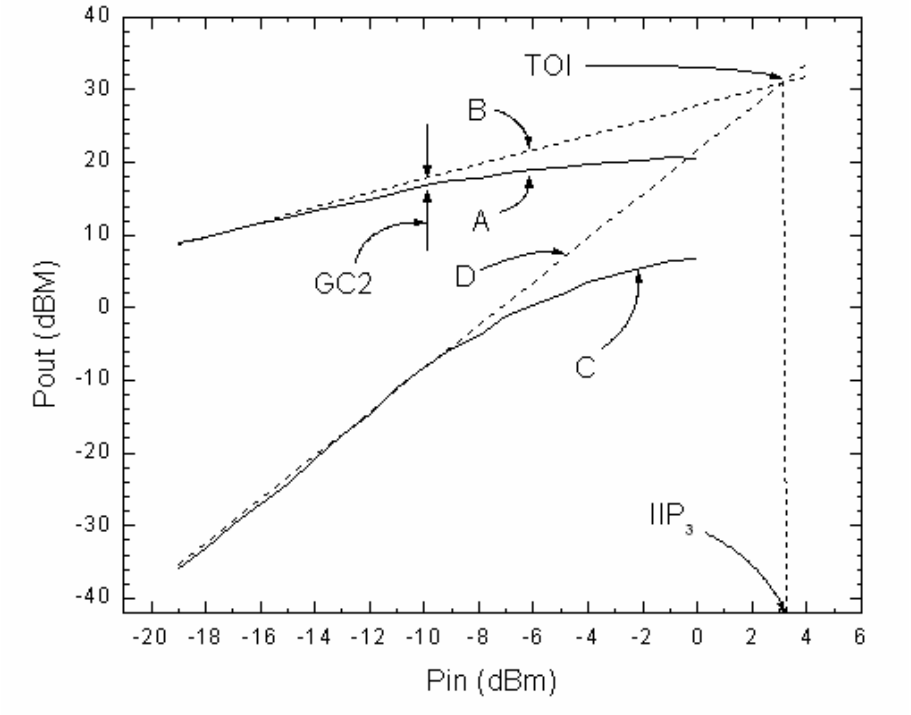

Figure 6-6 The measurement data of two-tone test of the amplifier C

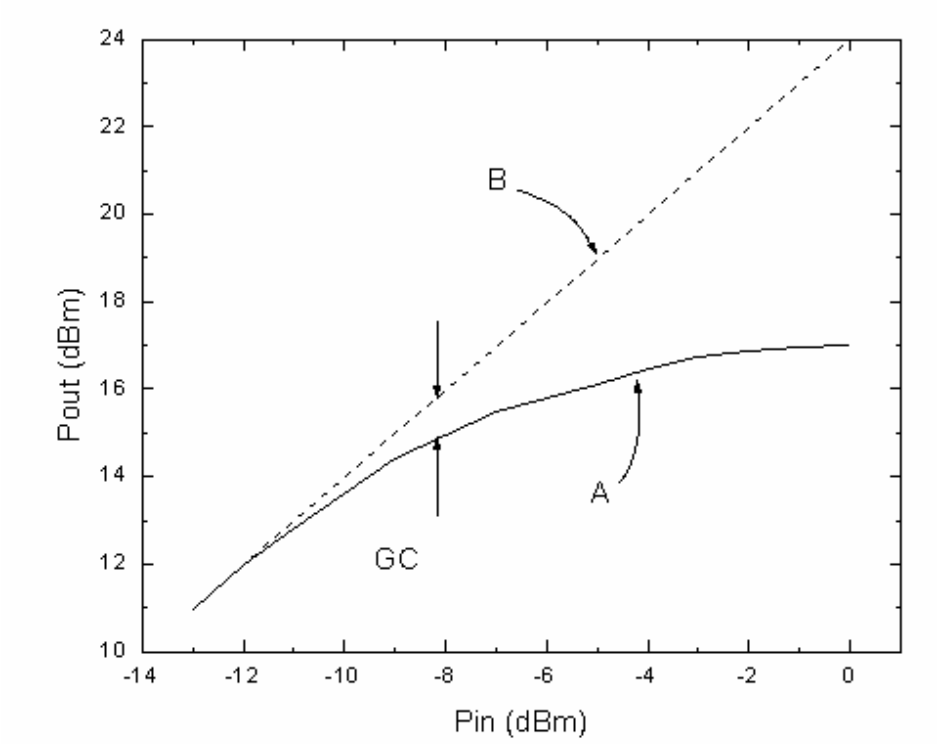

Figure 6-7 The measurement data of one-tone test of the amplifier D

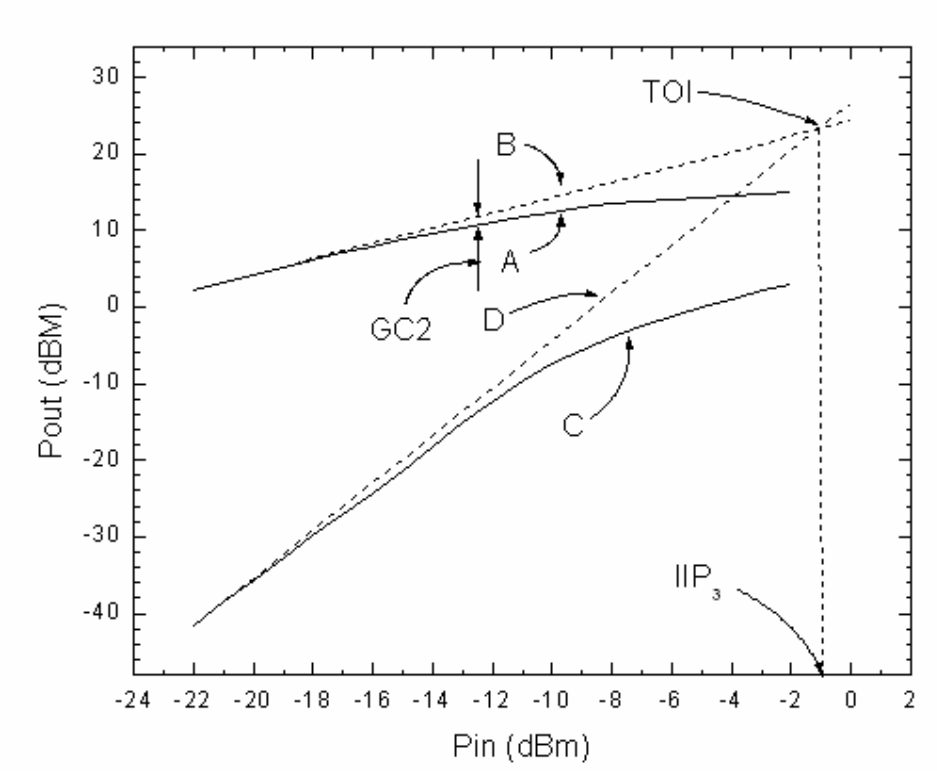

Figure 6-8 The measurement data of two-tone test of the amplifier D

Table 6-1 The summary of the measurement results of commercial PAs

Device Name	$IP_{1\text{-}dB}$*	$IP_{1\text{-}dB,2}$**	IIP_3**	IIP_3-$IP_{1\text{-}dB}$
Amplifier A	-11 dBm	-16 dBm	-4.4 dBm	6.6 dB
Amplifier B	-8 dBm	-13 dBm	0 dBm	8 dB
Amplifier C	-6 dBm	-10 dBm	3 dBm	9 dB
Amplifier D***	-8 dBm	-12.5 dBm	-1 dBm	7 dB

*One-tone test : Source frequency = 2.45 GHz
**Two-tone test : frequencies = 2.45 GHz, 2.46 GHz
*** Amplifier D is tested at 5.2 GHz (and 5.21 GHz).

of the one-tone test of the amplifier D. The input frequency in this one-tone test is 5.2 GHz. $IP_{1\text{-}dB}$ is -8 dBm in this figure. The applied two frequencies in two-tone test are 5.2 GHz and 5.21 GHz. IIP_3 is -1 dBm and $IP_{1\text{-}dB,2}$ is -12.5 dBm. The measurement data of these amplifiers are summarized in Table 6-1. In this table, the difference between 1 dB gain compression point and third-order intercept point is not constant.

6.3 IIP_3 Estimation from the One-tone Data

A robust algorithm which analyzes the measurement data with error is used for the wideband RF amplifier. In RF power amplifier, another algorithm is required to examine the nonlinear characteristics since the nonlinear behavior of power amplifier is somewhat different from that of wideband RF amplifier.

A fitting method which extracts the nonlinear coefficients simultaneously from one-tone data and is used in the analysis of simulation data in chapter 4 is useful in the nonlinear analysis of RF power amplifiers. The fitting range is adjusted through linear regression analysis. The increase of fitting range reduces the standard error of each coefficient but the residual, the difference between real model and fitting model, increases since the high amplifier input power includes energy in higher-order nonlinear factors than that of fitting model. Both the analysis of the residual and that of standard

errors of each coefficients help to define the appropriate range for the fitting model. Third-order intercept point can be estimated using the extracted nonlinear coefficients after fitting this range. In this section, two fitting models are applied to the data of commercial power amplifiers. One of two fitting model is

$$y = K_1 x + \frac{3}{4} K_3 x^3 \tag{6-1}$$

Equation (6-1) is the simplest form for the explanation of the nonlinear gain curve. The other model applied to the fitting gain curve is

$$y = K_1 x + \frac{3}{4} K_3 x^3 + \frac{5}{8} K_5 x^5 \tag{6-2}$$

The difference between two fitting models is whether or not to include the fifth-order nonlinear coefficient in the fitting model. Through the application of these two models to the data of commercial PAs, the effect of adding fifth-order nonlinear coefficient is investigated.

The first fitting model, equation (6-1) is applied to the one-tone data of the amplifier A shown in Figure 6-1. Figure 6-9 shows the value of coefficient K_1 from the fitting results. In this graph, the x-axis represents the end point of fitting range from the starting point, -16 dBm. When the fitting range changes, the fitted result changes also. Figure 6-10 shows the value of coefficient K_3. The best fitting range should be chosen using the standard errors of each coefficients and the sum of squares of the residuals which are explained in Chapter 4. The standard errors are defined in equation (4-2). Figure 6-11 shows the standard errors of coefficients K1 and K3. In this graph, Point A indicates the smallest value in both the standard errors of K1 and K3. From the standard error of the coefficients, the fitting range (-16 dBm, -9 dBm) is chosen. The sum of

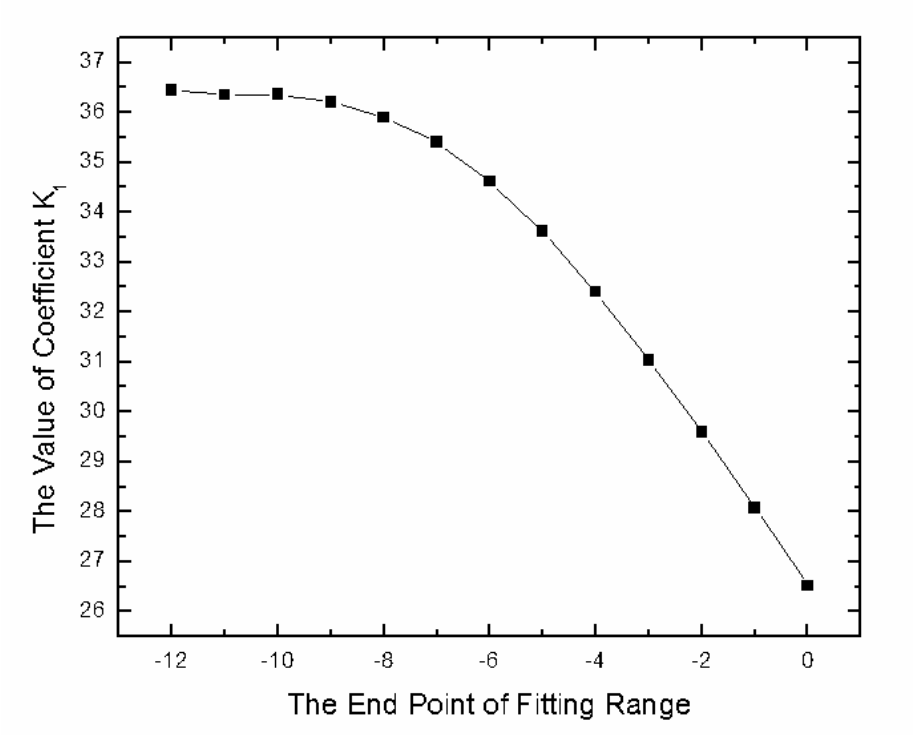

Figure 6-9 The value of coefficient K_1 (amplifier A)

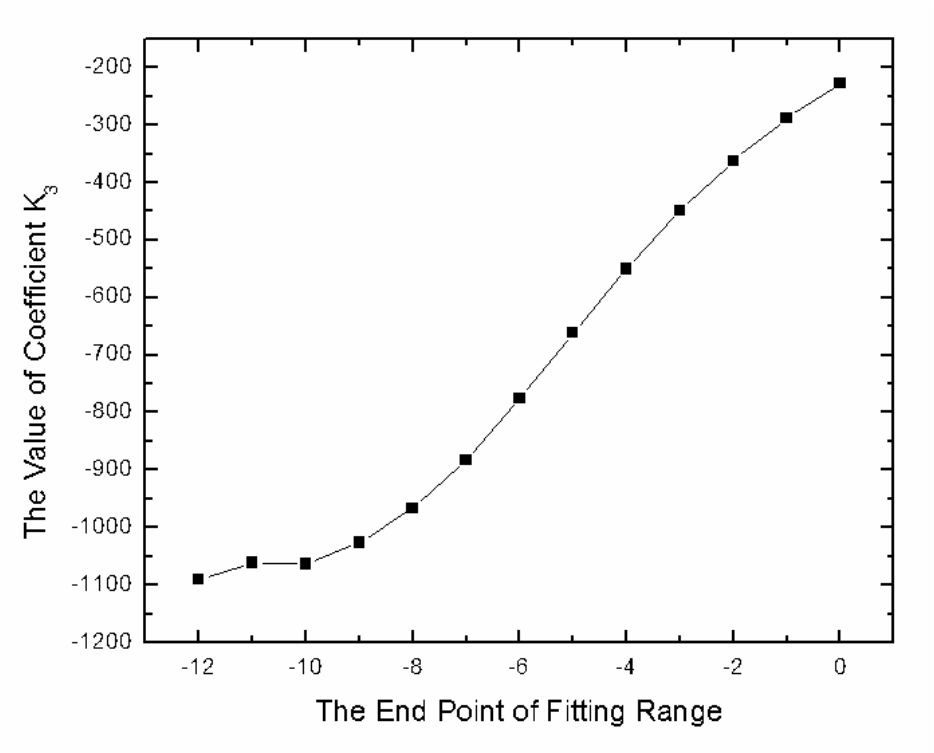

Figure 6-10 The value of coefficient K_3 (amplifier A)

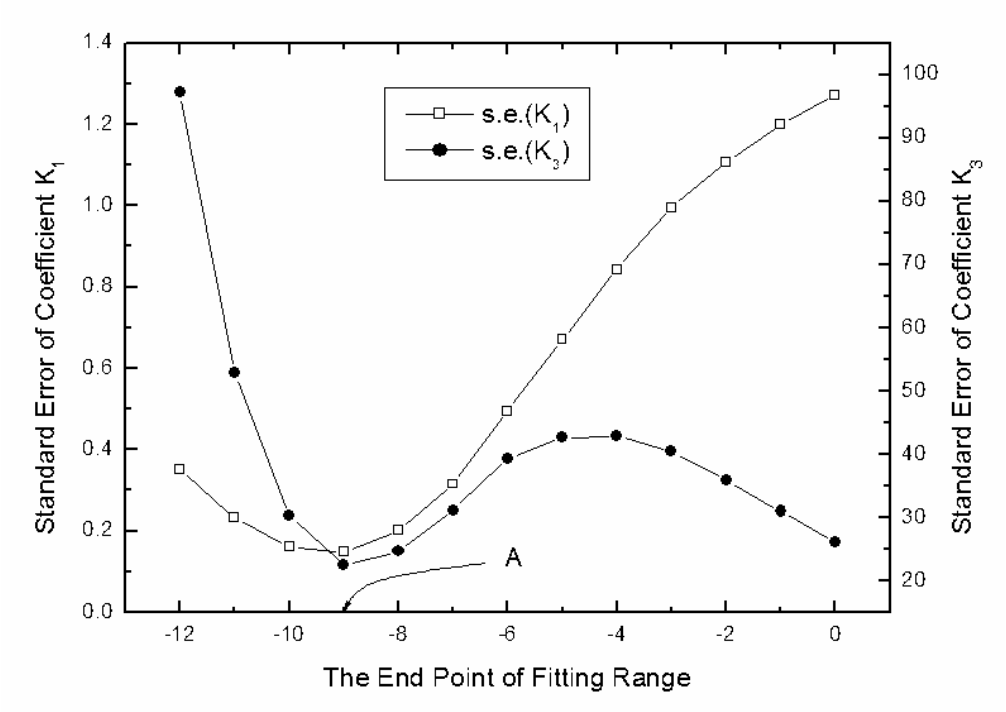

Figure 6-11 Standard errors of K_1 and K_3 (amplifier A)

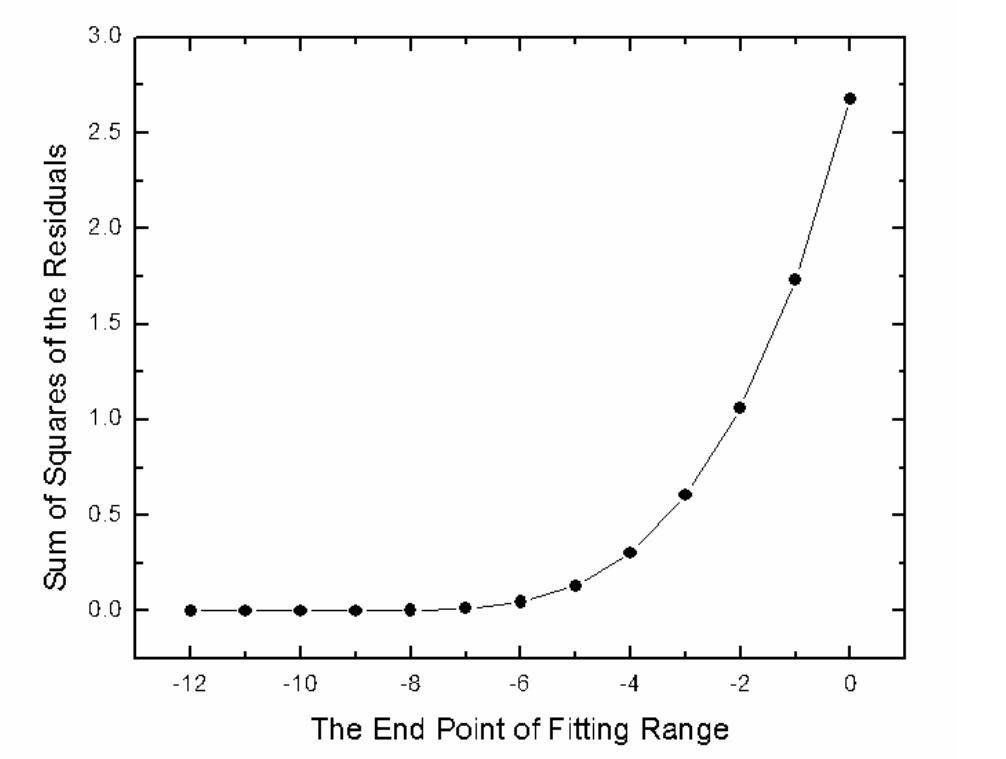

Figure 6-12. Sum of squares of the residuals (Amplifier A)

Table 6-2 The summary of fitting results (amplifier A)

Parameters	Values
Coefficient K_1	36.20
s.e.(K_1)	0.15
Coefficient K_3	-1026
s.e.(K_3)	22
Calculated IIP_3	-3.27 dBm

squares of the residual in this fitting range is also small in Figure 6-12. The fitting results are summarized in Table 6-2. The calculated IIP_3 is -3.27 dBm in this table. The difference between the estimated IIP_3 and the measured IIP_3 is 1.13 dB since the measured IIP_3 is -4.4 dBm in Table 6-1.

The second fitting model, equation (6-2) is applied the same data of the amplifier A. Figure 6-13, 6-14 and 6-15 show the values of K_1, K_3 and K_5 respectively. From these graphs, the values of nonlinear coefficients will be chosen after the best fitting range is decided. From Figure 6-16 and 6-17, Point A denotes the end point of the best fitting range which satisfies the condition that the standard errors of nonlinear coefficients become small simultaneously. The best fitting range in this fitting process is (-16 dBm, -5 dBm). In this range, the sum of squares of the residuals is small in Figure 6-18. The result of the fitting application is summarized in Table 6-3. In this table, the calculated value, -4.31 dBm is very close to the measured value, -4.4 dBm. The first fitting model has less standard errors of each coefficient than the second fitting model.

The data of the amplifier B in Figure 6-3 is used for the IIP_3 prediction from one-tone measurement. Using fitting model, equation (6-1), the values of K_1 and K_3 are shown in Figure 6-19 and Figure 6-20. Figure 6-21 shows the standard errors of nonlinear

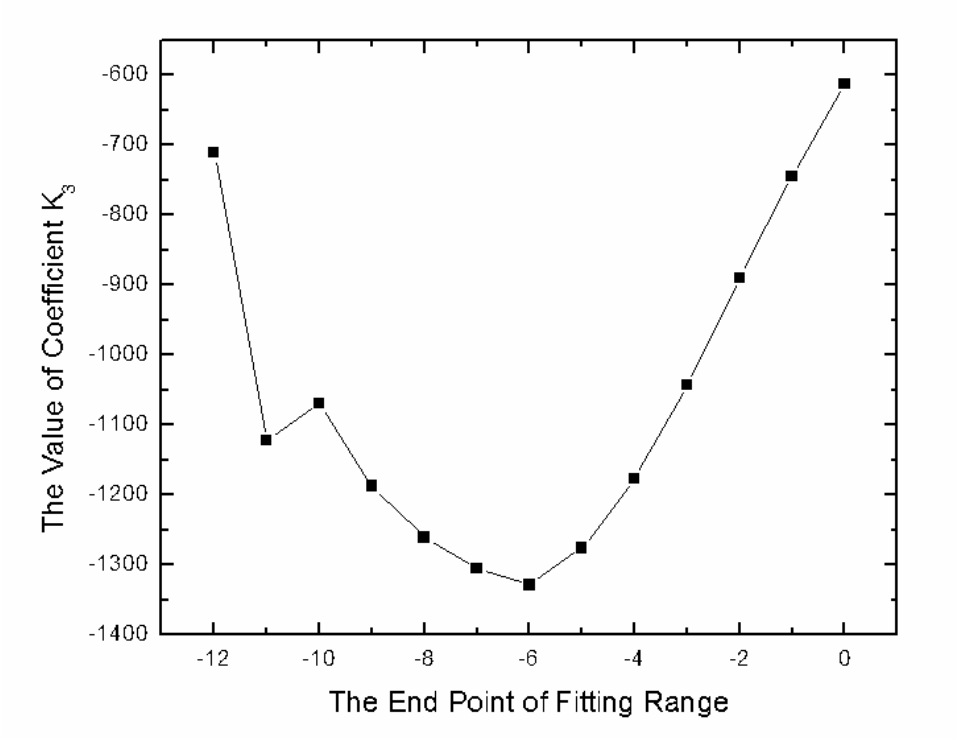

Figure 6-13 The value of coefficient K_1 (amplifier A)

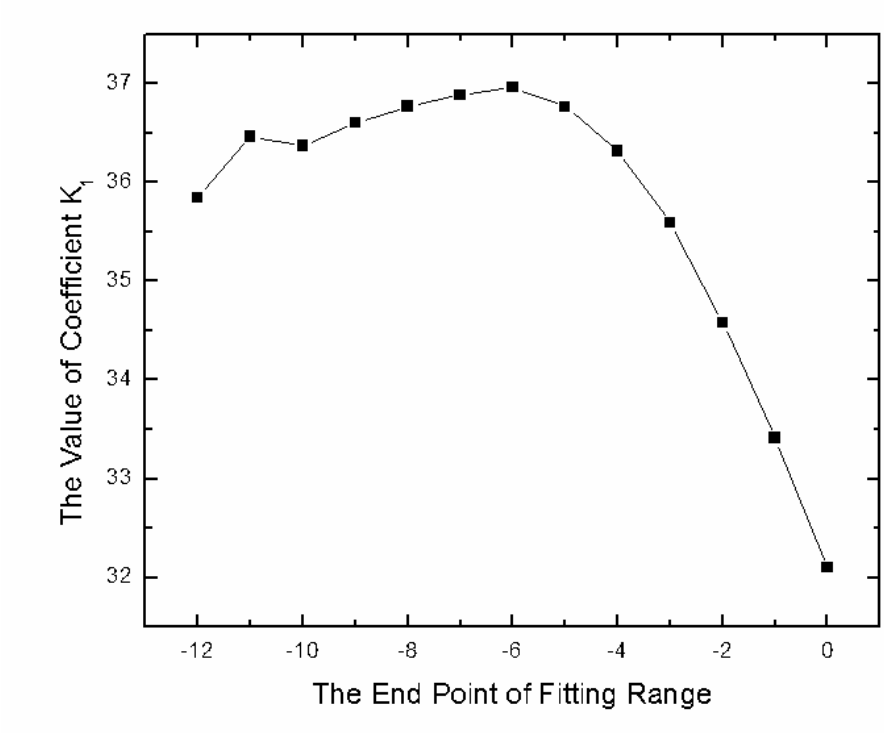

Figure 6-14 The value of coefficient K_3 (amplifier A)

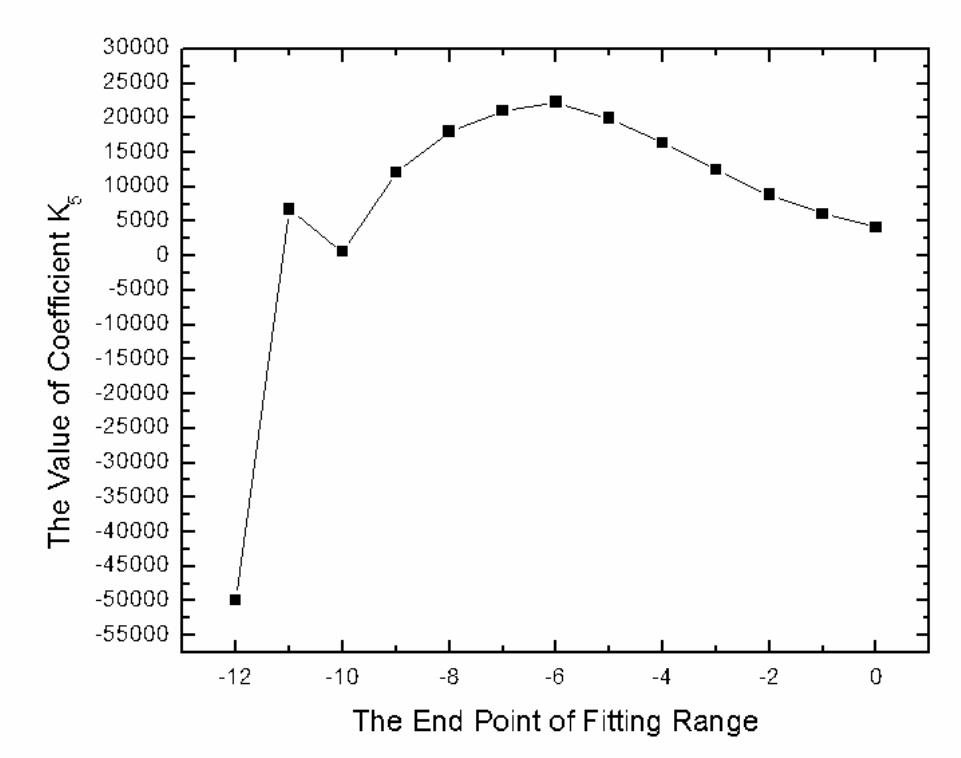

Figure 6-15 The value of coefficient K_5 (amplifier A)

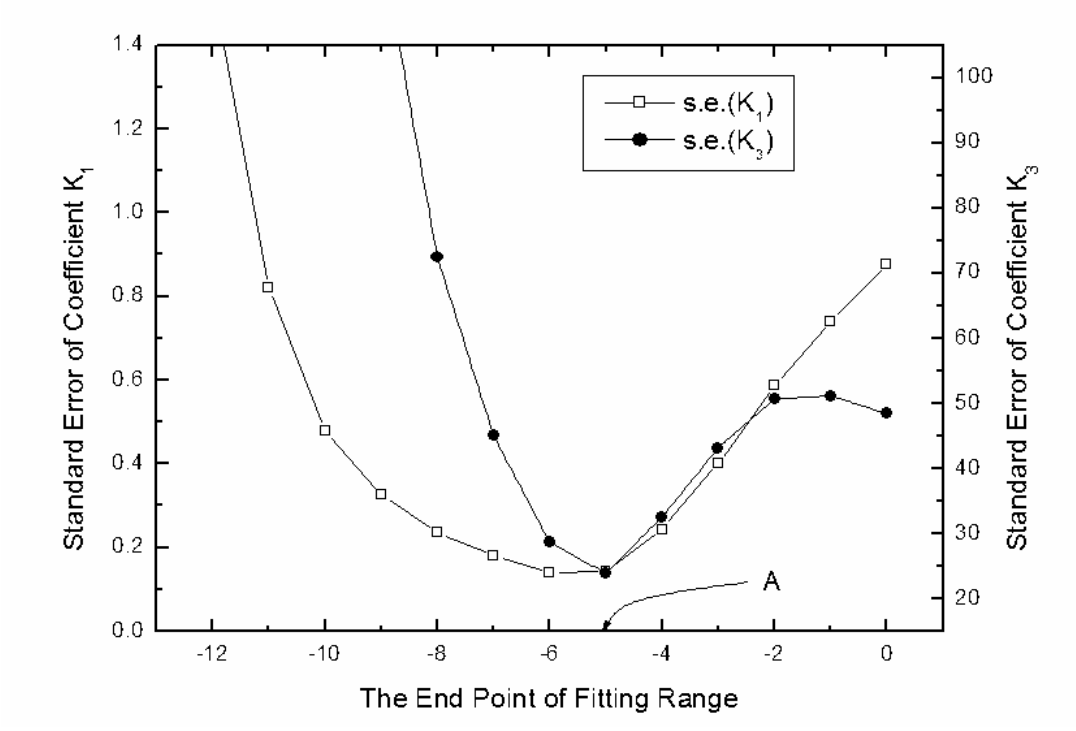

Figure 6-16 Standard errors of K_1 and K_3 (amplifier A)

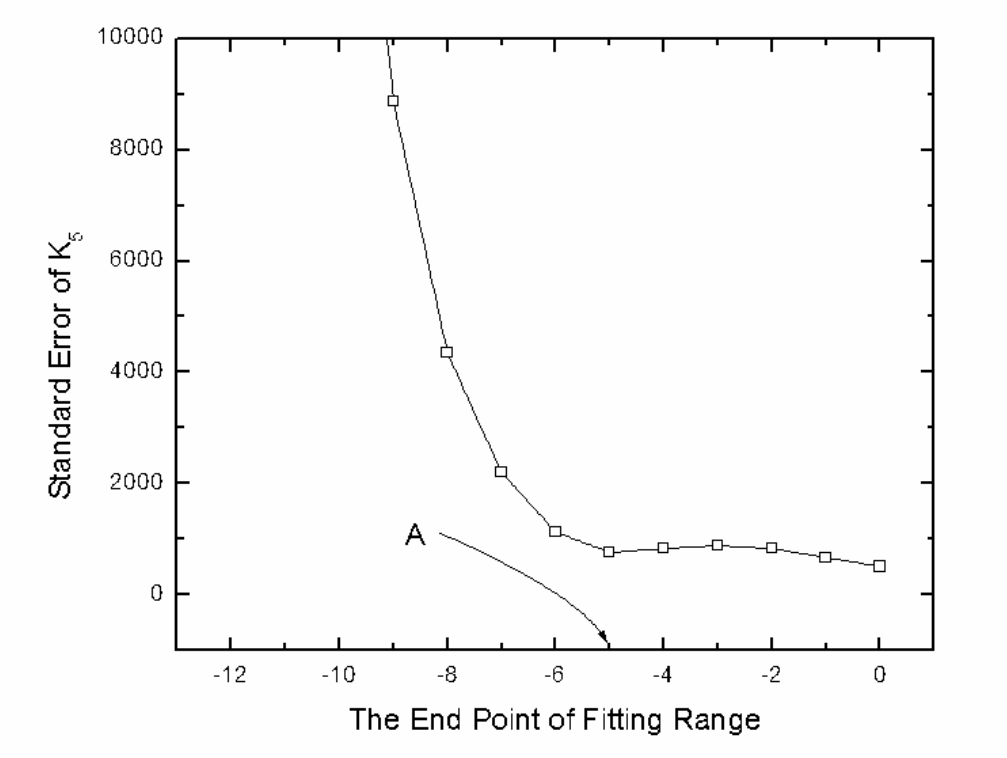

Figure 6-17 Standard error of K_5 (amplifier A)

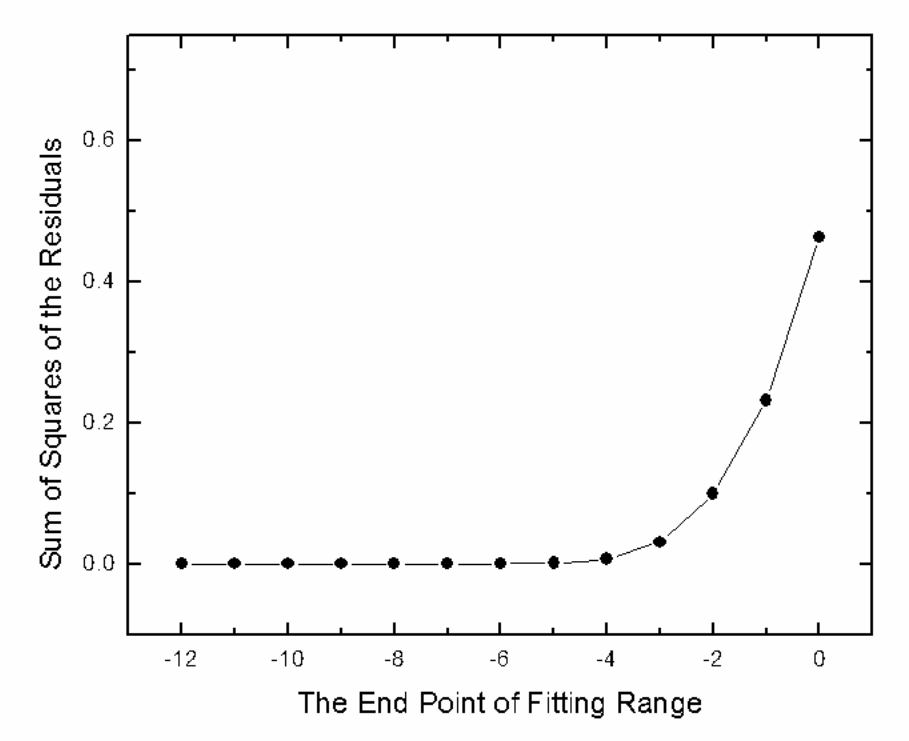

Figure 6-18 Sum of squares of the residuals (amplifier A)

Table 6-3 The summary of fitting results (amplifier A)

Parameters	Values
Coefficient K_1	36.96
s.e.(K_1)	0.14
Coefficient K_3	-1329
s.e.(K_3)	29
Coefficient K_5	22276
s.e.(K_5)	1126
Calculated IIP_3	-4.31 dBm

Table 6-4 The summary of fitting results of the first model (amplifier B)

Parameters	Values
Coefficient K_1	34.50
s.e.(K_1)	0.11
Coefficient K_3	-404
s.e.(K_3)	7
Calculated IIP_3	0.43 dBm

coefficients. In this figure, point A is the best region of this fitting. In the application of the first fitting model, the best fitting range is from -17 dBm to -5 dBm. In the graph of sum of squares of the residuals, Figure 6-22, the value of sum of squares of the residual is under 0.1. In this best fitting range, the fitting result is summarized in Table 6-4. Using extracted nonlinear coefficients, the calculated IIP_3 is 0.43 dBm. Compared to the measured IIP_3, 0 dBm, the estimated IIP_3 is close to the measured value. When the second fitting model is applied to the amplifier B, the values of K_1, K_3 and K_5 extracted from one-tone gain curve in Figure 6-3 are drawn in Figure 6-23, 6-24 and 6-25 separately. The standard errors of K_1 and K_3 are shown in Figure 6-26 and the standard

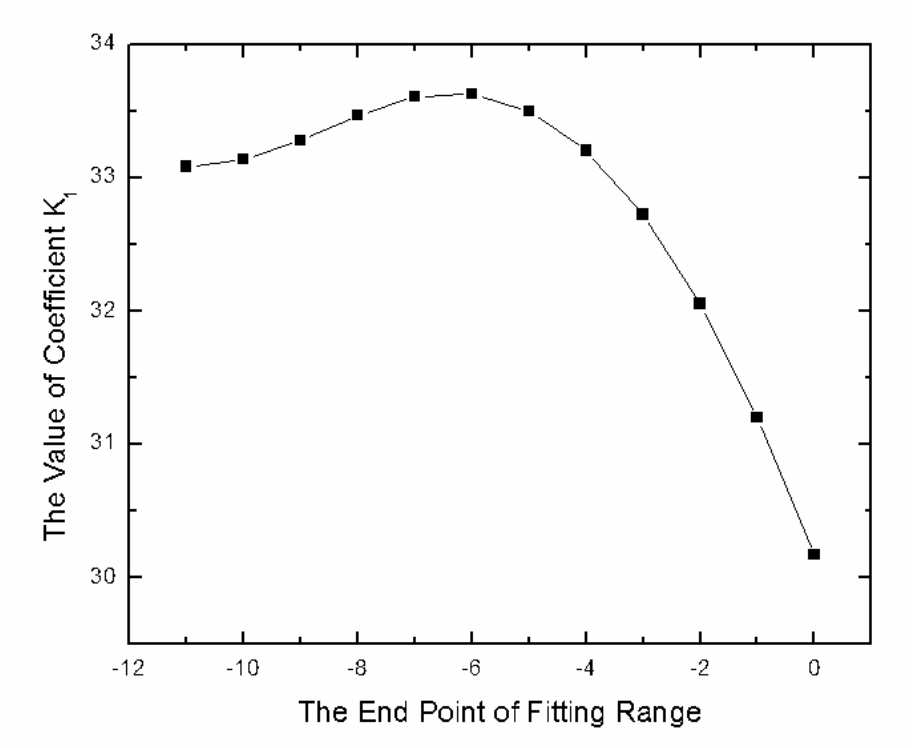

Figure 6-19 The value of coefficient K_1 (amplifier B)

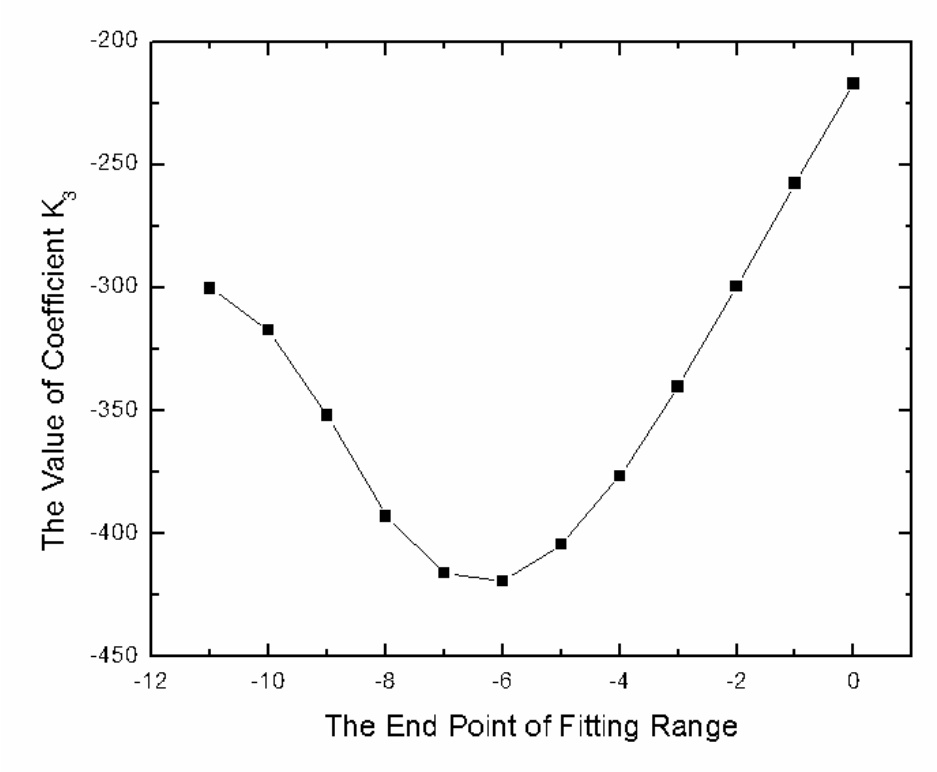

Figure 6-20 The value of coefficient K_3 (amplifier B)

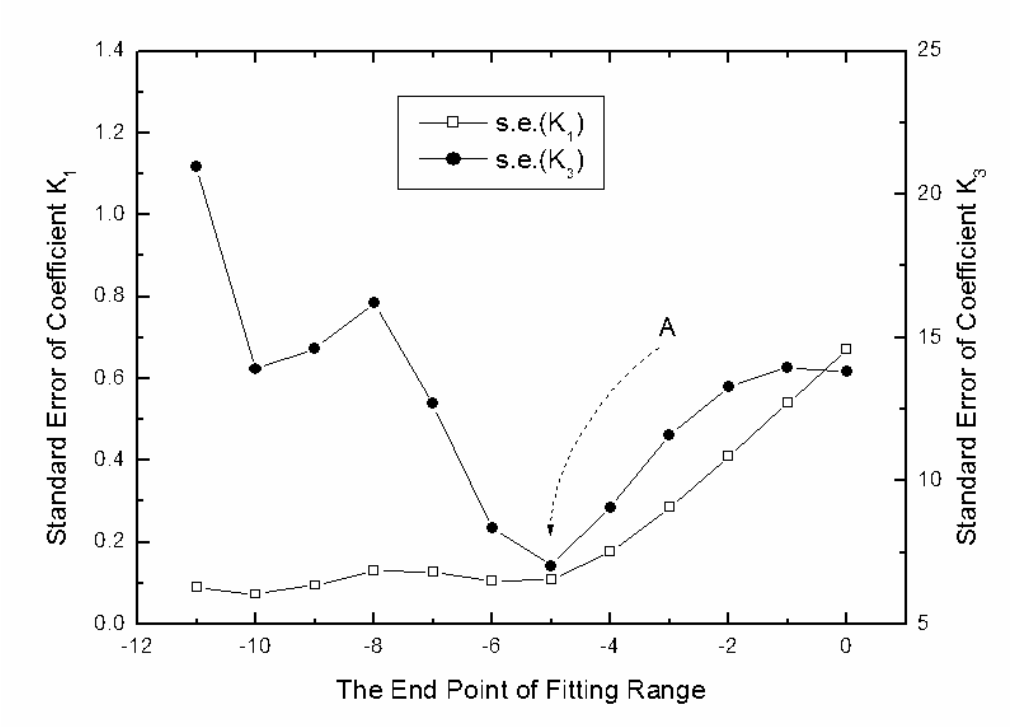

Figure 6-21 Standard errors of K_1 and K_3 (amplifier B)

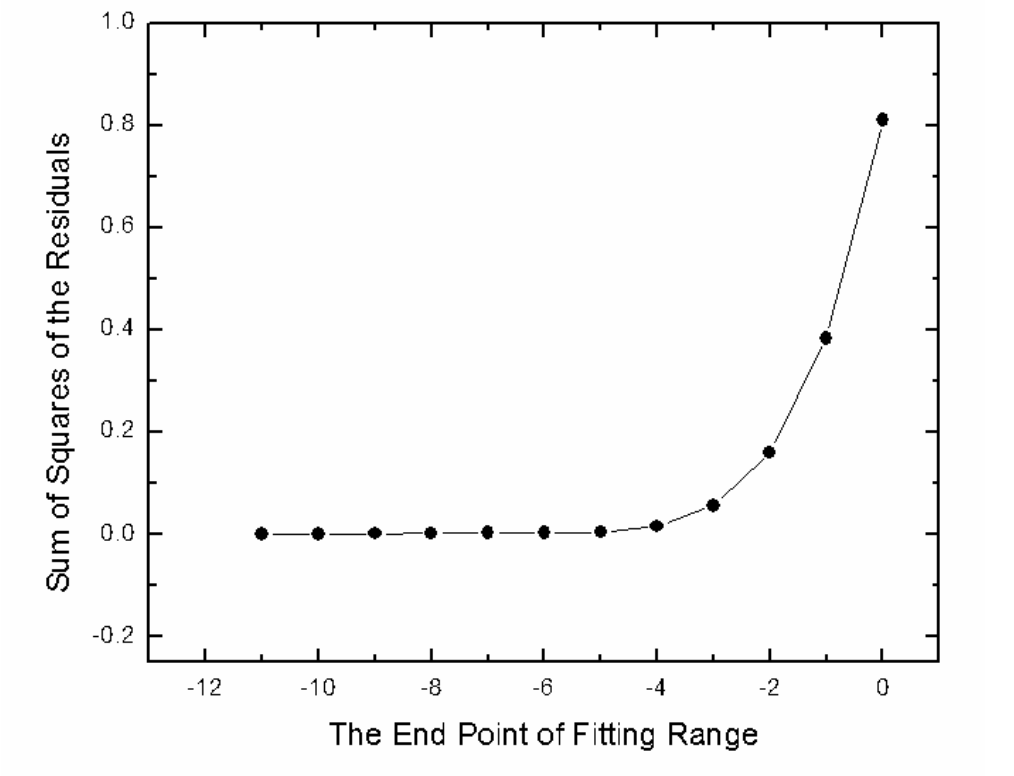

Figure 6-22 Sum of squares of the residuals (amplifier B)

error of K5 is shown in Figure 6-27. It is difficult to find the end point of fitting range which gives small values simultaneously in the standard errors of nonlinear coefficients in Figure 6-26 and 6-27. To choose the best fitting range, three regions denoted by point A, point B and point C in these figures are compared in the standard errors with extracted nonlinear coefficients in Table 6-5. From this table, the region C has the smallest standard errors of three nonlinear coefficients and is chosen for the best fitting region. In this region C, the sum of squares of the residuals are not big in Figure 6-28. Estimated IIP_3 is -0.28 dBm calculated from the fitting result of fitting region (-17 dBm, - 1 dBm) is near around the measured IIP_3, 0 dBm.

The one-tone data of the amplifier C is the third example for the application of fitting algorithm which estimates the third-order intercept point using nonlinear coefficients extracted from the one-tone data of the amplifier. The applied fitting algorithm to this example is the same as that of the previous examples. First, the fitting model represented by equation (6-1) is applied to the gain compression curve of the amplifier C. The values of nonlinear coefficients K_1 and K_3 from fitting results are shown in Figure 6-29 and 6-30. The best fitting range is chosen in the standard errors of

Table 6-5 The summary of fitting results according to fitting region (amplifier B)

Parameters	Region A (-8 dBm)	Region B (-2 dBm)	Region C (-1 dBm)
Coefficient K_1	32.85	33.97	33.77
s.e.(K_1)	0.07	0.14	0.15
Coefficient K_3	-173	-505	-481
s.e.(K_3)	22	12	10
Coefficient K_5	-13790	3471	3003
s.e.(K_5)	1352	198	135
Calculated IIP_3	4.05 dBm	-0.48 dBm	-0.28 dBm

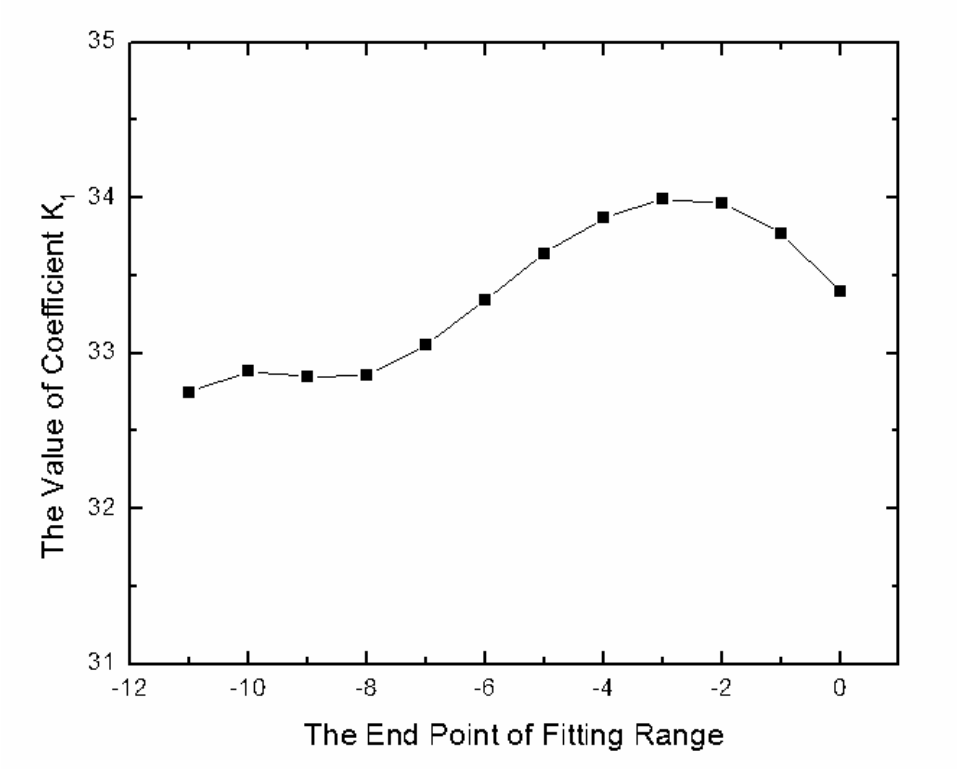

Figure 6-23 The value of coefficient K_1 (amplifier B)

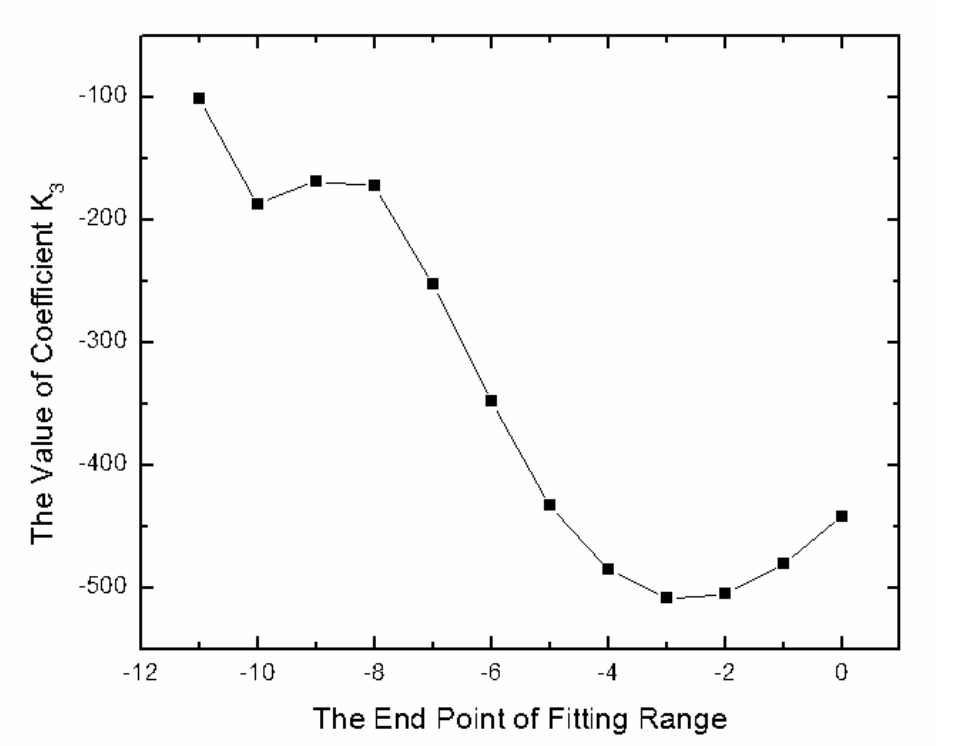

Figure 6-24 The value of coefficient K_3 (amplifier B)

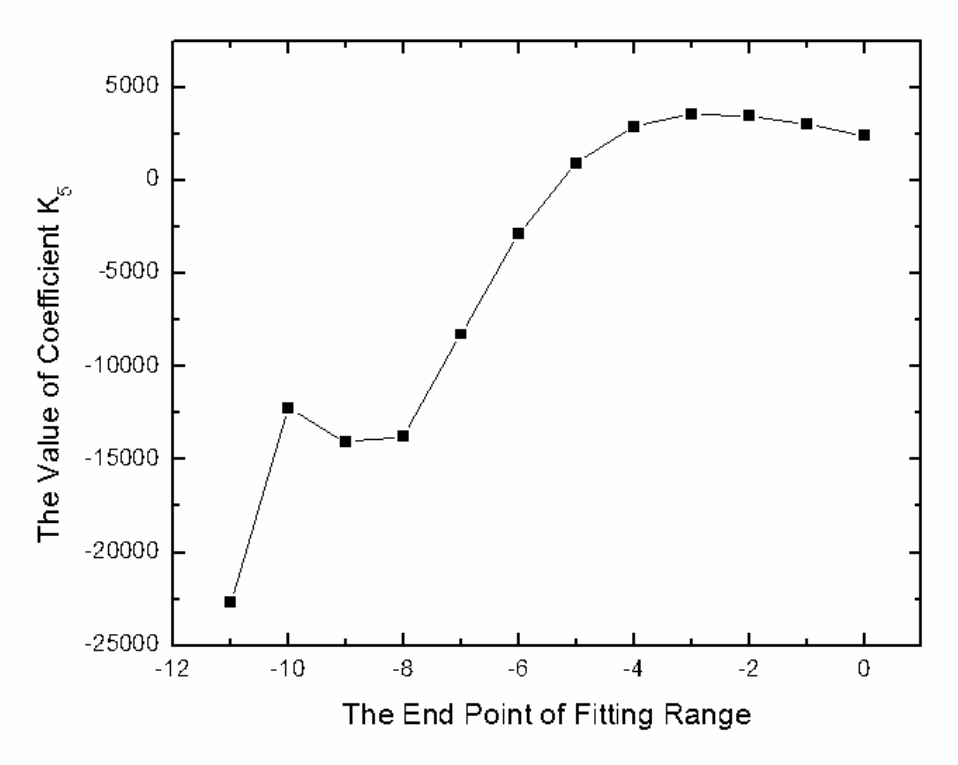

Figure 6-25 The value of coefficient K_5 (amplifier B)

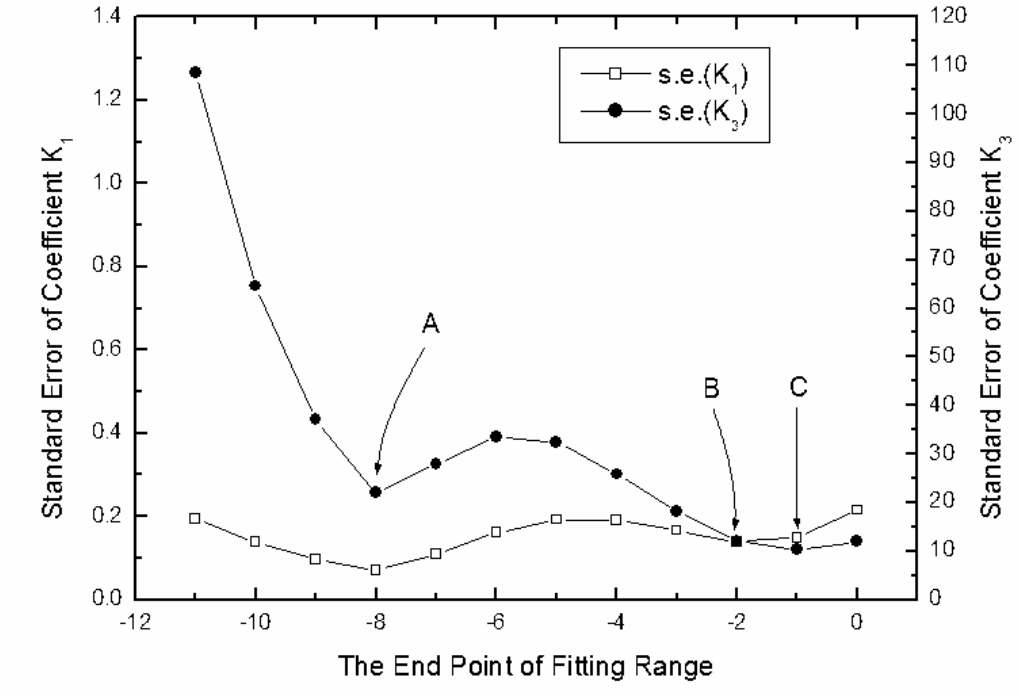

Figure 6-26 Standard errors of K_1 and K_3 (amplifier B)

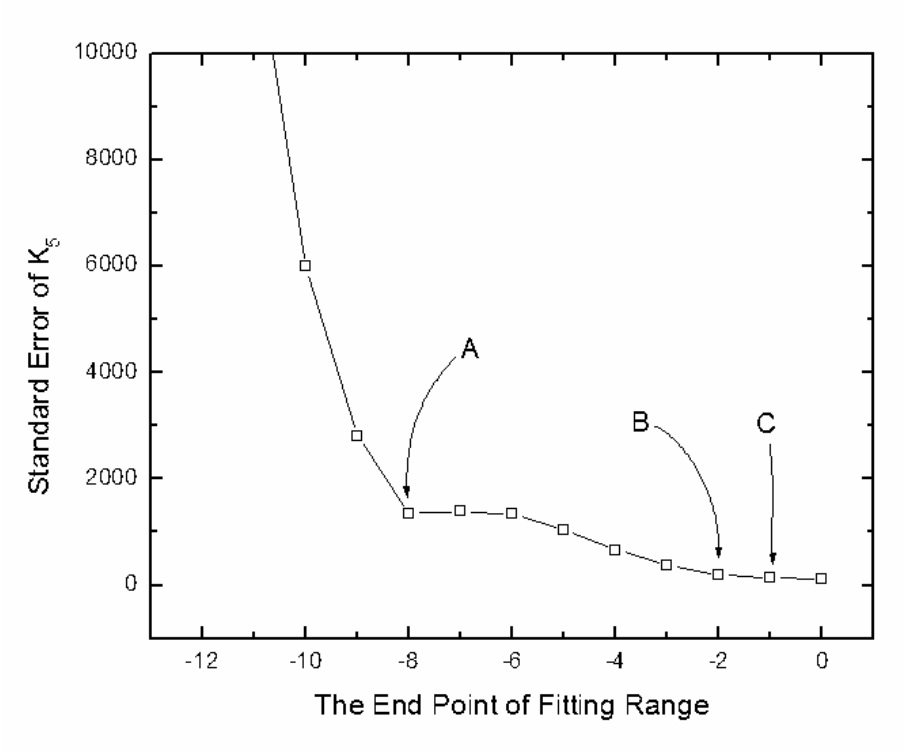

Figure 6-27 Standard error of K_5 (amplifier B)

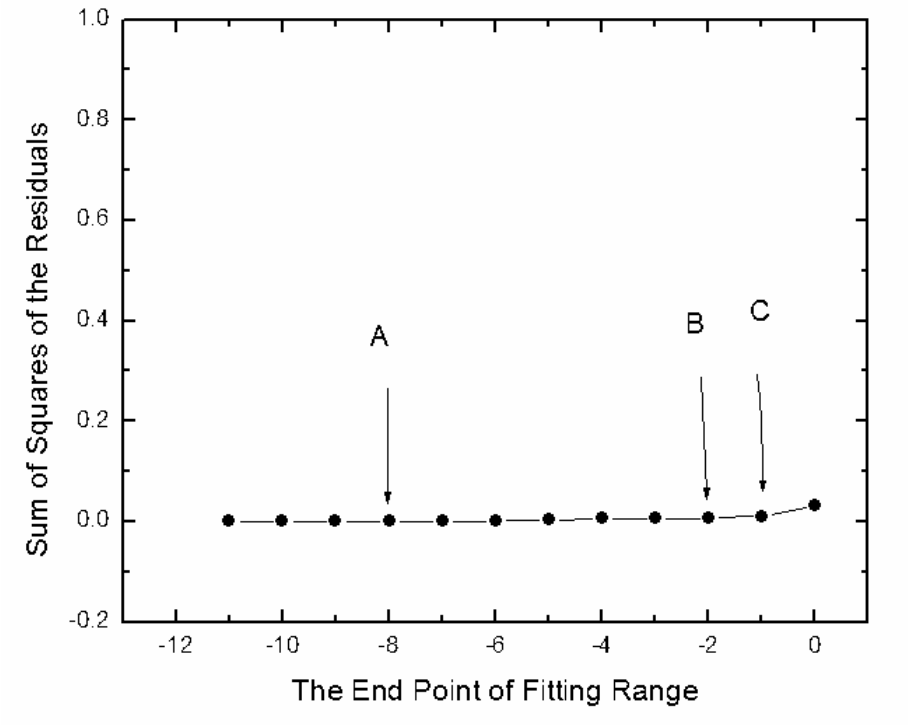

Figure 6-28 Sum of squares of the residuals (amplifier B)

Table 6-6 The summary of fitting results of the first model (amplifier C)

Parameters	Values
Coefficient K_1	24.50
s.e.(K_1)	0.19
Coefficient K_3	-196
s.e.(K_3)	8
Calculated IIP_3	2.2 dBm

K_1 and K_3 in Figure 6-31. Point A indicates the best fitting range from -14 dBm to -3 dBm. To confirm this range in the aspects of the residuals, the sum of squares of the residuals is checked in Figure 6-32. The value of sum of squares of the residuals is small in this fitting range. The fitting results are listed in Table 6-6. The calculated IIP_3 is 2.2 dBm. Figure 6-33, 6-34 and 6-35 shows the values of K_1, K_3 and K_5 when the second fitting model is applied to the one-tone data of the amplifier C in Figure 6-5. To determine the values of the nonlinear coefficients, the best fitting range is chosen in the standard error graphs of Figure 6-36 and 6-37. In Figure 6-36 and 6-37, the standard errors of K_1, K_3 and K_5 decrease when the fitting width increases. The best fitting range in this example is from -14 dBm to 0 dBm. The sum of squares of the residuals in Figure 6-38 is also small in this fitting range. Table 6-7 summarizes the fitting result in the fitting range from -14 dBm to 0 dBm. The calculated value of IIP3 is 1.16 dBm. The measured IIP3 of the amplifier C is 3 dBm in Table 6-1. The fitting result of the first model is better than that of the second model in this example.

The one-tone data of the amplifier D in Figure 6-7 is used as the final example of the fitting algorithm. In this example, the two fitting models are applied to this gain curve in Figure 6-7. The input frequency of the one-tone data is 5.2 GHz and is different from

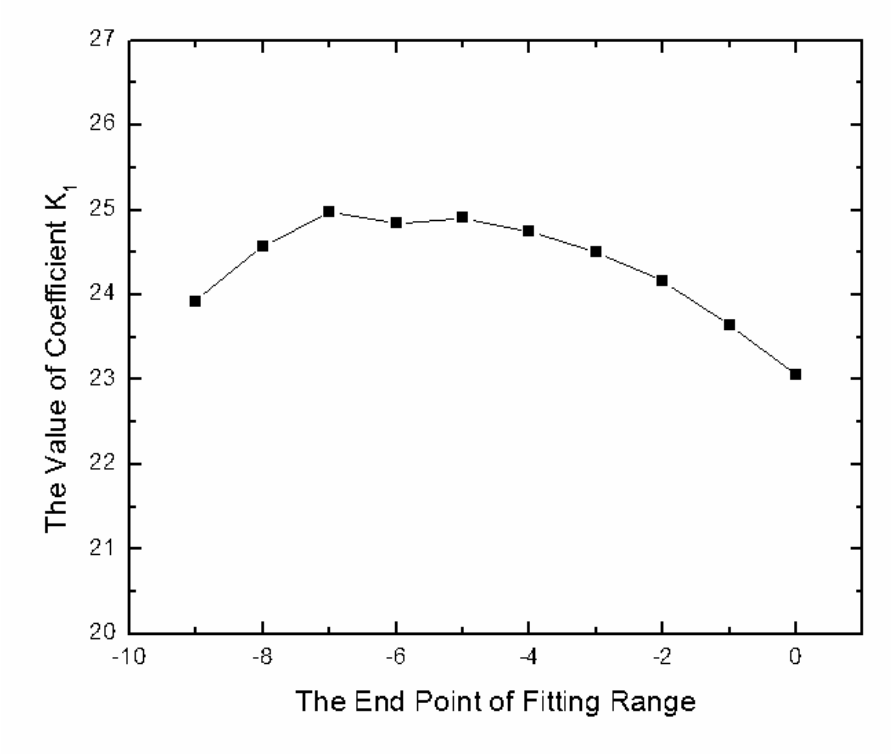

Figure 6-29 The value of coefficient K_1 (amplifier C)

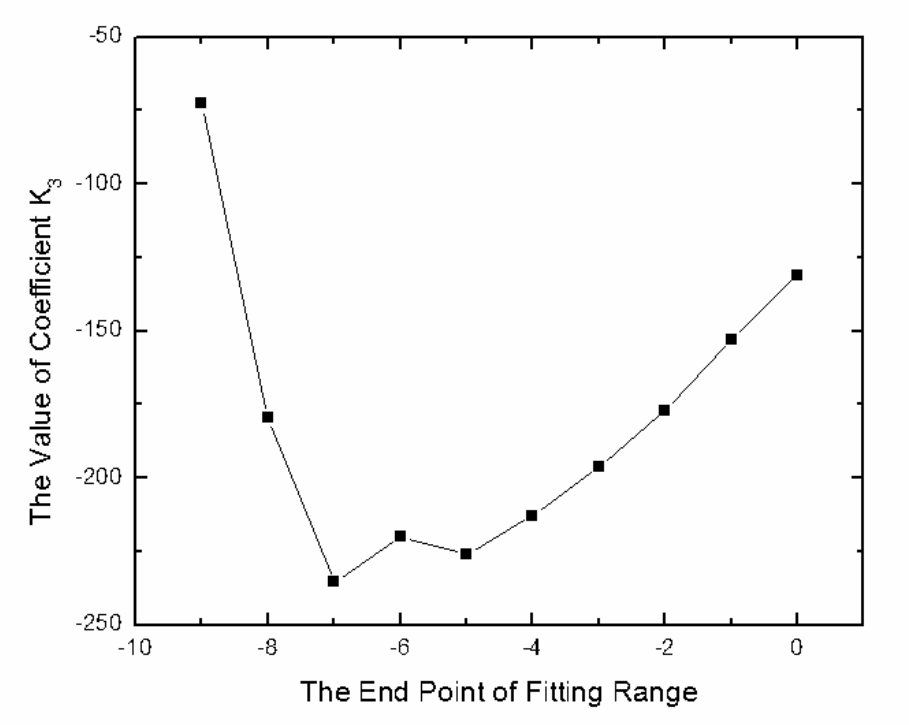

Figure 6-30 The value of coefficient K_3 (amplifier C)

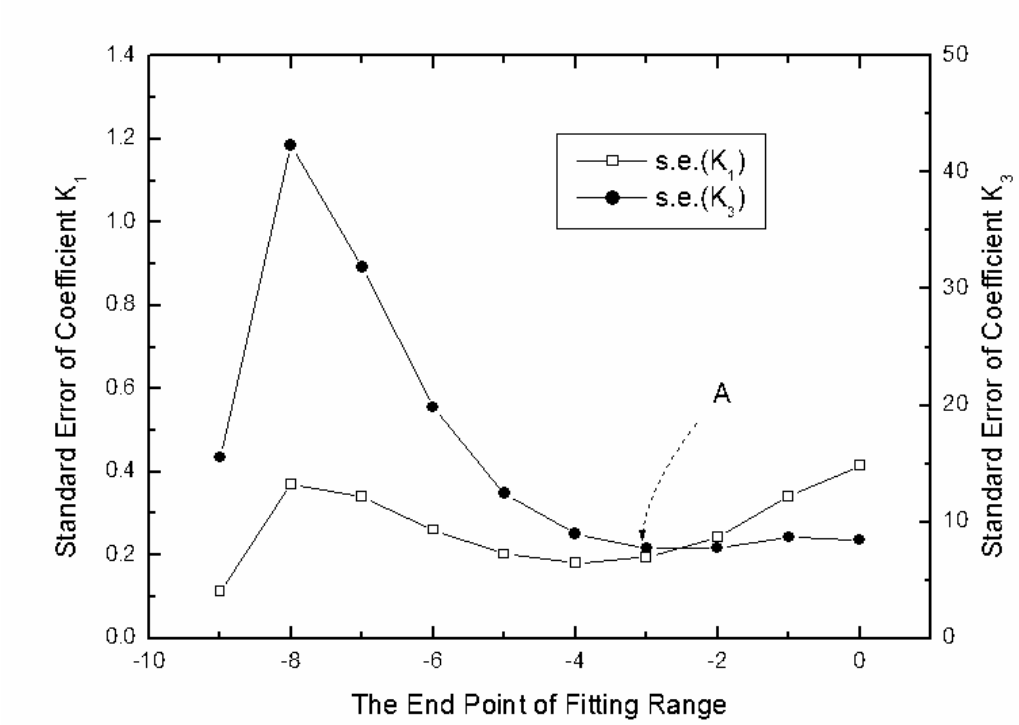

Figure 6-31 Standard errors of K_1 and K_3 (amplifier C)

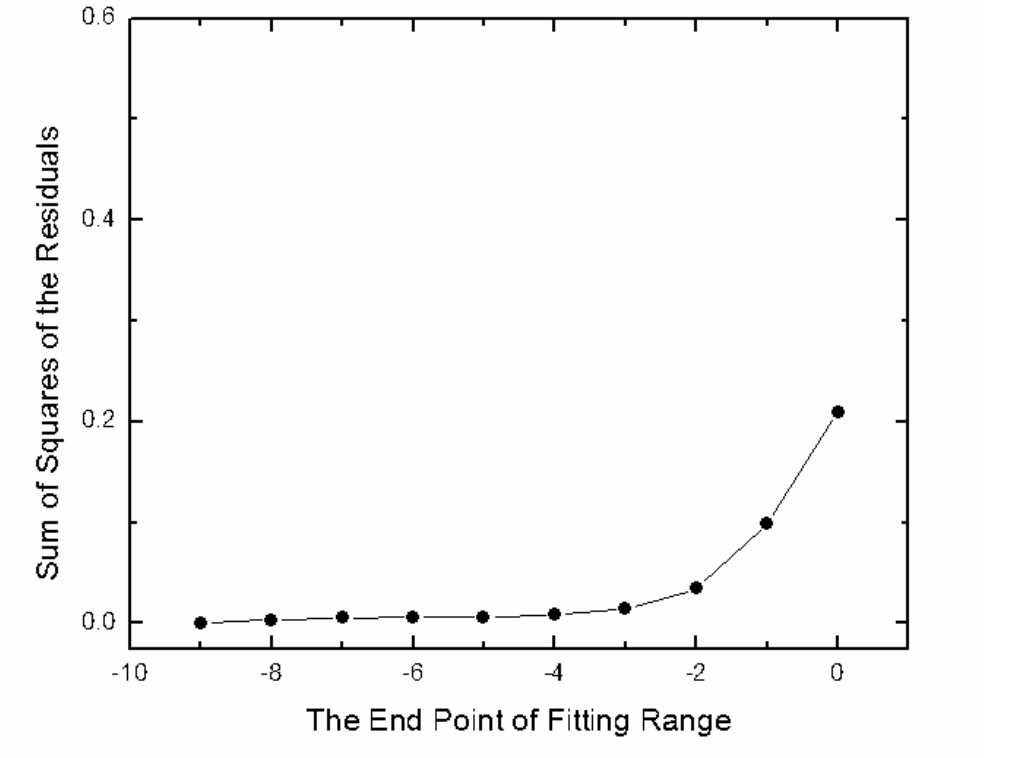

Figure 6-32 Sum of squares of the residuals (amplifier C)

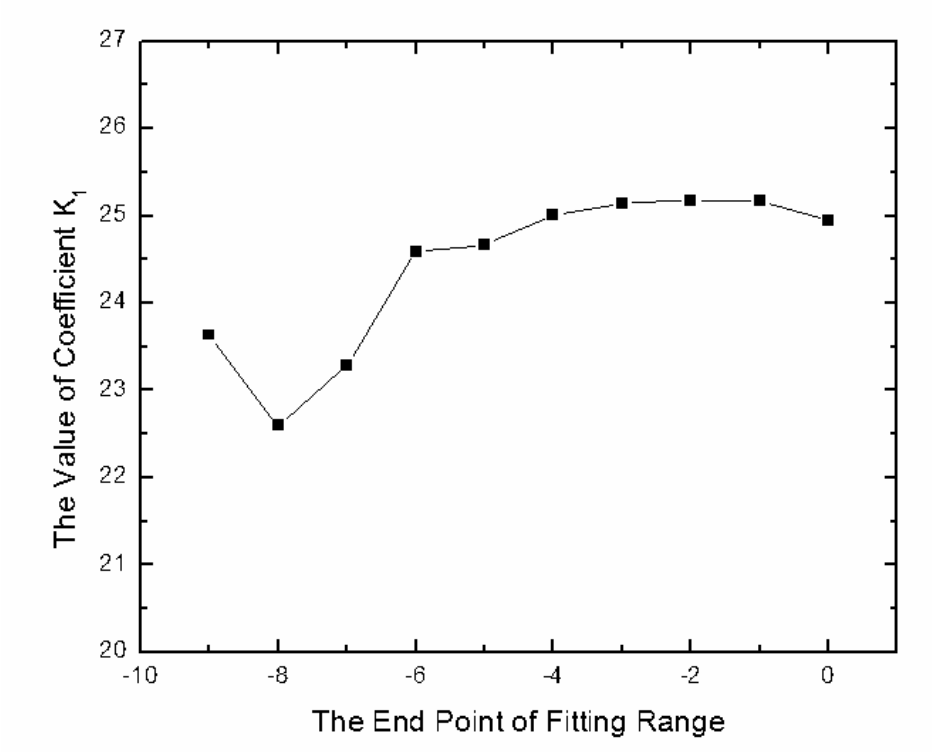

Figure 6-33 The value of coefficient K_1 (amplifier C)

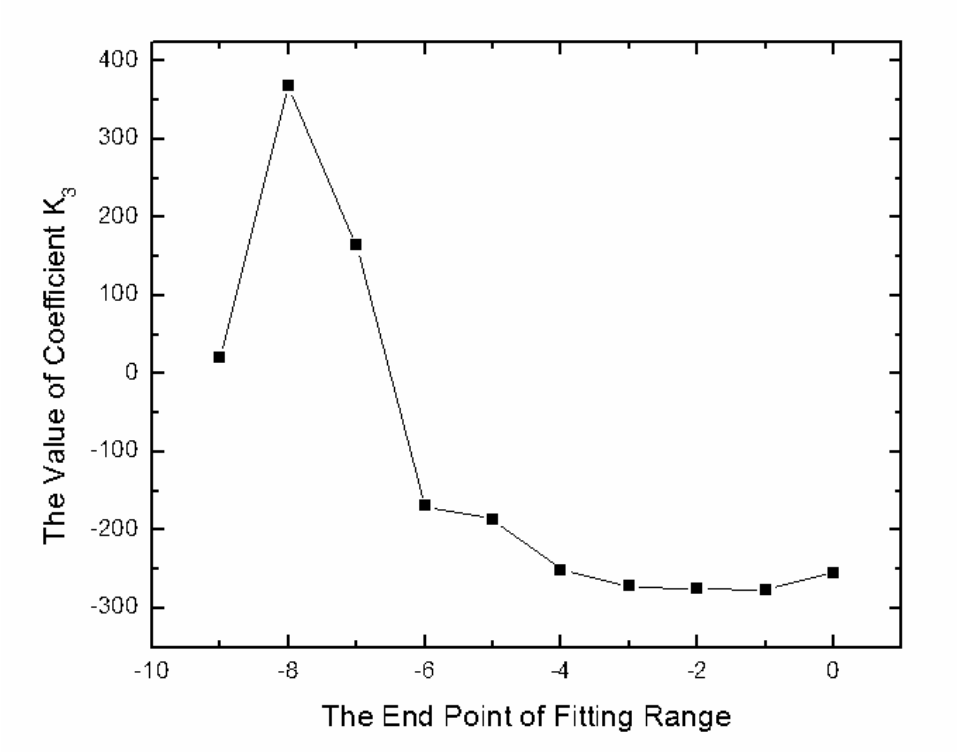

Figure 6-34 The value of coefficient K_3 (amplifier C)

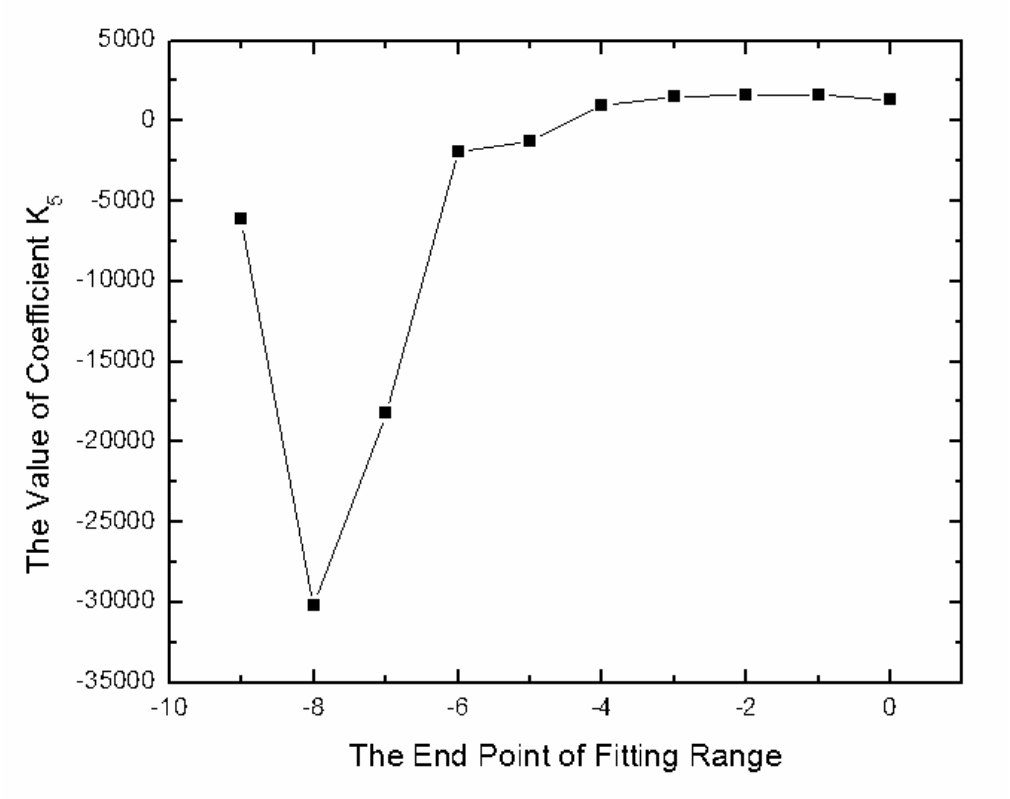

Figure 6-35 The value of coefficient K_5 (amplifier C)

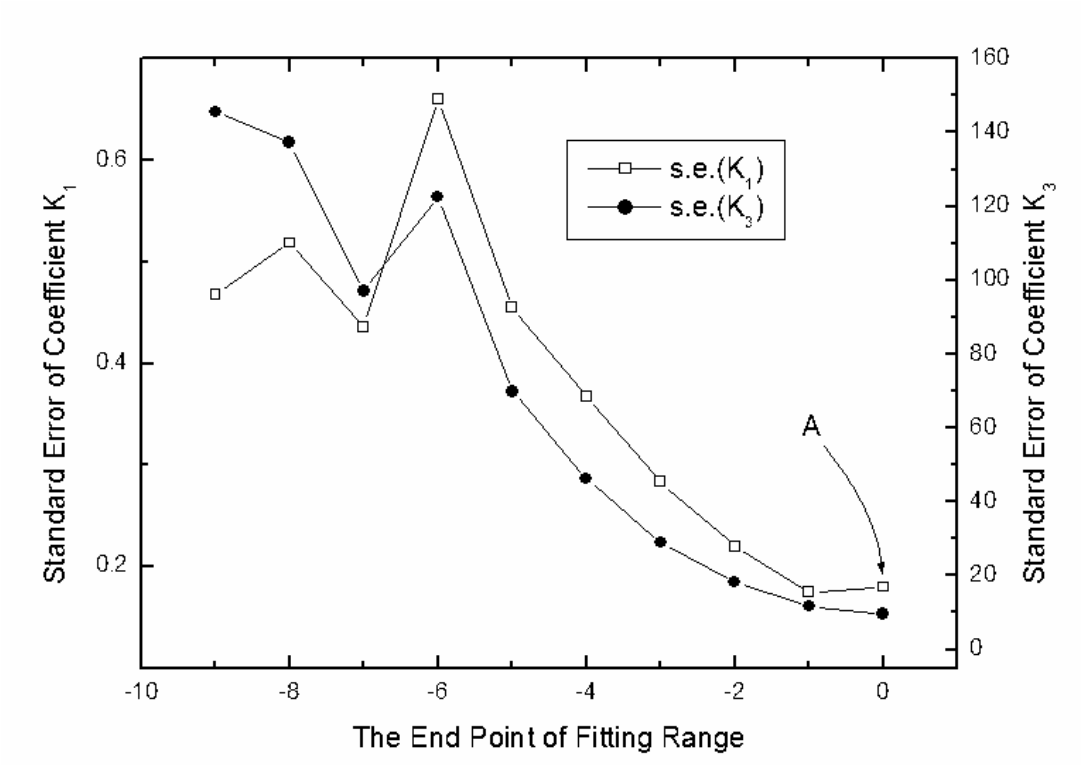

Figure 6-36 Standard errors of K_1 and K_3 (amplifier C)

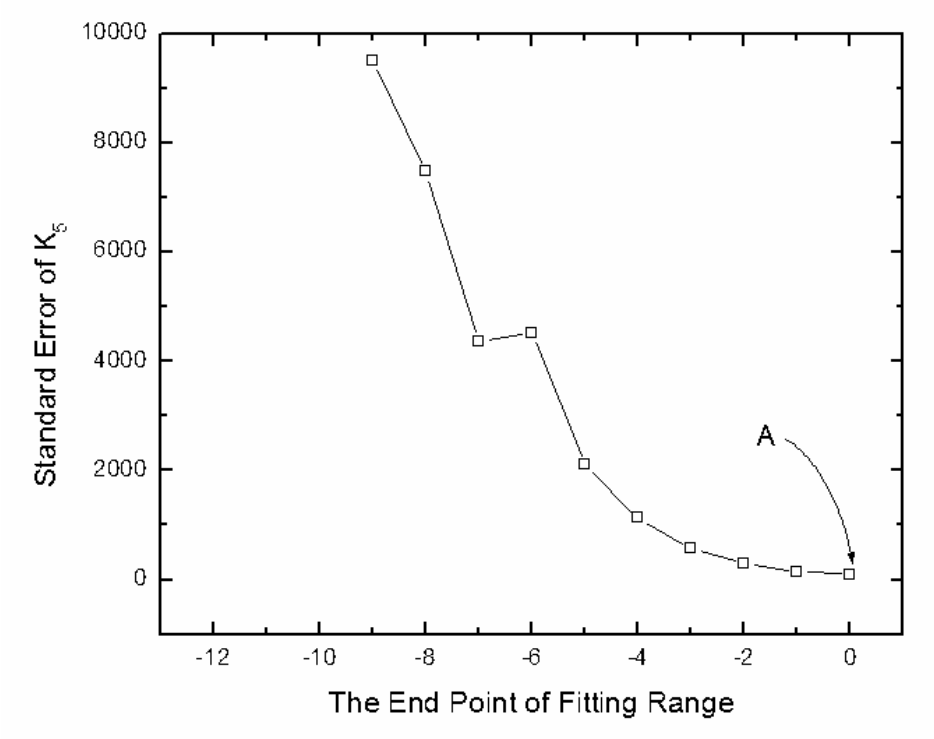

Figure 6-37 Standard error of K_5 (amplifier C)

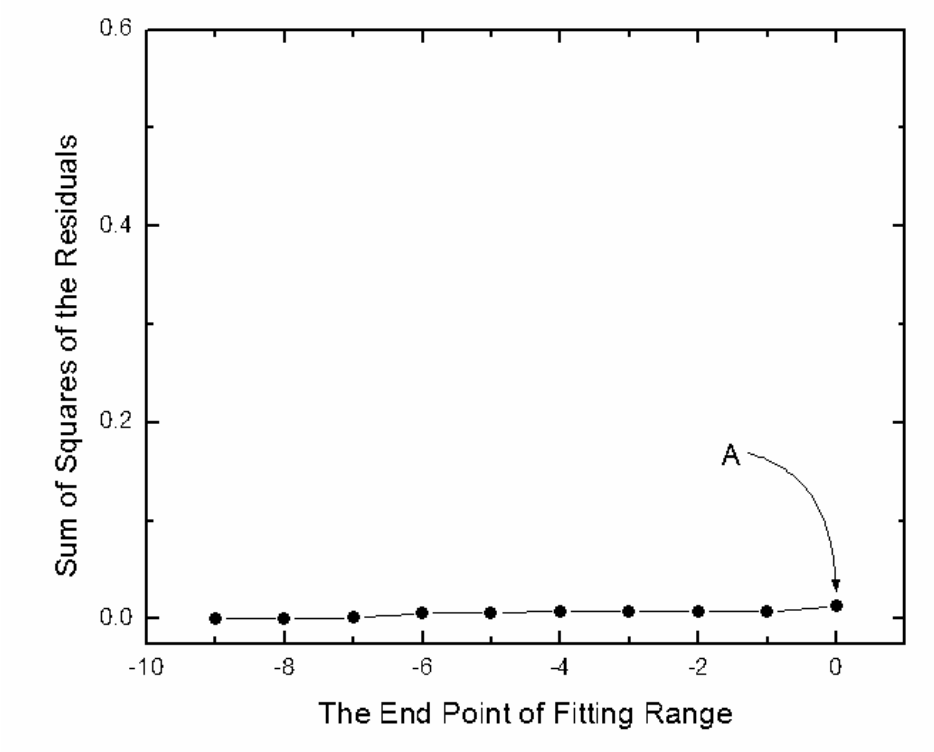

Figure 6-38 Sum of squares of the residuals (amplifier C)

Table 6-7 The summary of fitting results (amplifier C)

Parameters	Values
Coefficient K_1	24.94
s.e.(K_1)	0.18
Coefficient K_3	-255
s.e.(K_3)	10
Coefficient K_5	1297
s.e.(K_5)	99
Calculated IIP_3	1.16 dBm

the previous three examples which is measured at 2.45 GHz. The application algorithm is the same as that applied to the previous examples. Since the applied fitting algorithm to this example is the same as that to the previous, the analysis of the fitting result is also the same. Figure 6-39 shows the value of K_1 according to the fitting range. The value of K_3 can be found simultaneously with the value of K_1 during fitting process. Figure 6-40 shows the value of K_3. Figure 6-41 shows the standard errors of nonlinear coefficients K_1 and K_3. From this graph, the best fitting range is chosen by point A which indicates small values of the standard errors of K_1 and K_3. The range from -13 dBm to -6 dBm is chosen for the best fitting range. The sum of squares of the residual in this range is small in Figure 6-42. The fitting results are listed in Table 6-8. The application of the second fitting model to the one-tone gain curve of the amplifier D is summarized in Table 6-9. The fitting range is chosen from -13 dBm to -3 dBm. Figure 6-43, 6-44 and 6-45 show the extracted values of K_1, K_3 and K_5 respectively. Figure 6-46 shows the standard errors of K_1 and K_3. Point A is defined as the best fitting range which is from -13 dBm to -3 dBm. Table 6-10 shows the summary of the application of two fitting model to commercial PAs. Both fitting models give good results for the estimated IIP_3 compared

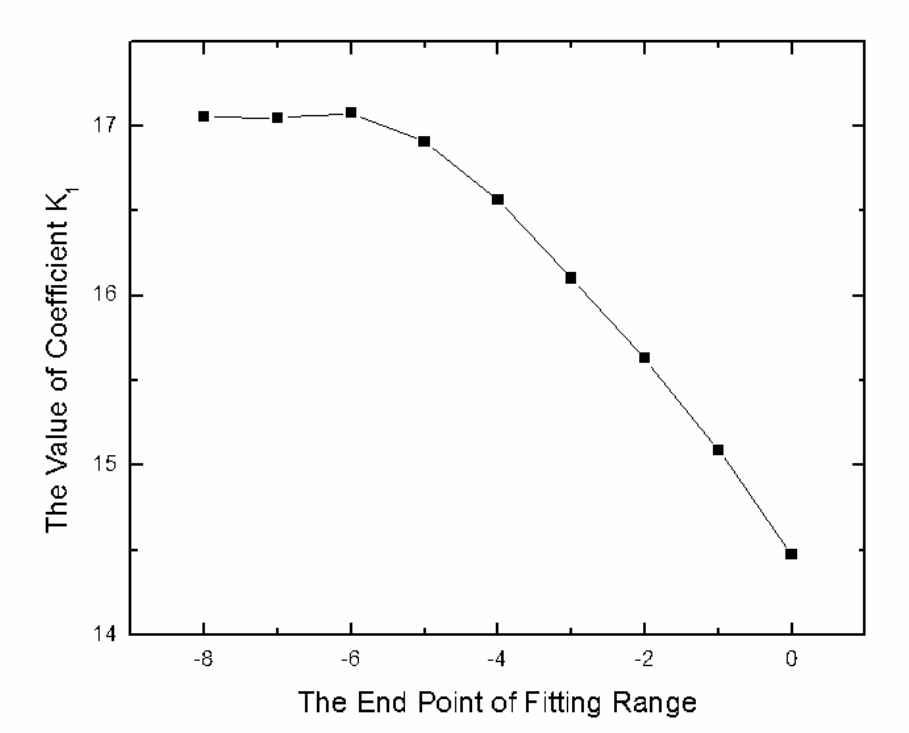

Figure 6-39 The value of coefficient K_1 (amplifier D)

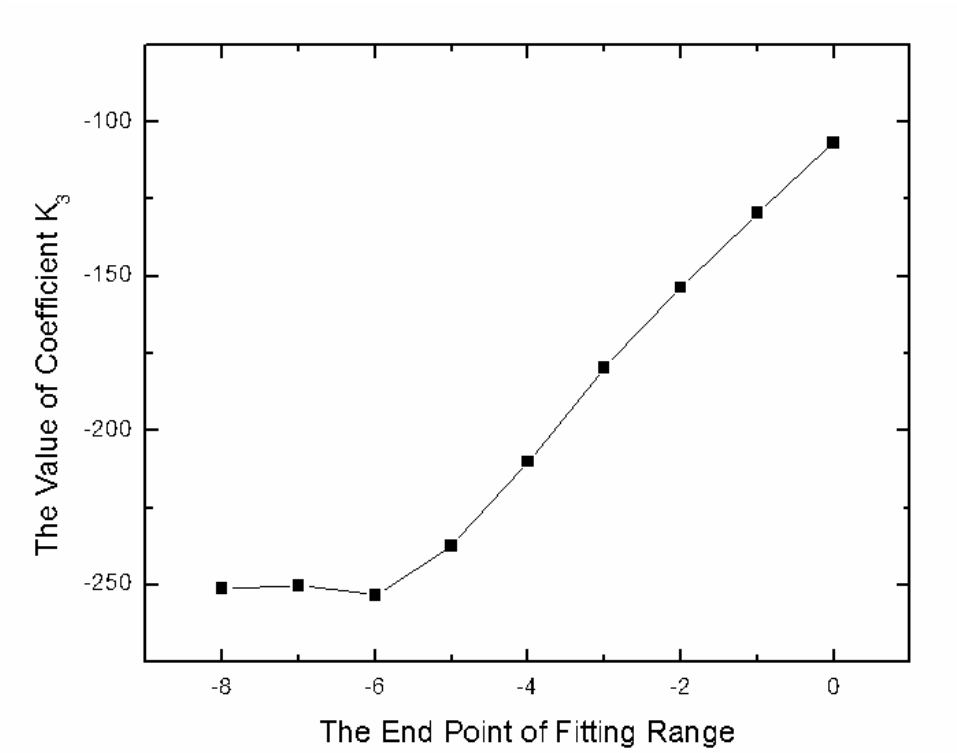

Figure 6-40 The value of coefficient K_3 (amplifier D)

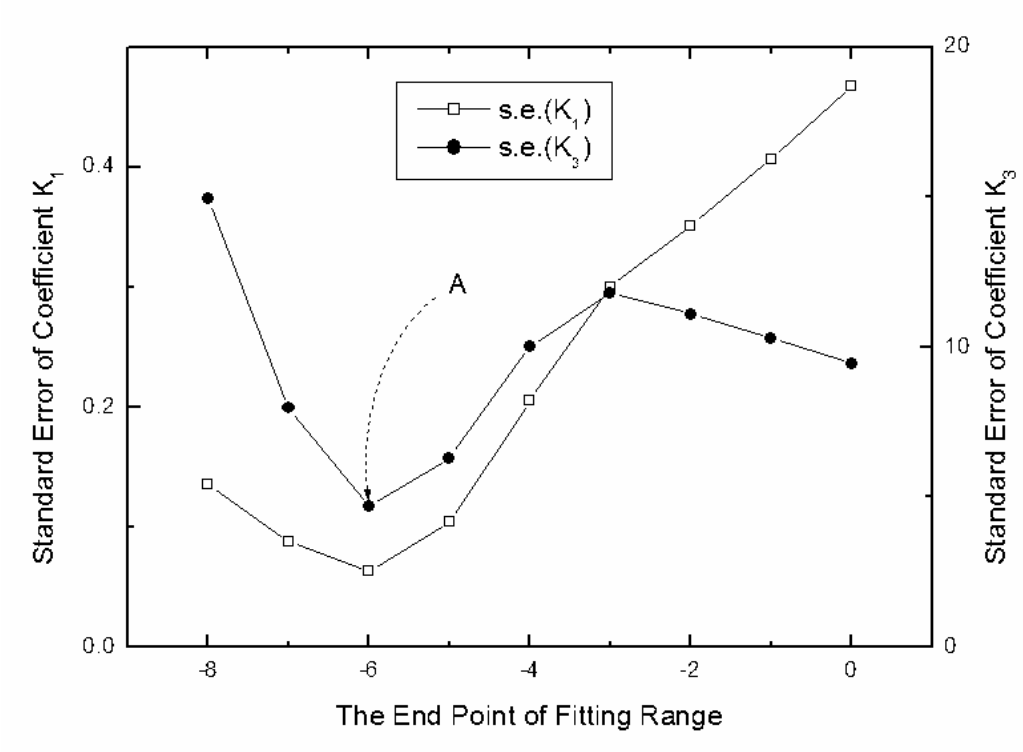

Figure 6-41 Standard errors of K_1 and K_3 (amplifier D)

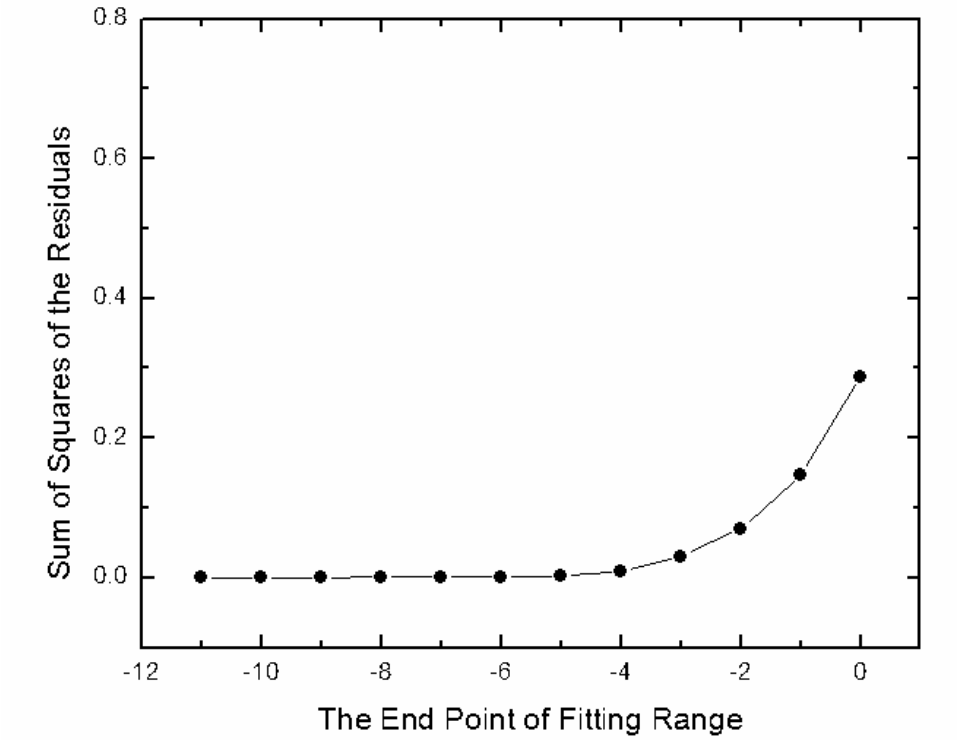

Figure 6-42 Sum of squares of the residuals (amplifier D)

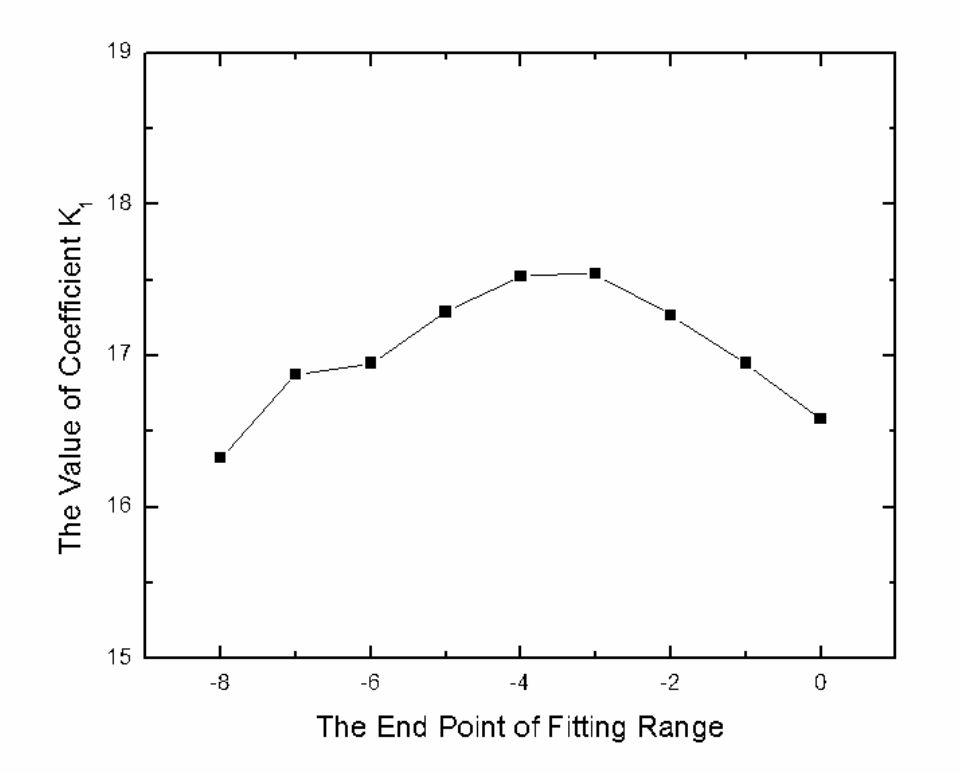

Figure 6-43 The value of coefficient K_1 (amplifier D)

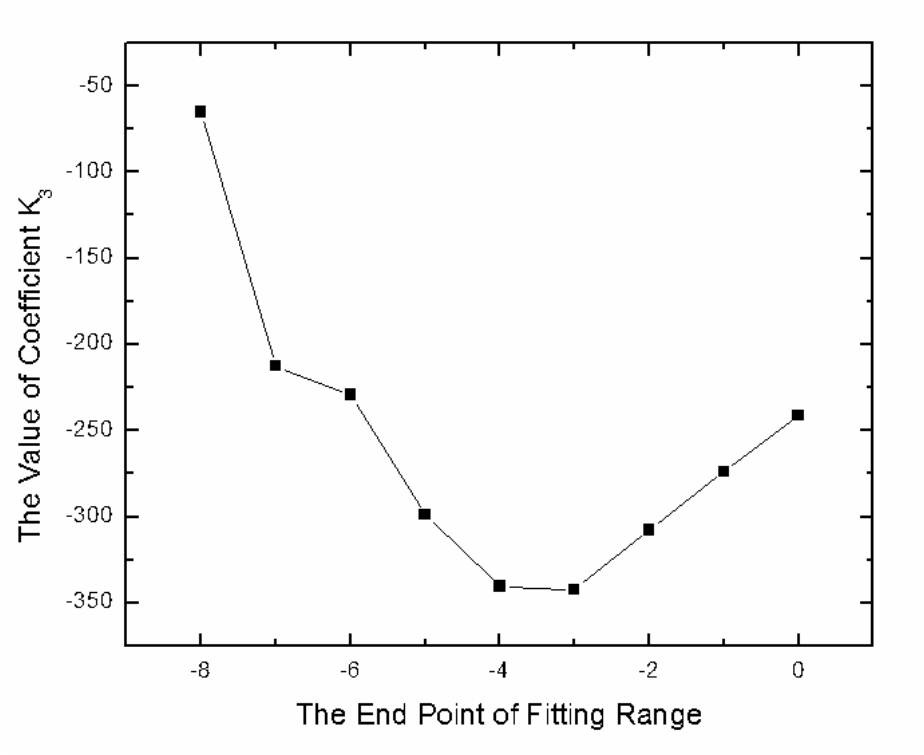

Figure 6-44 The value of coefficient K_3 (amplifier D)

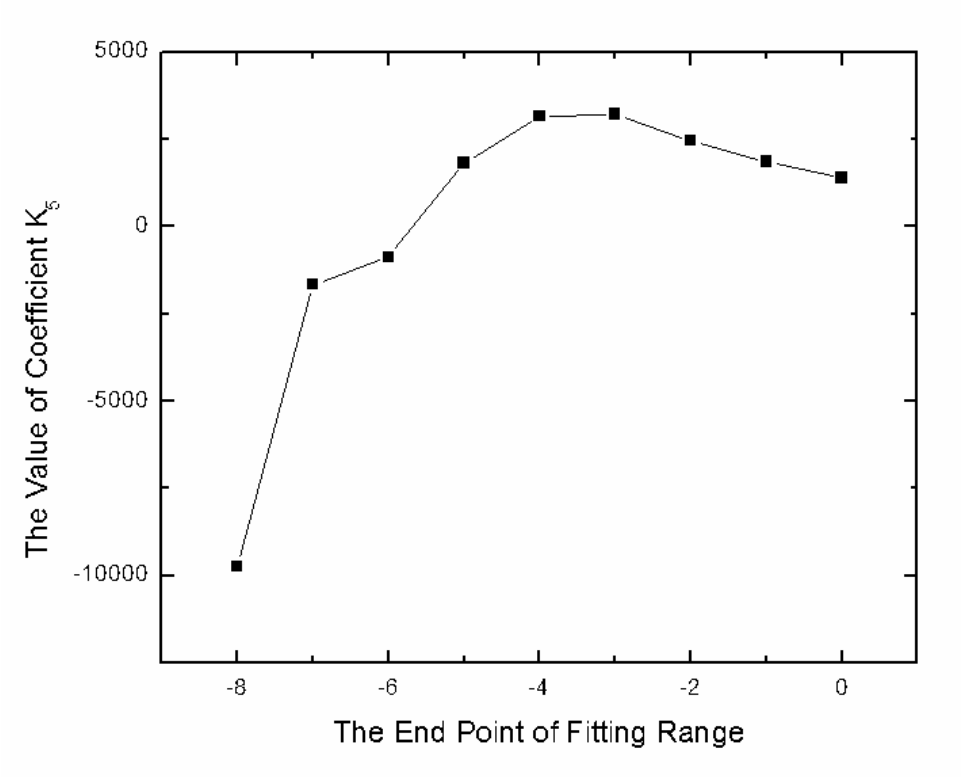

Figure 6-45 The value of coefficient K_5 (amplifier D)

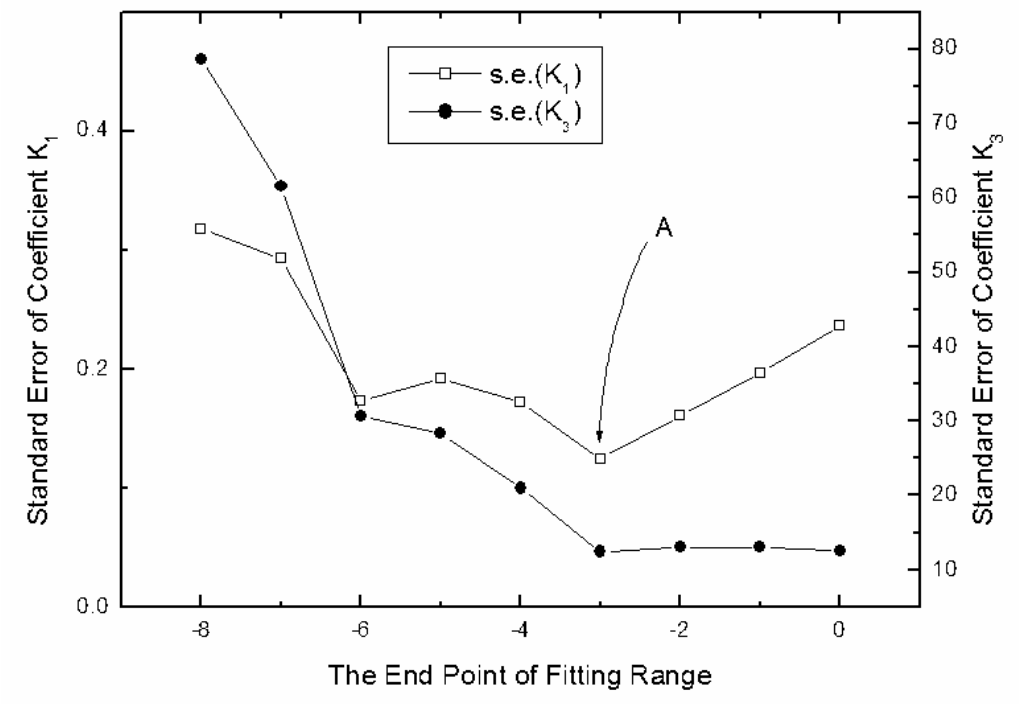

Figure 6-46 Standard errors of K_1 and K_3 (amplifier D)

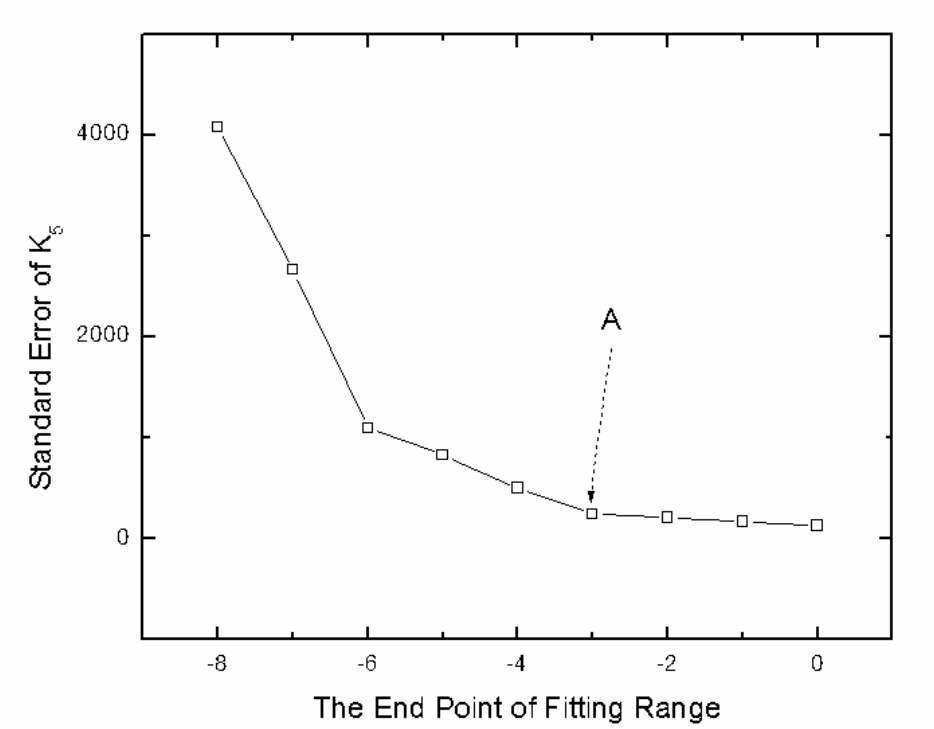

Figure 6-47 Standard error of K_5 (amplifier D)

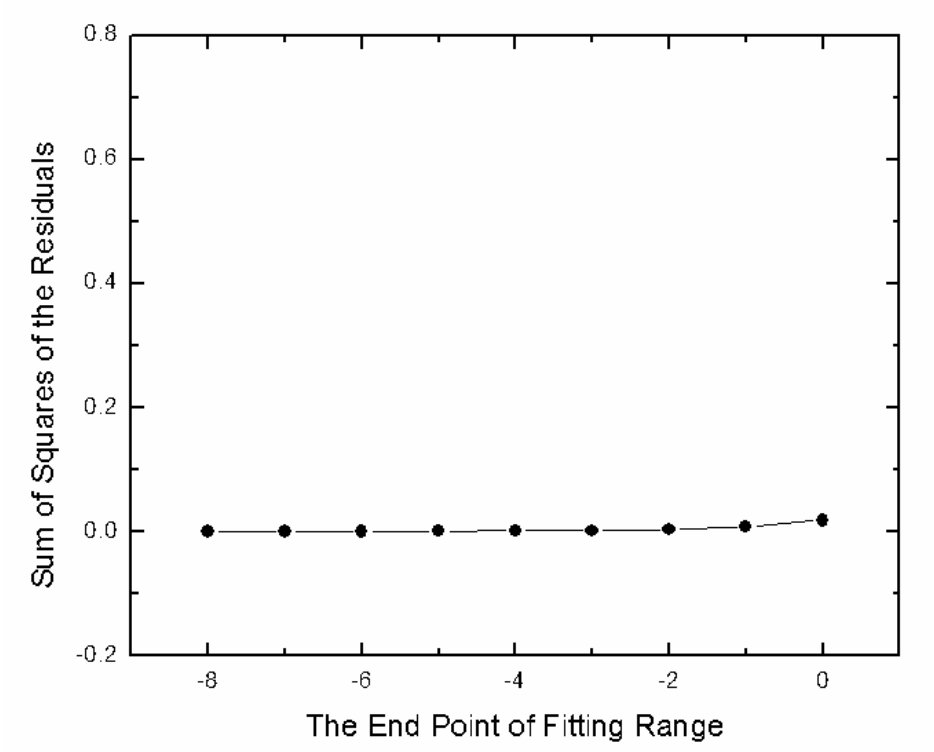

Figure 6-48 Sum of squares of the residuals (amplifier D)

Table 6-8 The summary of fitting results of the first model (amplifier D)

Parameters	Values
Coefficient K_1	17.08
s.e.(K_1)	0.06
Coefficient K_3	-253
s.e.(K_3)	5
Calculated IIP_3	-0.47 dBm

Table 6-9 The summary of fitting results (amplifier D)

Parameters	Values
Coefficient K_1	17.54
s.e.(K_1)	0.12
Coefficient K_3	-342
s.e.(K_3)	12
Coefficient K_5	3218
s.e.(K_5)	242
Calculated IIP_3	-1.65 dBm

Table 6-10 The comparison between two fitting models

Devices	IIP_3	Fitting Model 1	Fitting Model 2
Amplifier A	-4.4 dBm	-3.27 dBm	-4.31 dBm
Amplifier B	0 dBm	0.43 dBm	-0.28 dBm
Amplifier C	3 dBm	2.2 dBm	1.16 dBm
Amplifier D	-1 dBm	-0.47 dBm	-1.65 dBm

to the measured IIP_3. The fitting range for the fitting model 1, equation (6-1), is less than that for the fitting model 2, equation (6-2). These results are sufficient to choose the fitting model 1 for the IIP_3 estimation from the one-tone data of power amplifiers.

6.4 $IP_{1\text{-}dB}$ Estimation from the Two-tone Data

In addition, the estimation algorithm of the 1 dB gain compression point from two-tone data is applied to these power amplifiers. This algorithm is explained in section 5.4. The examples are shown also in section 5.4.

The amplifier A is considered as the first application example of this algorithm. IIP_3 of the amplifier A is -4.4 dBm in Table 6-1. The input amplitude at this point is

$$A_{IP3} = 10^{(IIP_3 - 10)/20} = 0.190 \tag{6-3}$$

where the unit of A_{IP3} is volt (V). The absolute value of the ratio, $\left|\frac{K_3}{K_1}\right|$ can be found in equation (6-3).

$$\left|\frac{K_3}{K_1}\right| = \frac{4}{3} \times 0.190^{-2} = 36.723 \tag{6-4}$$

The sign of above ratio $\left|\frac{K_3}{K_1}\right|$ is negative since the gain at the fundamental frequency compresses in Figure 6-2. From Table 6-1, the $IP_{1\text{-}dB,2}$ is -16 dBm. The input amplitude at this 1 dB compression point in the two-tone data is

$$A_{1-dB,2} = 10^{(IP_{1-dB,2} - 10)/20} = 0.050 \tag{6-5}$$

Using the value of $A_{1-dB,2}$ and the ratio $\left(\frac{K_3}{K_1}\right)$, the ratio $\left(\frac{K_5}{K_1}\right)$ is found in equation (5-4).

The calculated value of $\left(\frac{K_5}{K_1}\right)$ is

$$\left(\frac{K_5}{K_1}\right) = \left(-\frac{4}{25} A_{1-dB,2}{}^{-4}\right)\left(\frac{9}{4}\left(\frac{K_3}{K_1}\right) A_{1-dB,2}{}^{2} + 0.109\right) = 2499 \tag{6-6}$$

The 1 dB compression point in one-tone test is now found by solving equation (5-1). The

Table 6-11 The summary of the application results of the $IP_{1\text{-}dB}$ estimation algorithm

Device	Measured $IP_{1\text{-}dB}$	Estimated IIP_3
Amplifier A	-11 dBm	-12.2 dBm
Amplifier B	-8 dBm	-8.46 dBm
Amplifier C	-6 dBm	-5.47 dBm
Amplifier D	-8 dBm	-8.8 dBm

solution of this equation is 0.077. The calculated IP_{1-dB} is -12.2 dBm. The difference between the estimated IP_{1-dB} and the measured IP_{1-dB} is 1.2 dB. The same procedure is applied to three other amplifiers. The results of these applications are listed in Table 6-11.

6.5 Summary

In this chapter, the fitting algorithm which had been developed in chapter 4 has been verified through commercial RF power amplifiers. The inspection of the standard errors of fitting parameters has given the best fitting range for the extraction of nonlinear coefficients used for the calculation of the third-order intercept point. Two fitting models was applied to the data of four power amplifiers. The standard errors analyzed by linear regression analysis showed the accuracy of fitting algorithm. The chosen fitting range had to be confirmed by the quantity of sum of squares of the residuals. The estimated IIP_3 from one-tone measurement data was close to the measured IIP_3. The other method to predict $IP_{1\text{-}dB}$ from two-tone measurement was applied successfully to these commercial RF power amplifiers.

CHAPTER 7
SUMMARY AND SUGGESTIONS FOR FUTURE WORK

7.1 Summary

In this dissertation, nonlinear characteristics of amplifiers were discussed, and a fitting algorithm which estimates the third-order intercept point by extracting the nonlinear coefficients from the one-tone measurement was proposed and verified, and a method to predict the 1 dB gain compression point from the two-tone measurement was proposed and applied to some examples. Commercial wideband RF amplifiers and RF power amplifiers are tested and used for the verification of the proposed algorithm. A typical RF/Mixed-signal production test may use this algorithm or method to avoid the difficulty of the two-tone measurement or to remove the one-tone measurement test step. The major contributions for this thesis work are summarized as follows.

In chapter 3, a new relationship between the 1 dB gain compression point and the third-order intercept point has been derived. First, this relationship between the third-order intercept point and the 1 dB gain compression point was reviewed in classical analysis. The difference between two nonlinear characteristics was 9.6 dB and constant. The classical analysis included only a third-order nonlinear coefficient. The new relationship has derived by expanding nonlinear analysis on the gain compression curve up to the fifth-order nonlinear coefficients. The difference between $IP_{1\text{-}dB}$ and IIP_3 is not fixed and is explained by the equation including nonlinear coefficients. The fitting algorithm to estimate IIP_3 from one-tone measurement and the calculation method to

predict $IP_{1\text{-}dB}$ from two-tone measurement are devised. The linear regression theory required for the fitting algorithm has been reviewed and modified to apply the algorithm.

In chapter 4, the proposed fitting algorithm has been verified through the simulation of a common-source amplifier. The best fitting range has been chosen through the standard errors of nonlinear coefficients and the sum of squares of the residuals. The effect of measurement error was explored by adding random noise to the simulation data. Frequency effect on the fitting algorithm was examined up to 30 GHz. The IIP_3 estimation error is less than 2 dB up to 30 GHz. Through the Volterra series analysis, the load effect on the algorithm was investigated and was not affected by the active load except for the change caused by the operating frequency.

In chapter 5, the robust algorithm to predict IIP3 has been developed for the wideband RF amplifier. Given the situation, a global extraction of the LNA power series expansion coefficients was not stable with small changes in the data set. Adding a few more data points at the high-power range would create large changes in the K_3 and K_5 extracted coefficients. To counteract this problem, which would be seen in ATE systems doing manufacturing test, a new parameter extraction methodology had to be created. After experimenting with many ways of performing this parameter extraction, a regional parameter extraction methodology was devised. The $IP_{1\text{-}dB}$ prediction from two-tone measurement has been applied to these wideband amplifiers. Through several steps of simple calculation using the third-order intercept point and the gain compression at the fundamental frequency, $IP_{1\text{-}dB}$ has been estimated well under 1 dB error.

In chapter 6, the fitting algorithm that had been developed in chapter 4 has been verified through commercial RF power amplifiers. The inspection of the standard errors

of fitting parameters has given the best fitting range for the extraction of nonlinear coefficients used for the calculation of the third-order intercept point. Two fitting models were applied to the data of four power amplifiers. The standard errors analyzed by linear regression analysis showed the accuracy of the fitting algorithm. The chosen fitting range had to be confirmed by the quantity of sum of squares of the residuals. The estimated IIP_3 from one-tone measurement data was close to the measured IIP_3. The other method to predict $IP_{1\text{-}dB}$ from two-tone measurement was applied successfully to these commercial RF power amplifiers.

In conclusion, a fitting algorithm to estimate IIP_3 from the one-tone test and a modified robust algorithm for the wideband RF amplifiers has been developed and verified through simulation and measurement of wideband RF amplifiers and the commercial RF power amplifiers. A useful calculation method to predict $IP_{1\text{-}dB}$ from two-tone measurement has been developed because of nonlinear analysis and has been established in the application of wideband RF amplifiers and RF power amplifiers. These methods developed in this thesis are useful to typical RF/Mixed-signal production tests. By developing the relationship between the 1 dB gain compression point and the third-order intercept point, a simple embedded test model used avoiding the difficulty and test cost of two-tone measurement.

7.2 Suggestions for Future Work

A simple embedded test using a direct conversion mixer can be realized to measure the nonlinear characteristics of an amplifier. In this chapter, the nonlinear characteristics of a mixer are reported and the mixer embedded test is suggested.

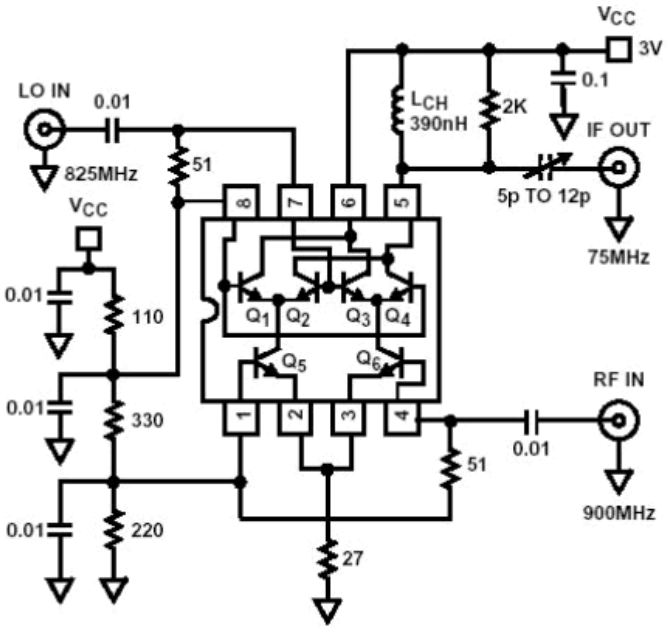

Figure 7-1 A schematic of a gilbert cell mixer

7.2.1 Nonlinearity of a Mixer

A mixer performs a frequency translation by multiplying two signals. A downconversion mixer employed in the receive path has two distinctly different inputs, called the RF port and the LO port. The RF port senses the signal to be downconverted and the LO port is the periodic waveform from the receiver local oscillator. In the receiver, the signal amplified by the LNA is applied to the RF port of the mixer [Raz98].

If a mixer operates with a differential LO signal and a single-ended RF signal, it is called as a single-balanced mixer. If a mixer accommodates both differential LO and RF inputs, it is called as a double balanced mixer and has the form of a Gilbert cell. To study of nonlinear characteristics of a mixer, a BJT Gilbert cell mixer is used. The schematic of the Gilbert cell mixer is shown in Figure 7-1. The one-tone test is performed with different LO powers. The gain of mixers must be carefully defined to avoid confusion. The power conversion gain of the mixer is defined as the ratio of the power of

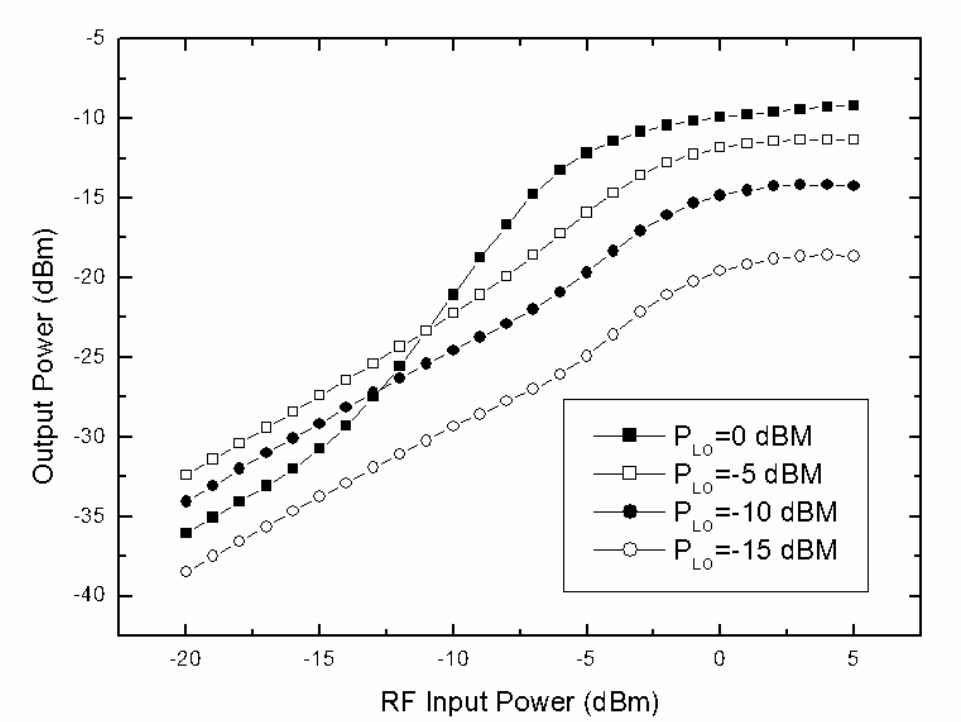

Figure 7-2 The result of one-tone test with different LO powers

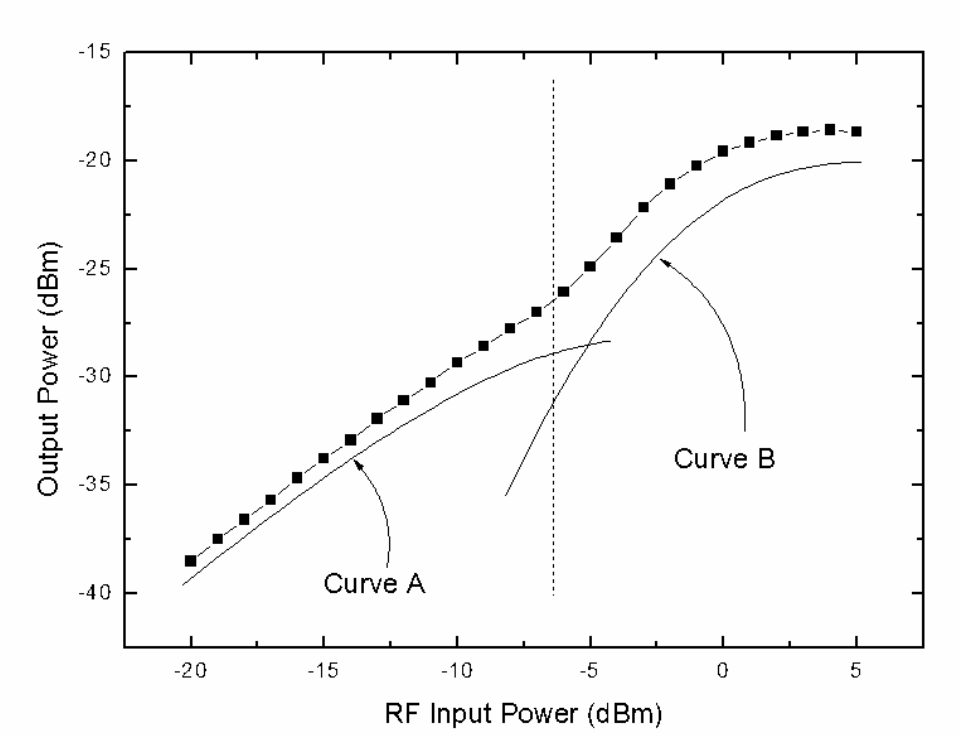

Figure 7-3 The analysis of the gain curve at -15 dBm LO power

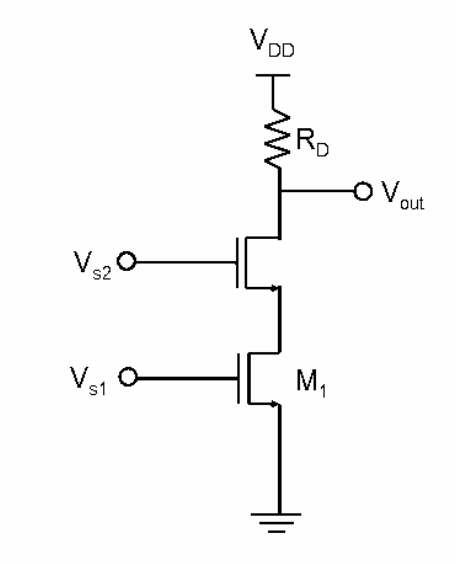

Figure 7-4 A cascode structure

the IF signal to the power of the RF signal. The result of the one-tone test can be seen in Figure 7-2. In this test, the IF output power shows a distinct behavior different from that of the amplifier. The gain curve of the mixer is assumed to be the sum of two different gain curves. Figure 7-3 shows the assumption that the gain curve at -15 dBm of LO power is the combination of the curve A and the curve B. To verify this assumption, the hand analysis of a cascode structure with two input signals is given in Figure 7-4. The result of the hand analysis is

$$\begin{aligned} i_{out} = V_{s2}\{&-2\beta_2\alpha_1 V_{s1} + \left(-2\beta_2\alpha_2 + 3\beta_3\alpha_1^{\,2}\right)V_{s1}^{\,2} + \left(-2\beta_2\alpha_3 + 6\beta_3\alpha_1\alpha_2 - 4\beta_4\alpha_1^{\,3}\right)V_{s1}^{\,3} \\ &+ \left(-2\beta_2\alpha_4 + 6\beta_3\alpha_1\alpha_3 + 3\beta_3\alpha_2^{\,2} - 12\beta_4\alpha_1^{\,2}\alpha_2 + 5\beta_5\alpha_1^{\,4}\right)V_{s1}^{\,4} \\ &+ \left(-2\beta_2\alpha_5 + 6\beta_3\alpha_1\alpha_4 + 6\beta_3\alpha_2\alpha_3 - 12\beta_4\alpha_1^{\,2}\alpha_3 - 12\beta_4\alpha_1\alpha_2^{\,2} + 20\beta_5\alpha_1^{\,3}\alpha_2\right)V_{s1}^{\,5} \\ &+ \ldots\} \\ + V_{s2}^{\,3}\{&-4\beta_4\alpha_1 V_{s1} + \left(-4\beta_4\alpha_2 + 10\beta_5\alpha_1^{\,2}\right)V_{s1}^{\,2} + \left(-4\beta_4\alpha_3 + 20\beta_5\alpha_1\alpha_2\right)V_{s1}^{\,3} \\ &+ \left(-4\beta_4\alpha_4 + 20\beta_5\alpha_1\alpha_3 + 10\beta_5\alpha_2^{\,2}\right)V_{s1}^{\,4} \\ &+ \left(-4\beta_4\alpha_5 + 20\beta_5\alpha_1\alpha_4 + 20\beta_5\alpha_2\alpha_3\right)V_{s1}^{\,5} + \ldots\} \\ &+ \ldots \end{aligned} \tag{7-1}$$

Equation (7-1) shows that the IF output is composed of two gain curves. One of them is linear to LO amplitude and the other is linear to triple times of LO amplitude. From this

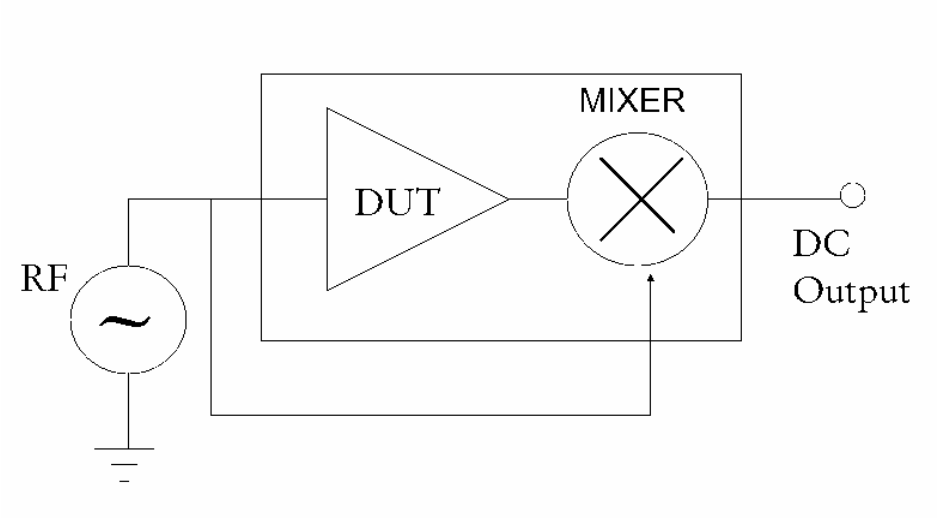

Figure 7-5 Simple embedded system with a mixer

analysis, it is possible to assume that the cascode structure with two input signals make the two compression curves. In the future, the nonlinear characteristic with multiple inputs and multiple nonlinear systems need to be investigated in the future.

7.2.2 Modeling a Mixer Embedded Test

Simple embedded test schemes for device under test can be seen in Figure 7-5. Through developing the relationship between IIP_3 and $IP_{1\text{-}dB}$, embedded test for IIP_3 requires only the one-tone test. For embedded test, new algorithm that predicts IIP_3 without the two-tone test was developed and verified in amplifiers. Through the one-tone test using this simple embedded scheme, nonlinear characteristics can be measured.

The direct downconversion of the mixer in the receiver can be adopted in the suggested simple test scheme. One of the problems of the direct downconversion receiver architecture is the envelope distortion due to the even-order nonlinearities [Kiv01]. Several mismatch factors cause even order intermodulation distortion in a Gilbert cell type mixer. The calibration technique for the dc offset caused by even-order nonlinearities is introduced for the direct downconversion mixer [Hot04]. For the

realization of the mixer embedded test, the effect of the mismatches and phase offset need to be investigated in the future

APPENDIX A
BSIM3 MODEL OF N-MOS AND P-MOS TRANSISTOR

In Chapter 4, the used transistor is TSMC 0.25um MOSFET. The BSIM3 model of n-MOSFET is listed in Table A-1 and the BSIM3 model of p-MOSFET is summarized in Table A-2.

Table A-1 BSIM3 model of n-MOSFET

LEVEL = 49 VERSION = 3.1 TNOM = 27 TOX = 5.7E-9
+XJ = 1E-7 NCH = 2.3549E17 VTH0 = 0.4122189
+K1 = 0.4555302 K2 = 5.728531E-3 K3 = 1E-3
+K3B = 2.9233592 W0 = 1.816641E-7 NLX = 2.10175E-7
+DVT0W = 0 DVT1W = 0 DVT2W = 0
+DVT0 = 0.4608679 DVT1 = 0.5163149 DVT2 = -0.5
+U0 = 318.8665069 UA = -9.32302E-10 UB = 2.162432E-18
+UC = 3.868128E-11 VSAT = 1.458598E5 A0 = 1.626434
+AGS = 0.3003966 B0 = -4.103132E-7 B1 = 5E-6
+KETA = -4.297464E-4 A1 = 0 A2 = 0.4274964
+RDSW = 116 PRWG = 0.5 PRWB = -0.2
+WR = 1 WINT = 0 LINT = 1.056485E-8
+XL = 3E-8 XW = -4E-8 DWG = -1.833849E-8
+DWB = 2.423085E-9 VOFF = -0.1085255 NFACTOR = 1.6188811
+CIT = 0 CDSC = 2.4E-4 CDSCD = 0
+CDSCB = 0 ETA0 = 4.244913E-3 ETAB = 5.001973E-4
+DSUB = 0.0551518 PCLM = 1.9563343 PDIBLC1 = 1
+PDIBLC2 = 7.485749E-3 PDIBLCB = -0.0349745 DROUT = 0.8869937
+PSCBE1 = 7.999904E10 PSCBE2 = 5E-10 PVAG = 0
+DELTA = 0.01 RSH = 4.4 MOBMOD = 1
+PRT = 0 UTE = -1.5 KT1 = -0.11 KT1L = 0
+KT2 = 0.022 UA1 = 4.31E-9 UB1 = -7.61E-18 UC1 = -5.6E-11
+AT = 3.3E4 WL = 0 WLN = 1 WW = 0 WWN = 1
+WWL = 0 LL = 0 LLN = 1 LW = 0
+LWN = 1 LWL = 0 CAPMOD = 2 XPART = 0.5
+CGDO = 6.08E-10 CGSO = 6.08E-10 CGBO = 1E-12
+CJ = 1.758361E-3 PB = 0.99 MJ = 0.4595413
+CJSW = 3.984847E-10 PBSW = 0.99 MJSW = 0.3488353
+CJSWG = 3.29E-10 PBSWG = 0.99 MJSWG = 0.3488353
+CF = 0 PVTH0 = -0.01 PRDSW = -10
+PK2 = 2.330213E-3 WKETA = 7.327459E-3 LKETA =-6.323718E-3

Table A-2 BSIM3 model of p-MOSFET

```
LEVEL   = 49
+VERSION = 3.1          TNOM    = 27          TOX     = 5.6E-9
+XJ      = 1E-7         NCH     = 4.1589E17   VTH0    = -0.5572867
+K1      = 0.611414     K2      = 4.87747E-3  K3      = 0
+K3B     = 10.9112779   W0      = 1E-6        NLX     = 1E-9
+DVT0W   = 0            DVT1W   = 0           DVT2W   = 0
+DVT0    = 2.3635216    DVT1    = 0.8955611   DVT2    = -0.2135943
+U0      = 113.0309435  UA      = 1.42794E-9  UB      = 1E-21
+UC      = -9.95235E-11 VSAT    = 2E5         A0      = 0.9647086
+AGS     = 0.2047206    B0      = 1.359601E-6 B1      = 5E-6
+KETA    = 9.05781E-3   A1      = 3.192059E-3 A2      = 0.3
+RDSW    = 1.107652E3   PRWG    = 0.1255776   PRWB    = -0.2785571
+WR      = 1            WINT    = 0           LINT    = 3.560404E-8
+XL      = 3E-8         XW      = -4E-8       DWG     = -3.109864E-8
+DWB     = 3.826099E-9  VOFF    = -0.1311284  NFACTOR = 1.0570063
+CIT     = 0            CDSC    = 2.4E-4      CDSCD   = 0
+CDSCB   = 0            ETA0    = 0.677192    ETAB    = -0.4495342
+DSUB    = 1.23934      PCLM    = 1.2278829   PDIBLC1 = 4.941705E-3
+PDIBLC2 = 1.946865E-5  PDIBLCB = -1E-3       DROUT   = 0.0556797
+PSCBE1  = 1.766372E10  PSCBE2  = 1.433404E-9 PVAG    = 0
+DELTA   = 0.01         RSH     = 3.5         MOBMOD  = 1
+PRT     = 0            UTE     = -1.5        KT1     = -0.11
+KT1L    = 0            KT2     = 0.022       UA1     = 4.31E-9
+UB1     = -7.61E-18    UC1     = -5.6E-11    AT      = 3.3E4
+WL      = 0            WLN     = 1           WW      = 0
+WWN     = 1            WWL     = 0           LL      = 0
+LLN     = 1            LW      = 0           LWN     = 1
+LWL     = 0            CAPMOD  = 2           XPART   = 0.5
+CGDO    = 6.73E-10     CGSO    = 6.73E-10    CGBO    = 1E-12
+CJ      = 1.883162E-3  PB      = 0.9888002   MJ      = 0.46754
+CJSW    = 3.120022E-10 PBSW    = 0.5590324   MJSW    = 0.2692798
+CJSWG   = 2.5E-10      PBSWG   = 0.5590324   MJSWG   = 0.2692798
+CF      = 0            PVTH0   = 7.130423E-3 PRDSW   = 14.8296171
+PK2     = 3.224494E-3  WKETA   = 0.0282003   LKETA   = -7.320113E-3
```

APPENDIX B
VOLTERRA-KERNELS OF A COMMON-SOURCE AMPLIFIER

Volterra-kernels are calculated in this section for a common-source amplifier. The equivalent circuit for this calculation is shown in Figure B-1. In this calculation, all parasitic capacitors are assumed as linear capacitors for simplicity. Here, the nonlinear source is transconductance only. Cgd is only considered at high frequency. Nonlinear transconductance is represented by the bellows,

$$i = K_1 v_{gs} + K_2 v_{gs}^{\ 2} + K_3 v_{gs}^{\ 3} + K_4 v_{gs}^{\ 4} + K_5 v_{gs}^{\ 5} + \ldots \tag{B-1}$$

To calculate first-order Volterra-kernel, Kirchoff's current law is applied at both node 1 and node 2 in Figure B-1.

$$V_1 = V_{in} \tag{B-2}$$

$$K_1 V_1 + (G_L + sC_L) V_2 = 0 \tag{B-3}$$

Above two equations can be combined in one matrix equation:

$$\begin{bmatrix} 1 & 0 \\ K_1 & G_L + sC_L \end{bmatrix} \bullet \begin{bmatrix} V_1 \\ V_2 \end{bmatrix} = \begin{bmatrix} V_{in} \\ 0 \end{bmatrix} \tag{B-4}$$

It is clear that V_1 and V_2 reduce to the transfer functions of the voltages at node 1 and node 2. These transfer functions are denoted by $H_{1,1}(s)$ and $H_{1,2}(s)$. The first subscript represents the order of transfer function and the second subscript indicates the number of nodes. The matrix equation can be formed in terms of these transfer functions by replacing voltages to these transfer functions or Volterra-kernels.

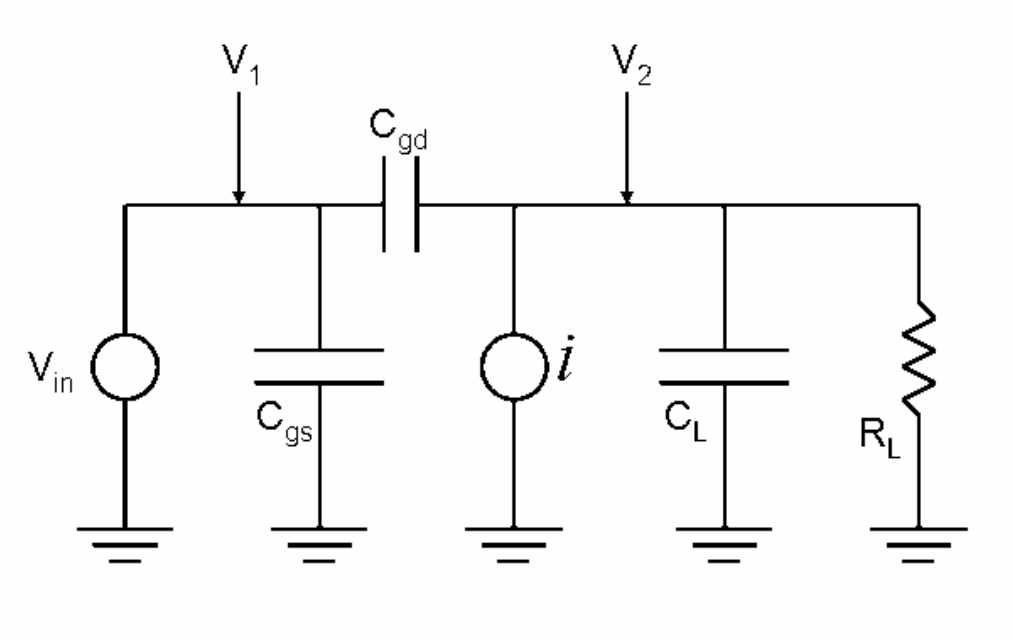

Figure B-1. An equivalent circuit of a common-source amplifier

$$\begin{bmatrix} 1 & 0 \\ \mathrm{K}_1 & G_L + sC_L \end{bmatrix} \bullet \begin{bmatrix} \mathrm{H}_{1,1}(s) \\ \mathrm{H}_{1,2}(s) \end{bmatrix} = \begin{bmatrix} 1 \\ 0 \end{bmatrix} \tag{B-5}$$

The solution of above matrix equation is as follows;

$$\mathrm{H}_{1,1}(s) = 1 \tag{B-6}$$

$$\mathrm{H}_{1,2}(s) = \frac{-K_1}{G_L + sC_L} \tag{B-7}$$

After finding the first kernel, the matrix for the second kernel can be made.

$$\begin{bmatrix} 1 & 0 \\ \mathrm{K}_1 & G_L + sC_L \end{bmatrix} \bullet \begin{bmatrix} \mathrm{H}_{2,1}(s_1, s_2) \\ \mathrm{H}_{2,2}(s_1, s_2) \end{bmatrix} = \begin{bmatrix} 0 \\ -\mathrm{K}_2 \mathrm{H}_{1,1}(s_1)\mathrm{H}_{1,1}(s_2) \end{bmatrix} = \begin{bmatrix} 0 \\ -\mathrm{K}_2 \end{bmatrix} \tag{B-8}$$

The second Volterra-kernel can be found by solving above matrix equation.

$$\mathrm{H}_{2,1}(s_1, s_2) = 0 \tag{B-9}$$

$$\mathrm{H}_{2,2}(s_1, s_2) = \frac{-K_2}{G_L + (s_1 + s_2)C_L} \tag{B-10}$$

Higher Volterra-kernels can be found by repeating the same process done before. Volterra-kernels have been calculated up to 5th order.

$$\mathrm{H}_{3,1}(s_1, s_2, s_3) = 0 \tag{B-11}$$

$$\mathrm{H}_{3,2}(s_1, s_2, s_3) = \frac{-K_3}{G_L + (s_1 + s_2 + s_3)C_L} \tag{B-12}$$

$$\mathrm{H}_{4,1}(s_1, s_2, s_3, s_4) = 0 \tag{B-13}$$

$$\mathrm{H}_{4,2}(s_1, s_2, s_3, s_4) = \frac{-K_4}{G_L + (s_1 + s_2 + s_3 + s_4)C_L} \tag{B-14}$$

$$\mathrm{H}_{5,1}(s_1, s_2, s_3, s_4, s_5) = 0 \tag{B-15}$$

$$\mathrm{H}_{5,2}(s_1, s_2, s_3, s_4, s_5) = \frac{-K_5}{G_L + (s_1 + s_2 + s_3 + s_4 + s_5)C_L} \tag{B-16}$$

At high frequency, Cgd should be considered in the Volterra-kernel. Like low frequency analysis, the matrix for the first Volterra-kernel can be formed by similar process including Cgd.

$$\begin{bmatrix} 1 & 0 \\ \mathrm{K}_1 - sC_{gd} & G_L + s(C_L + C_{gd}) \end{bmatrix} \bullet \begin{bmatrix} \mathrm{H}_{1,1}(s) \\ \mathrm{H}_{1,2}(s) \end{bmatrix} = \begin{bmatrix} 1 \\ 0 \end{bmatrix} \tag{B-17}$$

The first Volterra-kernel at high frequency is not the same as that at low frequency.

$$\mathrm{H}_{1,1}(s) = 1 \tag{B-18}$$

$$\mathrm{H}_{1,2}(s) = \frac{-(K_1 - sC_{gd})}{G_L + s(C_L + C_{gd})} \tag{B-19}$$

From second-order kernel, the Volterra-kernels are similar to those at low frequency only if C_L is replaced by (C_L+C_{gd}).

APPENDIX C
MATLAB PROGRAM FOR FITTING ALGORITHM

The MATLAB program for the fitting algorithm is listed as bellows,

```
% Extracting K1,K3,K5 coefficients
% device : Power amplifier
% frequency = 2.45GHz, one-tone data
close all
clear all
load PA.txt -ASCII;
Pin=PA(:,1)';
Pin=Pin(:);
Pout=PA(:,2)';
Pout=Pout(:);
Vin=10.^((Pin-10)./20);     % Data converting : power(dBm) to voltage(V)
Vout=10.^((Pout-10)./20);
% Extracting b1, b3, b5 ( y=b1*x+b3x^3+b5x^5+error )
Fit_start=5;                          % Define the first fitting range
Fit_end=length(Vin);
for Fit_n = Fit_start:Fit_end         % Sweeping the range for fitting
   clear xx                           % local parameter xx and yy for for-loop
   clear yy
   xx=Vin(1:Fit_n);                   % Define fitting data (voltage)
```

```
yy=Vout(1:Fit_n);
n=length(xx);
Pinx(Fit_n-Fit_start+1)=Pin(Fit_n);     % Define fitting data in dBm unit
% Polynomial regression model : y=b0+b1*x+error
% Vector form : estimate of Vector b
clear X                          % Construct X
X(:,1) = ones(n,1);
X(:,1) = xx.*X(:,1);
X(:,2) = xx.^2.*X(:,1);
X(:,3) = xx.^2.*X(:,2);
C=inv(X'*X);
bb=C*(X'*yy);                    % estimation of vector bb = [(X'X)^-1]*(X'Y)
b1=bb(1);
b3=bb(2);
b5=bb(3);
Coeff_b1(Fit_n-Fit_start+1)=b1;
Coeff_b3(Fit_n-Fit_start+1)=b3;
Coeff_b5(Fit_n-Fit_start+1)=b5;
% Analysis of Varianc
%    1. degrees of freedom
%    2. Sum of Squares
%    3. Mean Squares= SS/d.f.
%    4. F test
```

```
%    5. Standard Error and t-distribution and confidence interval
 Total_df(Fit_n-Fit_start+1)=n;                    % Degrees of freedom
Tcorrected_df(Fit_n-Fit_start+1)=Total_df(Fit_n-Fit_start+1)-1;
Regression_df(Fit_n-Fit_start+1)=length(bb)-1;
Residual_df(Fit_n-Fit_start+1)=Tcorrected_df(Fit_n-Fit_start+1)-
Regression_df(Fit_n-Fit_start+1);
Mx=mean(xx);                                      % Mean Value
My=mean(yy);
Regression_SS(Fit_n-Fit_start+1)=bb'*X'*yy-n*My^2;     % Sum of squares
T_corrected_SS(Fit_n-Fit_start+1)=yy'*yy-n*My^2;
Residual_SS(Fit_n-Fit_start+1)=T_corrected_SS(Fit_n-Fit_start+1)-
Regression_SS(Fit_n-Fit_start+1);
MSR(Fit_n-Fit_start+1)=Regression_SS(Fit_n-Fit_start+1)/Regression_df(Fit_n-
Fit_start+1);       % Mean Squares
MSE(Fit_n-Fit_start+1)=Residual_SS(Fit_n-Fit_start+1)/Residual_df(Fit_n-
Fit_start+1);
F0(Fit_n-Fit_start+1)=MSR(Fit_n-Fit_start+1)/MSE(Fit_n-Fit_start+1);
% F-test
F_1percent(Fit_n-Fit_start+1)=finv(0.99,Regression_df(Fit_n-
Fit_start+1),Residual_df(Fit_n-Fit_start+1));
disp('_____________________________________________________________________');
dispftest={'F-test   ','calculated F0=',num2str(F0),'    <=
','F(0.01,n1,n2)=',num2str(F_1percent)};
```

```
            disp(dispftest);
            disp('   ( > ) means H0:b1=b3=b5=0 is rejected ');
            %The coefficient of multiple determination
            RR(Fit_n-Fit_start+1)=Regression_SS(Fit_n-Fit_start+1)/T_corrected_SS(Fit_n-
Fit_start+1);
          disp('_____
__');
            dispRR=['The coefficient of multiple determination R^2:',num2str(RR) ];
            disp(dispRR);
            Cov_b=MSE(Fit_n-Fit_start+1).*C;
 % Covariance matrix of Vector b : Cov(Vector b)=sig^2(X'X)^-1, Matrix C=(X'X)^-1
           disp('_____
___');
            disp('Covariance of estimation beta');
            disp(Cov_b);
            se_b1(Fit_n-Fit_start+1)=sqrt(Cov_b(1,1));
% Standard error of beta se(bi)=sqrt(Cjj*sig^2)
            se_b3(Fit_n-Fit_start+1)=sqrt(Cov_b(2,2));
            se_b5(Fit_n-Fit_start+1)=sqrt(Cov_b(3,3));
             tvalue=tinv(0.975,Residual_df);
          % Confidence interval using t distribution
            low_b1=b1-tvalue*se_b1;
            high_b1=b1+tvalue*se_b1;
```

```
    disp('_____');
    disp('95% Confidence interval');
    disp_b1=[num2str(low_b1),'<< b1 <<',num2str(high_b1)];
    disp(disp_b1);
% Nonlinear Coefficients
K5=(8/5).*Coeff_b5;
K3=(4/3).*Coeff_b3;
K1=Coeff_b1;
SEK5=(8/5).*se_b5;
SEK3=(4/3).*se_b3;
SEK1=se_b1;
% Third-order Intercept Point
AIP3=sqrt(abs(4.*K1./(3.*K3)));
IIP3=20.*log10(AIP3)+10;
Calculated_IIP3=IIP3(Index_reg)
WriteMatrix(:,1)=Pinx';
WriteMatrix(:,2)=K1';
WriteMatrix(:,3)=SEK1';
WriteMatrix(:,4)=K3';
WriteMatrix(:,5)=SEK3';
WriteMatrix(:,6)=K5';
WriteMatrix(:,7)=SEK5';
WriteMatrix(:,8)=Residual_SS';
```

```
WriteMatrix(:,9)=IIP3';
dlmwrite('p7analysis.txt',WriteMatrix,'\t');
```

LIST OF REFERENCES

[Dra98] N. R. Drapper and H. Smith, *Applied Regression Analysis*, 3rd ed., New York :John Wiley & Sons, 1998.

[Eis01] W. R. Eisenstadt and S. Choi, "Programmable Embedded IF Source For Wireless Test," 1st Workshop on Test of Wireless Circuits and Systems, Atlantic, NJ, November 1-2, 2001.

[Eis02] W. R. Eisenstadt, C. Cho, R. Stengel, and E. Ferrer, "Third-order intercept Point(IIP3) from Gain Compression Curve," 2nd Workshop on Test of Wireless Circuits and Systems, Baltimore, MD, October 10-11,2002.

[Fag02] C. Fager, J.C. Pedro, N. B. Carvalho, and H. Zirath, "Prediction of IMD in LDMOS Transistor Amplifiers using a New Large-Signal Model," IEEE Trans. On Microwave Theory and Techniques, vol. 50, pp. 2834-2842,2002.

[Fon98] K. L. Fong and R. G. Meyer "High-Frequency Nonlinearity Analysis of Common-Emitter and Differential-Pair Transconductance Stages", IEEE Journal on Solid-State Circuits, vol. 33, No. 4, pp. 548-555, April 1998

[Gon97] G. Gonzalez, *Microwave Transistor Amplifers*, 2nd ed., Upper Saddle River : Prentice Hall, 1997.

[Gra93] P. R. Gray and R. G. Meyer, *Analysis and Design of Analog Integrated Circuits*, 3rd ed., New York :John Wiley & Sons, 1993.

[Hot04] M. Hotti, J. Ryynanen, K. Kivekas, and K. Halonen, "An IIP2 Calibration technique for direct conversion," ISCAS 2004, pp. IV-257-IV-260, 2004.

[Kan03] S. Kang, B. Choi, and B. Kim, "Linearity Analysis of CMOS for RF Application," IEEE Transactions on Microwave Theory and Techniques, vol. 51, No.3, pp. 972-977, March 2003.

[Kiv01] K. Kivekas, A. Parssinen, and K. Halonen, "Characterization of IIP2 amd DC-OFFSETS in Transconductance Mixers," IEEE Transactions on Circuits and systems-II: Analog and Digital Signal Processing, vol. 48, pp. 1028-1038, Nov. 2002.

[Maa88] S. A. Maas, *Nonlinear Microwave Circuits*, Norwood :Artech House, 1988.

[Mon01] D.C. Montgomery, E. A. Peck, and G. G. Vining, *Introduction to Linear Regression Theory*, 3rd ed., New York :John Wiley & Sons, 2001.

[Mcc99] J. H. McClellan, R. W. Schafer and M. A. Yoder, *DSP First*, Upper Saddle River :Prentice Hall, 1999.

[Ped91] D. O. Pederson and K. Mayaram, *Analog Integrated Circuits for Communication: principles, simulation and design*, Boston :Kluwer Academic Publishers, 1991.

[Raz98] B. Razavi, *RF Microelectronics*, Upper Saddle River :Prentice-Hall, 1998

[Ros98] D. A. Ross, *Master Math :Calculus*, Franklin Lakes: CAREER PRESS, 1998.

[San73] W. M. C. Sansen and R. G. Meyer, "Distortion in Bipolar Transistor Variable-Gain Amplifiers," IEEE Journal on Solid-State Circuits, vol. 8, pp. 275-282, August 1973.

[San99] W. Sansen, "Distortion in Elementary Transistor circuits," IEEE Transactions on Circuits and systems, vol. 46, pp. 315-325, March 1999.

[Vuo03] J. Vuolevi and T. Rahkonen, *Distortion in RF Amplifers*, Norwood :Artech House, 2003.

[Wam98] P. Wambacq and W. Sansen, *Distortion Analysis of Analog Integrated Circuits*, Boston :Kluwer Academic Publishers, 1998.

[Wei80] D. D. Weiner and J. E. Spina, Sinusoidal Analysis and Modeling of Weakly Nonlinear Circuits, *Distortion Analysis of Analog Integrated Circuits*, New York :Van Nostrand Reinhold Company, 1980.

BIOGRAPHICAL SKETCH

Choongeol Cho was born in Korea, in 1969. He received a BS degree and a MS degree in physics from Yonsei University, South Korea, in 1991 and 1993, respectively. During his MS program, he had majored in solid-state physics for II-VI compound heterojunction structures.

He worked as a process engineer for six years at Samsung Semiconductor research lab. During this time, he joined a process team that developed 256M DRAM and 1G DRAM. Since June 2001, he has been working on his Ph.D. degree in Radio Frequency Test Research Group at the University of Florida as a graduate research assistant.

His research interests are nonlinear analysis of analog/RF mixed circuits, RF receiver design, and embedded test. He is particularly interested in the improvement of linearity of RF components.